Interactions of hadrons at high energies.

A.B.Kaidalov

Lecture at ITEP Winter School

February 2009.

Plan of lectures:

1. Introduction.

- S-matrix. Cross sections. Kinematics.
- Crossing. Mandelstam variables.
- Unitarity and optical theorem.
- Partial wave expansion.
- Analyticity and dispersion relations.
- Gribov-Froissart representation.
- Froissart theorem.
- Pomeranchuk theorem.

Plan of lectures

2. Regge poles.

- The reggeon concept.
- Complex angular momentum method.
- Properties of reggeons.
- Pomeron.
- Regge poles in QCD. 1/N-expansion.
- Pomeron in QCD and glueballs.

Plan of lectures

3. Reggeon calculus and multi-particle production.

- s-channel picture of reggeons.
- Regge cuts and their properties.
- AGK-cutting rules.
- Multi-particle production and topological expansion.
- Quark Gluon Strings Model.
- Comparison with experiment.

Plan of lectures

4. Hadronic physics at LHC.

- Small-x physics and “saturation” of partons.
- Interactions of pomerons.
- Diffractive processes and exclusive Higgs production.
- Predictions for LHC.
- Conclusions.

Books and reviews:

- V.Berestetsky, E.Lifshitz, L.Pitaevsky. Relativistic quantum theory. Chapter VIII.
- R.J.Eden, P.V.Landshoff, D.I.Polkinghorne. The analytic S-matrix. 1966.
- P.D.B.Collins. An introduction to Regge theory and high energy physics, 1977.
- A.B.Kaidalov. Regge poles in QCD. At Frontiers of Particle Physics.vol.1, 609.
- A.B.Kaidalov. Pomeranchuk singularity and high-energy hadronic interactions, Usp. Fiz. Nauk, 46, 1153 , 2003.

S-matrix formalism.

1 S matrix

initial state $(t=-\infty)$ $|i\rangle$

final state $(t=+\infty)$ $\langle f|$

$$\langle f | i \rangle \equiv S_{fi} -$$

- scattering or S-matrix

$|S_{fi}|^2$ determines a probability of a given final state

In absence of interaction $\hat{S} = \hat{I}$

In general $S_{fi} = \delta_{fi} + i(2\pi)^4 \delta^4(P_f - P_i) T_{fi}$

T_{fi} – scattering amplitude

$\hbar = c = 1$

Normalization

$$\langle \vec{p}', i' | \vec{p}, i \rangle = (2\pi)^3 \cdot 2E \cdot \delta^3(p'-p)\,\delta_{i'i}$$

phase space: $\dfrac{d^3p}{(2\pi)^3 \cdot 2E}$

Cross sections.

$$d\sigma = \frac{dw}{j}$$

dw - probability of transition to the phase space element $d\tau$ per unit time

$$j = \frac{4I}{V}$$ - flux factor

Volume V does not enter into physical quantities

$$I = \sqrt{(p_1 p_2)^2 - m_1^2 m_2^2}$$

$I = p \cdot W$ in c.m

$$d\sigma = (2\pi)^4 \delta^4(P_f - P_i)\,|T_{fi}|^2 \frac{1}{4I} \prod_{a=1}^{n} \frac{d^3p_a}{(2\pi)^3 2E_a} \equiv$$

$$\equiv \frac{|T_{fi}|^2}{4I}\, d\tau_n$$

For two-body final state $1+2 \to 3+4$

$$d\tau_2 = \frac{1}{16\pi^2}\frac{p'}{W}\, d\Omega' \qquad \left(\begin{array}{l} p' - \text{c.m. momentum} \\ W = E_3 + E_4 \end{array}\right)$$

and

$$\frac{d\sigma}{d\Omega'} = \frac{1}{64\pi^2 W^2}\frac{p'}{p}|T|^2 \quad ; \quad (I = p \cdot W)$$

For elastic scattering $(1=3,\ 2=4)$ $p = p'$

$$\frac{d\sigma}{d\Omega} = \frac{1}{64\pi^2 W^2}|T|^2 = |f|^2;$$

$$f \equiv \frac{1}{8\pi W}\, T$$

Helicity amplitudes T_{λ_f, λ_i} for particles with spins.

$$|T_{fi}|^2 \rightarrow \frac{1}{(2S_1+1)(2S_2+1)} \sum_{\lambda_i, \lambda_f} |T_{\lambda_f, \lambda_i}|^2$$

Useful formula for phase space:

$$d\tau_n = d\tau_{n_1} \cdot d\tau_{n_2} \, \frac{dM^2_{n1}}{2\pi} \, \frac{dM^2_{n2}}{2\pi} \, d\tau_2(w^2, M^2_{n1}, M^2_{n2})$$

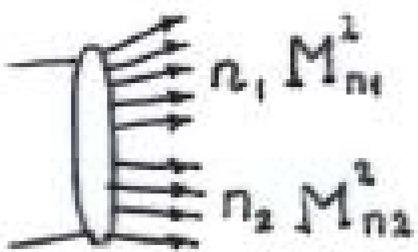

$n = n_1 + n_2$

Problem: Prove this formula

Lorentz invariance.

Amplitudes (for spinless particles) are functions of invariants.

Example:

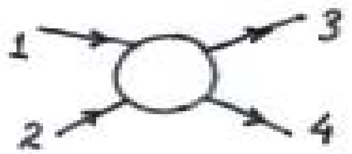

$$s = (p_1 + p_2)^2$$
$$t = (p_1 - p_3)^2$$
$$u = (p_1 - p_4)^2$$

$$s + t + u = \sum_{i=1}^{4} m_i^2 \equiv h$$

2 independent invariant variables

In the case of n-point amplitude

$3n - 10$ independent variables

In c.m. $s = W^2$; $t = m_1^2 + m_3^2 - 2(\varepsilon_1 \varepsilon_3 - pp' \cos\theta)$

$$p = \frac{\lambda^{1/2}(s, m_1^2, m_2^2)}{2\sqrt{s}} \; ; \qquad \lambda = [s - (m_i + m_k)^2][s - (m_i - m_k)^2]$$

$$p' = \frac{\lambda^{1/2}(s, m_3^2, m_4^2)}{2\sqrt{s}} \; ;$$

Crossing.

In relativistic quantum theory an outgoing particle with momentum $-p$ (negative energy) corresponds to ingoing antiparticle with momentum p.

Thus the amplitude $T(s,t,u)$ describes not only the process

$1+2 \to 3+4$ s-channel but also

$1+\bar{3} \to \bar{2}+4$ t-channel

$1+\bar{4} \to 3+\bar{2}$ u-channel

However kinematical regions of s,t,u where these processes are physical are different

For example ($m_i = m$)

s-channel: $s \geq 4m^2 \quad t \leq 0 \;, \; u \leq 0$

t-channel: $t \geq 4m^2 \quad s \leq 0 \;, \; u \leq 0$

u-channel: $u \geq 4m^2 \quad s \leq 0 \;, \; t \leq 0$

Mandelstam plane.

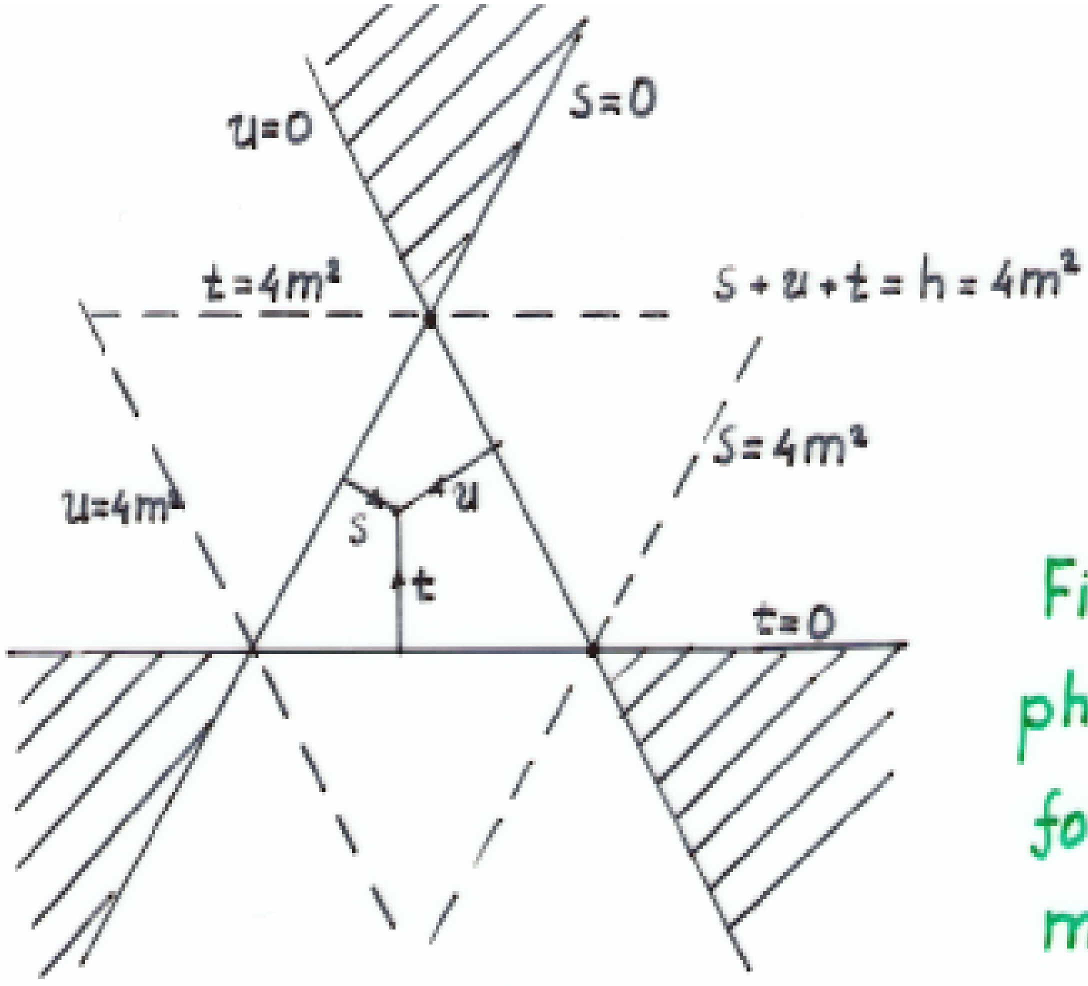

Problem:

Find borders of physical regions for arbitrary masses m_i.

Analyticity allows to connect these different kinematical regions.

Crossing symmetry.

if $2=\bar{3}$ (e.g. $\pi^+ + \pi^- \to \pi^+ + \pi^-$)

then s and t-channels are the same and

$T(s,t)$ is symmetric under $s \rightleftarrows t$

if $\bar{4}=2$ ($p\pi^0 \to p\pi^0$)

T is symmetric under $s \rightleftarrows u$

Unitarity of S-matrix.

$$\sum_f S^*_{fi} S_{fi} = 1$$

using also the superposition principle we obtain

$$S^+ S = \hat{I}$$

$$S = \hat{I} + i(2\pi)^4 \delta^4(P_f - P_i)\hat{T}.$$

$$i(T^+ - T)_{fi} = \sum_n \int d\tau_n T^+_{fn} T_{ni}$$

from t-invariance $T_{if} = T_{fi}$

$$\mathrm{Im}\, T_{fi} = \frac{1}{2} \sum_n \int d\tau_n T^*_{nf} T_{ni}$$

For forward elastic scattering $i = f$

$$\mathrm{Im}\, T(s,0) = 2I\sigma^{(tot)}_{(s)} = 2p\sqrt{s}\,\sigma^{(tot)}_{(s)}$$ optical theorem

at larges $p = \frac{\sqrt{s}}{2}$ $\quad \mathrm{Im}\, T(s,0) \simeq s\,\sigma^{(tot)}_{(s)}$

Partial wave amplitudes.

Partial wave expansion of elastic amplitude

$$f(s, \cos\theta_s) = \frac{T(s,t)}{8\pi\sqrt{s}} = \frac{1}{p}\sum_{\ell=0}^{\infty}(2\ell+1) f_\ell(s) P_\ell(\cos\theta_s)$$

$$f_\ell(s) = \frac{p}{2}\int_{-1}^{1} f(s,z) P_\ell(z)\, dz \quad ; \quad z \equiv \cos\theta_s$$

for $m_i = m$ $\quad z = 1 + \dfrac{2t}{s-4m^2}$

Unitarity for partial waves.

$$\mathrm{Im}\, f_\ell(s) = |f_\ell(s)|^2 + G_\ell^{in}(s) \;; \qquad G_\ell^{in}(s) = \sum_n |f_\ell^{in(n)}|^2 \geq 0$$

so $\quad \mathrm{Im}\, f_\ell(s) \geq |f_\ell(s)|^2 \longrightarrow \underline{|f_\ell(s)| \leq 1}$

$f_\ell(s)$ can be written in the form

$$f_\ell(s) = \frac{1}{2i}\left(e^{2i\delta_\ell(s)} - 1\right)$$

if $G_\ell^{in} = 0 \quad (s \leq s_{th}^{in}) - \delta_\ell(s)$ is real

In general $\quad \mathrm{Im}\, \delta_\ell(s) \geq 0$

$$\delta_\ell = \mathrm{Re}\,\delta_\ell + i\eta_\ell \quad ; \qquad G_\ell^{in}(s) = \frac{1}{4}\left(1 - e^{-4\eta_\ell(s)}\right)$$

So: $\quad G_\ell^{in}(s) \leq \frac{1}{4}$

Analyticity.

Unitarity shows that $\mathrm{Im}\, T \neq 0$ for $s > s_{th}$

(for 2-body final state $s_{th} = (m_3 + m_4)^2$)

$\tau_2 \sim p' \sim \sqrt{s - (m_3 + m_4)^2}$

Amplitudes have branch points singularities at corresponding thresholds.

Problem: What is the type of the singularity at - n-particle threshold ?

Cuts in the compex s-plane

5

Can be poles (in nonphys. regions) due to transition to a single-particle state

$$\frac{g^2}{s - m_N^2}$$

If we decrease s $\quad u = h - s - t$ can become larger than threshold value u_{1th}. So there is a branch point at $\bar{s}_{1th} = h - t - u_{1th}$

There are in general right-hand and left-hand cuts and poles. Between cuts an amplitude is real

$$T(s+i\varepsilon)=T^{*}(s-i\varepsilon)$$

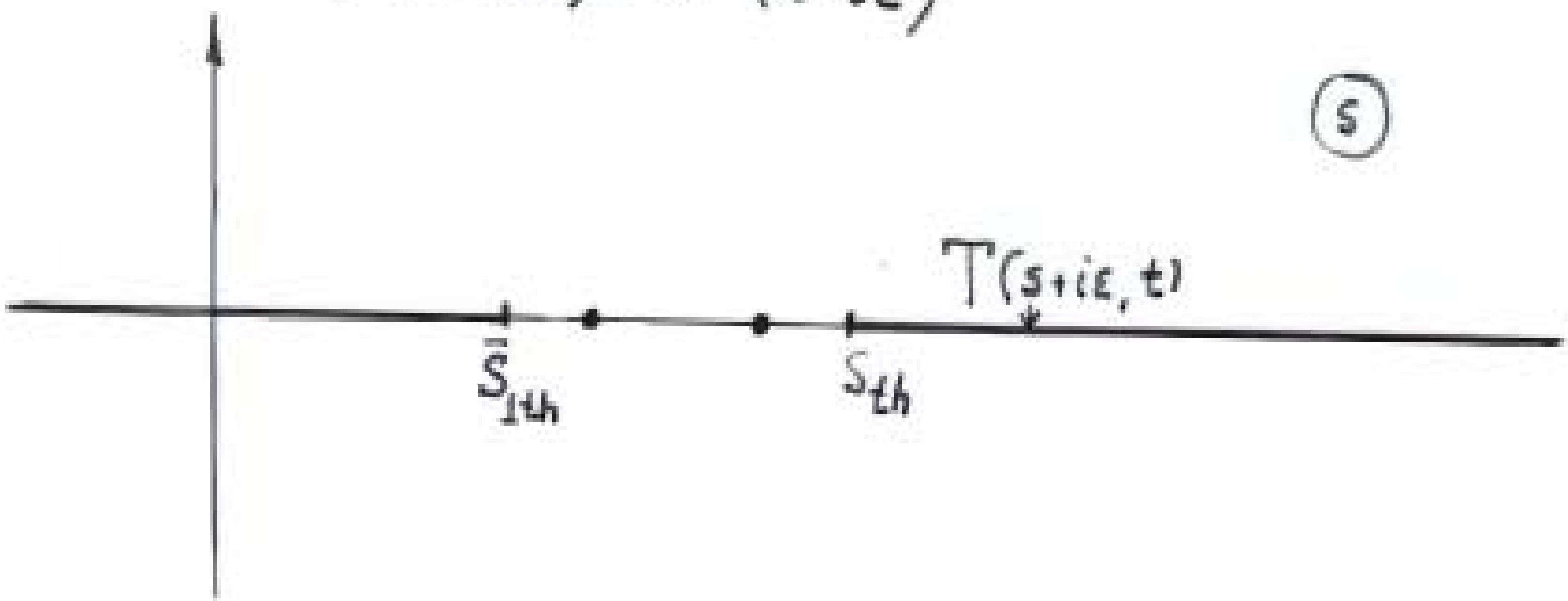

Rigorous proof of analyticity is possible from microcasuality (in some cases)

Dispersion relations.

An amplitude with analyticity properties discussed above can be written as

$$T(s,t) = \frac{1}{2\pi i}\int_C \frac{ds'\,T(s',t)}{s'-s}$$

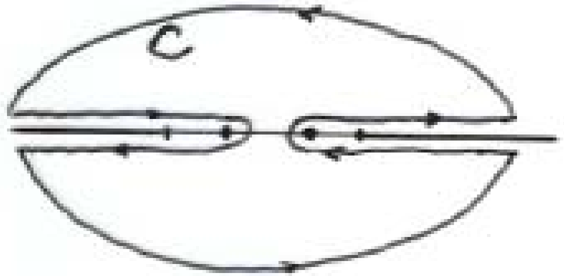

if $T(s',t) \to 0 \quad s' \to \infty$

$$T(s,t) = \frac{r_s}{s-m_s^2} + \frac{r_u}{u-m_u^2} + \frac{1}{2\pi i}\int_{s_{th}}^{\infty} \frac{ds'\,T_s(s',t)}{s'-s} + \frac{1}{2\pi i}\int_{u_{th}}^{\infty} \frac{du'\,T_u(u',t)}{u'-u}$$

where $T_s \equiv \mathrm{Disc}_s T = 2i\,\mathrm{Im}\,T(s,t)$ (in the phys. region of s-channel)

T_u is the same for u-channel

$$\frac{1}{s'-s-i\varepsilon} = P\frac{1}{s'-s} + i\pi\delta(s'-s)$$

$$\mathrm{Re}\,T(s,t) = \frac{r_s}{s-m_s^2} + \frac{r_u}{u-m_u^2} + \frac{1}{\pi}\int_{s_{1th}}^{\infty}\frac{\mathrm{Im}\,T(s',t)\,ds'}{s'-s} +$$

$$+\frac{1}{\pi}\int_{u_{1th}}^{\infty}\frac{\mathrm{Im}\,T(u',t)\,du'}{u'-u}\,;$$ Dispersion relation

Usually $T(s,t)$ does not decrease as $s \to \infty$ and it is necessary to write dispersion relations with "substractions".

If $T(s,t) \sim s^{N-1}$ as $s \to \infty$ N - substract.

$$F(s,t) = \frac{T(s,t)}{(s-s_1)(s-s_2)\dots(s-s_N)} \to 0 \qquad s \to \infty$$

Write dispersion relation for $F(s,t)$

$$\mathrm{Re}\,T(s,t) = \phi_N(s,t) + \frac{r_s \cdot (s-s_1)\dots(s-s_N)}{(s-m_s^2)(m_s^2-s_1)\dots(m_s^2-s_N)} + \frac{r_u \cdot (s-s_1)\dots(s-s_N)}{(u-m_u^2)(m_u^2-u_1)\dots(m_u^2-u_N)} +$$

$$+ \frac{(s-s_1)\dots(s-s_N)}{\pi}\left(P\int_{s_{th}}^{\infty} \frac{ds'\,\mathrm{Im}\,T(s',t)}{(s'-s)(s'-s_1)\dots(s'-s_N)} + \int_{u_{th}}^{\infty} \frac{du'\,\mathrm{Im}\,T(u',t)}{(u'-u)(u'-u_1)\dots(u'-u_N)} \right)$$

where $u_i = h - s_i - t$

$$\phi_N = T(s_1,t)\frac{(s-s_2)\ldots(s-s_N)}{(s_1-s_2)\ldots(s_1-s_N)} + T(s_2,t)\frac{(s-s_1)(s-s_3)\ldots(s-s_N)}{(s_2-s_1)(s_2-s_3)\ldots(s_2-s_N)} + \ldots$$

polinomial N-1 degree

For $t=0$ $\quad \mathrm{Im}\, T(s_i',0) = 2p(s')\sqrt{s'}\,\sigma^{(tot)}(s')$

In $\pi^- p$-inter. $\quad \mathrm{Im}\, T_s(s',0) = 2p(s')\sqrt{s'}\,\sigma^{(tot)}_{\pi^- p}(s')$

$$\mathrm{Im}\, T_u(u',0) = 2p(u')\sqrt{u'}\,\sigma^{(tot)}_{\pi^+ p}(u')$$

Gribov-Froissart representation.

$$T(s,z) = \sum_{\ell} (2\ell+1)\, T_{\ell}(s)\, P_{\ell}(z) \; ; \qquad z = \cos\theta_s$$

$$T_{\ell}(s) = \frac{1}{2}\int_{-1}^{1} dz\, T(s,z)\, P_{\ell}(z) = \underset{\substack{\parallel \\ 16\pi}}{\frac{8\pi\sqrt{s}}{p}}\, f_{\ell}(s) \qquad s \gg m_i^2$$

For fixed s the dispersion relation in t (u) has the form

$$T(s,t) = T_{pole} + \frac{1}{\pi}\int_{t_1}^{\infty} \frac{dt'\, A_t(t',s)}{t'-t} + \frac{1}{\pi}\int_{u_1}^{\infty} \frac{du'\, A_u(u',s)}{u'-u}$$

$$A_t = \frac{1}{2i}\left[T(t+i\epsilon, s) - T(t-i\epsilon, s)\right]$$

t and u are related to z

(For $m_i = m$ $\quad z = 1 + \frac{2t}{s-4m^2}$; $\quad z = -1 - \frac{2u}{s-4m^2}$)

So the dispersion relation can be written as

$$T(s,z) = T_{pole} + \frac{1}{\pi}\int_{z_{1t}}^{\infty} \frac{dz' A_t(z',s)}{z'-z} + \frac{1}{\pi}\int_{z_{1u}}^{\infty} \frac{dz' A_u(z',s)}{z'+z}$$

(For equal mass case $z_{1t} = z_{1u} = 1 + \frac{8m^2}{s-4m^2}$)

Using this in the eq. for $T_\ell(s)$ and applying the Neumann's formula

$$\frac{1}{2}\int_{-1}^{1} dz \frac{P_\ell(z)}{z'-z} = Q_\ell(z')$$ ← Legendre functions of the second kind

we obtain

$$T_\ell(s) = T_\ell^{pole} + \frac{1}{\pi}\int_{z_{1t}}^{\infty} dz' A_t(z';s)\, Q_\ell(z') - \frac{1}{\pi}\int_{z_{1u}}^{\infty} dz' A_u(z';s) \times$$
$$\times Q_\ell(-z') =$$

$$Q_\ell(-z) = -(-1)^\ell Q_\ell(z)$$ Gribov-Froissart repr.

$$= T_\ell^{pole} + \frac{1}{\pi}\int_{z_{1t}}^{\infty} dz' A_t(z';s)\, Q_\ell(z') + \frac{(-1)^\ell}{\pi}\int_{z_{1u}}^{\infty} dz' A_u(z';s)\, Q_\ell(z')$$

If N-substraction this eq. is true for $\ell \geq N$.

Note that $Q_\ell(z') \sim \frac{1}{(z')^{\ell+1}}$ for large z' and for $A_i \sim (z')^{N-1}$ integrals converge well for $\ell \geq N$.

G-F representation is useful for a study of analyticity of T_ℓ and analytic continuation to complex values of ℓ.

Froissart theorem.

We will find a bound for a possible increase of scattering amplitude as $s \to \infty$

$$T(s,t) = \sum_{\ell} (2\ell+1)\, T_\ell(s)\, P_\ell(z)$$

in the physical region $-1 \leq z \leq 1$ $\quad |P_\ell(z)| \leq 1$

From unitarity $|T_\ell(s)| = 16\pi |f_\ell(s)| \leq 16\pi$

How many partial waves can be important as $s \to \infty$

From G-F representation

$$Q_\ell(z) \sim \ell^{-\frac{1}{2}} \exp\left[-(\ell+\tfrac{1}{2}) \ln\{z + \sqrt{z^2-1}\}\right] \quad ; \quad \ell \to \infty$$

So the min. value of $z' > 1 \to z_{1t}$ gives a dominant contribution. $\quad z_{1t} = 1 + \frac{2t_{1th}}{s}$

$$\ln\left\{ z_{1t} + \sqrt{z_{1t}^2 - 1} \right\} \simeq \ln\left(1 + \sqrt{\frac{4t_{1th}}{s}}\right) = \sqrt{\frac{4t_{1th}}{s}} = \frac{4m_\pi}{\sqrt{s}}$$

So for $\ell \to \infty$

$$T_\ell(s) \sim s^N \exp\left(-\ell \frac{4m_\pi}{\sqrt{s}}\right) = \exp\left(-\ell \frac{4m_\pi}{\sqrt{s}} + N \ln\frac{s}{s_0}\right)$$

Thus $T_\ell(s) \ll 1$ for $\ell > \frac{\sqrt{s}\,N}{4m_\pi} \ln s \equiv L_{max}$

(It is possible to prove that $N \leq 2$)

$$|T(s,t)| \leq 16\pi \sum_{\ell}^{L_{max}} (2\ell+1) \simeq L_{max}^2 \cdot 16\pi = s \frac{\pi}{m_\pi^2} N^2 \ln^2\frac{s}{s_0}$$

$$\mathrm{Im}\, T(s,0) \leq s \frac{\pi}{m_\pi^2} N^2 \ln^2\frac{s}{s_0}$$

$$\sigma^{(tot)}(s) \leq \frac{\pi N^2}{m_\pi^2} \ln^2\frac{s}{s_0}$$

Froissart theorem

Radius of interaction can not increase faster with energy than $\ln s$.

$$\frac{d\sigma^{(el)}}{dt} = \frac{\left(\sigma^{(tot)}(s)\right)^2}{16\pi}(1+\alpha^2)\, e^{B(s)t} \qquad (\text{small } t)$$

$$\alpha = \frac{\mathrm{Re}\, T(s,0)}{\mathrm{Im}\, T(s,0)}\,; \qquad B(s) = \frac{d}{dt}\left(\ln \frac{d\sigma^{(el)}}{dt}\right)\Bigg|_{t=0} \leq \frac{C}{4m_\pi^2}\ln^2\frac{s}{s_0}$$

Slope of the diffraction cone.

Problem: Generalize Froissart theorem to inelastic processes.

Pomeranchuk theorem.

$a + b \to a + b$ s-channel

$\bar{a} + b \to \bar{a} + b$ u-channel

$$\sigma_{ab}^{(tot)}(s) - \sigma_{\bar{a}b}^{(tot)}(s) \to 0 \qquad s \to \infty$$

if $\dfrac{\mathrm{Re}\,T(s,0)}{\mathrm{Im}\,T(s,0)} \to 0$ $\quad (\mathrm{Re}\,T^{(-)}(s,0) / \ln(s)\,\mathrm{Im}\,T^{(-)}(s,0) \to 0)$

Consider $T^{(-)}(s,t) = T_{ab}(s,t) - T_{\bar{a}b}(s,t)$

$$T^{(-)} \to -T^{(-)} \qquad s \rightleftarrows u$$

$\nu = \dfrac{s-u}{4m_b}$ - Energy in the lab.

Dispersion relation for $T^{(-)}$

$$\mathrm{Re}\,T^{(-)}(\nu,t) = T^{(-)}_{pole} + \frac{\nu}{\pi}\int_{\nu_0}^{\infty} d\nu' \frac{\mathrm{Im}\,T^{(-)}(\nu',t)}{\nu'^2-\nu^2}$$

valid if $\frac{T^{(-)}(\nu')}{\nu'} \to 0$ $\nu' \to \infty$

$$\mathrm{Im}\,T^{(-)}(\nu,0) = 2p\sqrt{s}\left(\sigma^{tot}_{ab} - \sigma^{(tot)}_{\bar{a}b}\right)$$

Assume that $\Delta\sigma \neq 0$ as $\nu \to \infty$

'Subtraction' is necessary

$$\mathrm{Re}\,T^{(-)}(\nu,0) = T^{(-)}(\nu_1)\frac{\nu}{\nu_1} + \widetilde{T}^{(-)}_{pole} + \frac{\nu(\nu^2-\nu_1^2)}{\pi}\int_{\nu_0}^{\infty}\frac{d\nu'\,\mathrm{Im}\,T^{(-)}(\nu',0)}{(\nu'^2-\nu^2)(\nu'^2-\nu_1^2)}$$

For large ν (24)

$$\frac{\mathrm{Re}\,T^{(-)}(\nu,0)}{\nu} = \frac{\mathrm{Re}\,T^{(-)}(\nu_1)}{\nu_1} + \frac{1}{\pi}\int_{\nu_0}^{\bar{\nu}} \frac{d\nu'\, m_b \sqrt{\nu'^2 - m_b^2}}{(\nu'^2 - \nu_1^2)}\, \Delta\sigma(\nu') +$$

$\bar{\nu} \gg m_i \quad$ for $\nu > \bar{\nu} \quad \Delta\sigma = C$

$$+ \frac{\nu^2}{\pi}\int_{\bar{\nu}}^{\infty} \frac{d\nu'\, \nu' m_b\, C}{(\nu'^2 - \nu^2)\,\nu'^2} \approx C_1 + \frac{C m_b}{\pi} \ln\frac{\nu}{\nu_1}$$

But this contradicts to the assumption that $\mathrm{Re}\,T^{(-)}(\nu,0)/\mathrm{Im}\,T^{(-)}(\nu,0) \to 0 \quad (< \mathrm{Const}\,\ln s)$

Pomeranchuk assumed also that the radius of interaction $R \to Const$ as $s \to \infty$

But it can increase with energy.

It is possible to build models with $\Delta\sigma$ not decreasing as $s \to \infty$.

Extensions of Pomeranchuk theorem

$$\frac{(\sigma_{ab} - \sigma_{\bar{a}b})}{(\sigma_{ab} + \sigma_{\bar{a}b})} \to 0 \qquad s \to \infty$$

can be proved without extra assumptions

$$\frac{d\sigma_s}{dt} = \frac{d\sigma_u}{dt} \quad ; \; t\text{-fixed} \quad s \to \infty$$

For example: $\frac{d\sigma}{dt}(pp \to pp) \simeq \frac{d\sigma}{dt}(\bar{p}p \to \bar{p}p)$

$$\frac{1}{2}\frac{d\sigma}{dt}(\pi^- p \to p\pi^-) \simeq \frac{d\sigma}{dt}(\bar{p}p \to \pi^+\pi^-)$$

- There are no experimental indications on possible violations of the Pomeranchuk theorem at present

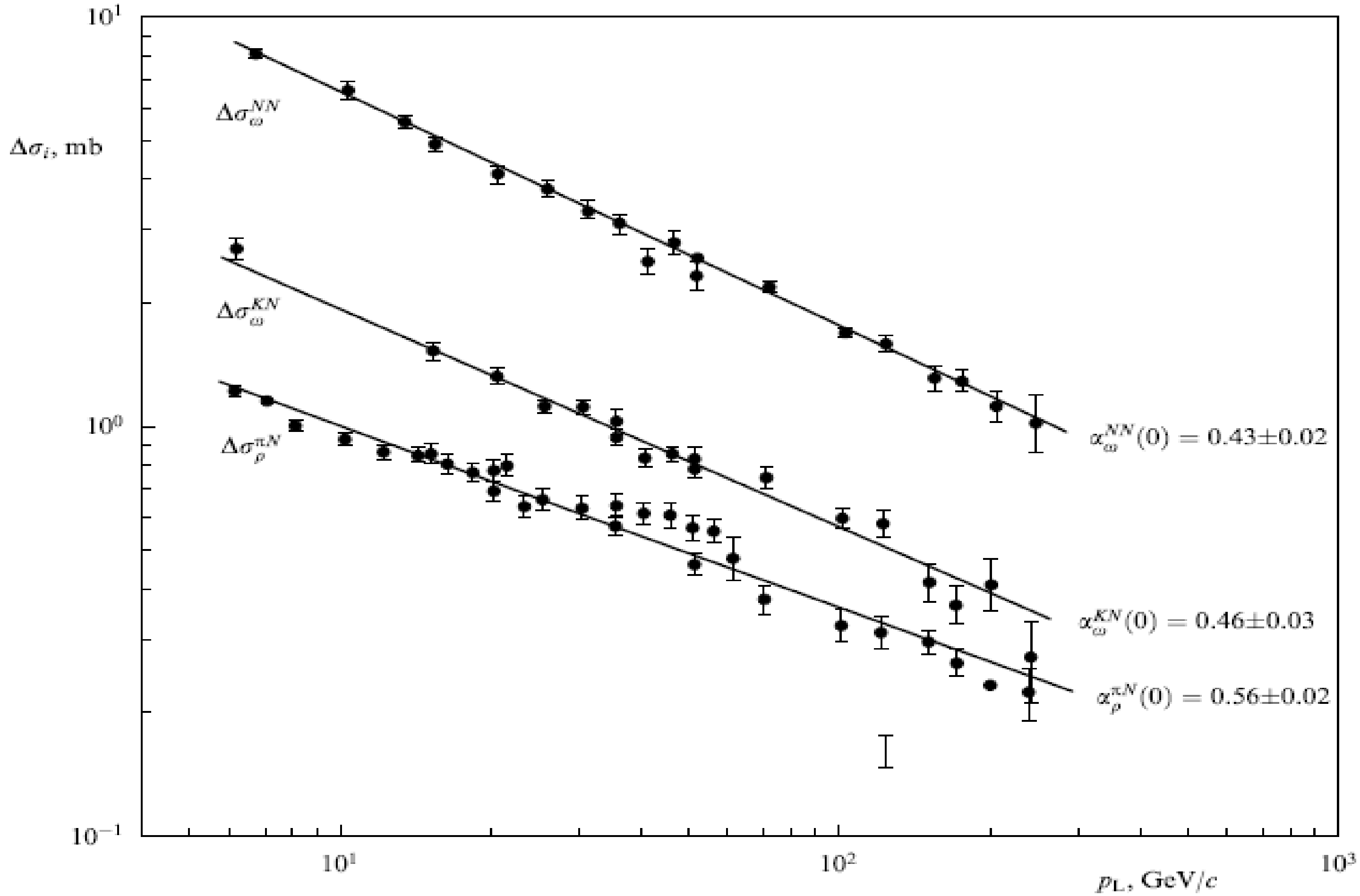

Lecture 2
Regge poles

The reggeon concept.

t-channel exchange picture

Exchange by a particle with spin J in the t-channel

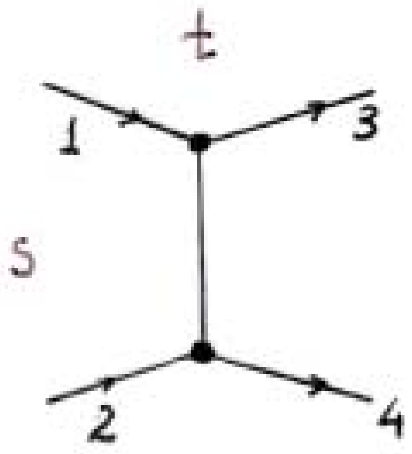

$$T(s,t) = \frac{g_{13}\, g_{24}}{t - m_J^2}\, s^J$$

$$s \gg m_i^2$$

Problem: Prove s^J behaviour

For large J it increases fast with s and for $J>1$ violates Froissart bound.

In fact it violates unitarity

$$f(s,b)=\int \frac{T(s,\vec{q}^{\,2})}{8\pi s}\, e^{-i\vec{q}\vec{b}}\, d^2q \quad ; \quad t=-\vec{q}^{\,2}$$

$$b=(\ell+\tfrac{1}{2})/p$$

$$f(s,b)\sim s^{J-1} \quad \text{for } s\to\infty \quad \text{violates } |f(s,b)|\leq 1$$

There are many particles (resonances) with $J>1$.

What is the solution?

Regge pole gives a generalization of a particle exchange in the t-channel and resolve this problem. It corresponds to an exchange in the t-channel by a state of noninteger spin $\alpha(t)$ (reggeon trajectory), which coincides with particles of spin J for $t = m_J^2$

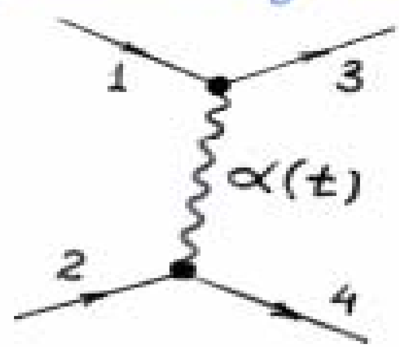

$$T(s,t) = g_{13}(t)\, g_{24}(t)\, \eta_\sigma(\alpha(t)) \left(\frac{s}{s_0}\right)^{\alpha(t)}$$

where $g_{ik}(t)$ - residues

$$\eta_\sigma(\alpha(t)) = -\frac{1 + \sigma e^{-i\pi\alpha(t)}}{\sin \pi\alpha(t)}$$

signature factor

$$\sigma = \begin{array}{ll} +1 & J\text{ - even} \\ -1 & J\text{ - odd} \end{array}$$

For $\alpha(t) \to J$, $t \to m_J^2$: $\eta_\sigma(\alpha(t)) \to \dfrac{2(-1)^{J+1}}{\pi\alpha'(t-m_J^2)}$

if $Im\,\alpha(m_J^2) \neq 0$ $(t > t_1)$

$$\eta_\sigma(\alpha(t)) \to \frac{2(-1)^{J+1}}{\pi\alpha'\left[t - m_J^2 + i\,\dfrac{Im\,\alpha(m_J^2)}{\alpha'(m_J^2)}\right]}$$

Corresponds to exchange by a resonance with $\Gamma_J = \dfrac{Im\,\alpha(m_J^2)}{m_J \cdot \alpha'(m_J^2)}$

Thus reggezation of particle exchanges will lead to amplitudes, which satisfy unitarity if $\alpha_i(t) \leq 1$ for $t \leq 0$.

Complex angular momentum method.

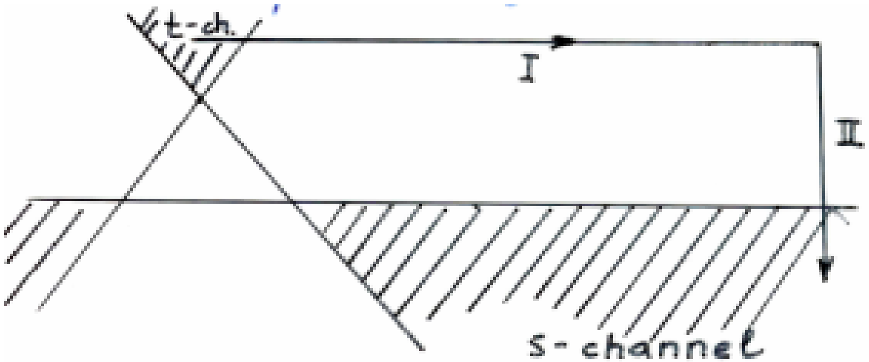

I step: From phys. region of t-channel $t > t_1$, $z_t \leq 1$ to unphys. region $t > t_1$, $s \gg m_i^2$ ($z_t \gg 1$)

II step: to phys. region of s-channel $s \gg m_i^2$, $t \leq 0$

In the physical region of the t-channel

$$T(s,t) = \sum_{\ell=0}^{\infty} (2\ell+1)\, T_\ell(t)\, P_\ell(z_t)$$

$$\left(z_t = 1 + \frac{2s}{t-4m^2} \quad \text{for } m_i = m \right)$$

This expression can not be continued to the region $z_t > 1$ ($P_\ell(z_t)$ exponentially increase in this region)

Use Sommerfeld-Watson method of complex angular momenta.

Let us obtain analytic continuation to complex values of ℓ of $T_\ell(t)$

G-F representation for $T_\ell(t)$

$$T_\ell(t) = \frac{1}{\pi}\int_{z_{1s}}^{\infty} Q_\ell(z)\,A_s(z,t)\,dz + \frac{(-1)^\ell}{\pi}\int_{z_{2u}}^{\infty} Q_\ell(z)\,A_u(z,t)\,dz$$

This is valid for $\mathrm{Re}\,j > \gamma$ if $A_i(z,t) \sim z^\gamma$ at large z

$$Q_j(z) \simeq \frac{\pi}{C(j)}\,\frac{1}{(2z)^{j+1}} \quad ; \quad C(j) = \pi^{\frac{1}{2}}\,\Gamma(j+\tfrac{3}{2})/\Gamma(j+1)$$

In order to have a unique analytic continuation from integer ℓ to complex values it is necessary to satisfy $T(j,t) < \exp(\pi j)$ as $j \to \infty$

$(-1)^{\ell} = \exp(-i\pi j)$ increases as $\exp(\pi j)$ as $Re\,j = c$ $Im\,j \to \infty$

So we introduce two functions

$$T^{\sigma}(j,t) = T^{1}(j,t) + \sigma T^{2}(j,t)$$

$\sigma = \pm$

$$T^{i}(j,t) = \frac{1}{\pi}\int_{z_i} Q_j(z) A_i(z,t)\,dz$$

$T^{+}(j,t) = T_{\ell}(t)$ for $j=\ell$ even

$T^{-}(j,t) = T_{\ell}(t)$ $j=\ell$ odd

σ- signature is closely related with $s \rightleftarrows u$ crossing properties of amplitudes.

Unitarity condition in the t-channel can be analytically continued to complex j.

Two particle unitarity ($4m^2 < t < 9m^2$)

$$\operatorname{Im} T_\ell(t) = \rho_2(t)\,|T_\ell(t)|^2 \quad ; \quad \rho_2(t) = \frac{1}{16\pi}\left(\frac{t-4m^2}{t}\right)^{1/2}$$

$$\downarrow$$

$$T_\ell(t_+) - T_\ell(t_-) = 2i\rho_2(t_+)\,T_\ell(t_+)\,T_\ell(t_-) ; \qquad T_\ell(t^*) = T_\ell^*(t)$$

$$t_\pm = t \pm i\varepsilon\,, \quad \varepsilon > 0\,, \quad \varepsilon \to 0$$

$$\downarrow$$

$$T^\sigma(j,t_+) - T^\sigma(j,t_-) = 2i\rho_2(t_+)\,T^\sigma(j,t_+)\,T^\sigma(j,t_-)$$

$$T(s,t) = \sum_{\sigma} \sum_{\ell=0}^{\infty} (2\ell+1) \frac{1}{2} \left(P_\ell(z_t) + \sigma P_\ell(-z_t) \right) T_\ell(t)$$

for large s $\quad z_t \cong \dfrac{s}{2 p_{13}(t) p_{24}(t)} \gg 1$

$$T(s,t) = \sum_{\ell=0}^{k-1} (2\ell+1) P_\ell(z_t) T_\ell(t) + \sum_{\sigma} \frac{1}{4i} \int_C \frac{2j+1}{\sin \pi j} \left(P_j(-z_t) + \sigma P_j(z_t) \right) \times$$
$$\times T^\sigma(j,t)\, dj$$

$k-1 < \gamma$
$k > \gamma$

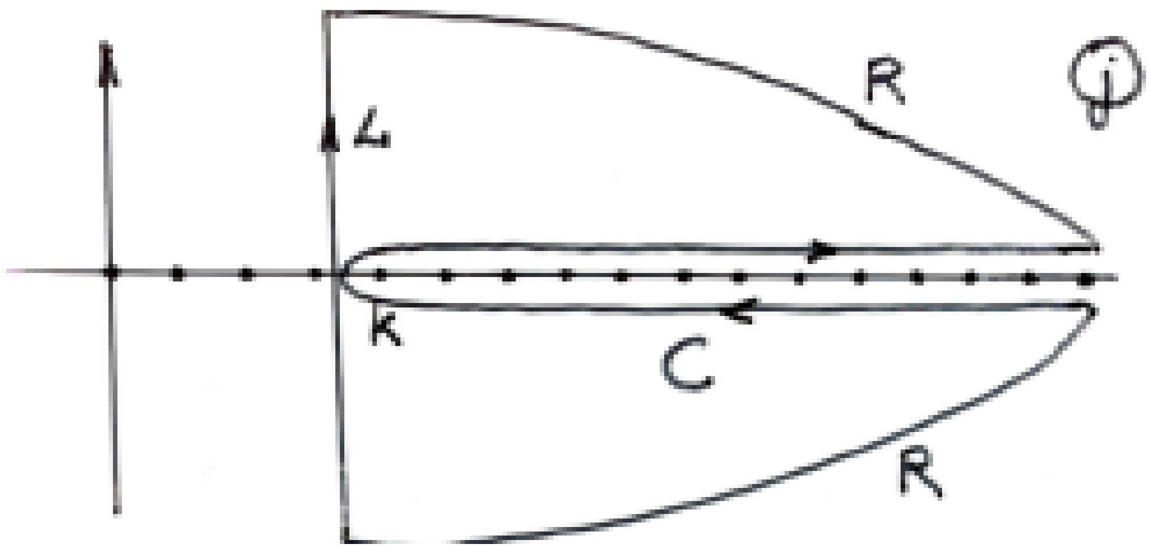

$P_j(z)$ are analytic functions of j

For $j \to \ell$ $\quad \dfrac{1}{\sin(\pi j)} \to \dfrac{(-1)^{\ell}}{\pi(j-\ell)}$

$$\int_C = \int_L$$

Integral over line L is absolutely convergent for any complex values of z. It gives an analytic continuation of an amplitude to the region of large z

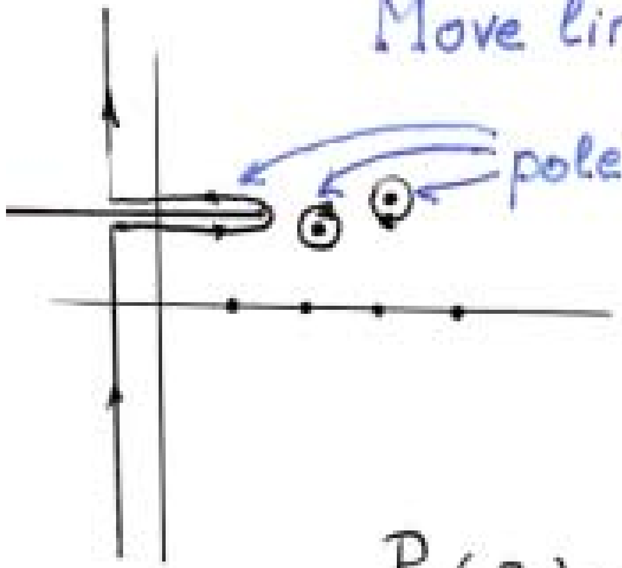

Move line L to the left.

poles and branch points of $T^{\sigma}(j,t)$

(If $T^{\sigma}(l,t)=T_l(t)$ the sum in expresion for $T(s,t)$ cancels)

$$P_j(-z_t)=\exp(-i\pi j)P_j(z_t)$$

for large z_t $\quad \pi(j+\frac{1}{2})P_j(z_t)\cong C(j)(2z_t)^j=C(j)\frac{s^j}{(p_{12}p_{34})^j}$

$$T(s,t)=\sum_{\sigma}\int_{L'}\pi\sigma(j+\tfrac{1}{2})T^{\sigma}(j,t)\eta_{\sigma}(j)P_j(z_t)\frac{dj}{2\pi i}=$$

$$(*)\quad T(s,t) = \int \Phi(j,t)\, s^j \frac{dj}{2\pi i}$$ Mellin transform

$$\Phi(j,t) = \sum_\sigma \eta_\sigma(j)\, \phi_\sigma(j,t)\ ; \qquad \phi_\sigma(j,t) = \frac{C(j)\,\sigma\, T^\sigma(j,t)}{(p_{13}(t)\cdot p_{24})^j}$$

$$\eta_\sigma(j) = -(1+\sigma \exp(-i\pi j))/\sin(\pi j)$$

Amplitudes $\phi_\sigma(j,t)$ do not contain kinematic singularities as $p_{ik}(t) \to 0$.

The expression can be continued to the physical region of s-channel ($t \leq 0$).

Contribution over vertical line can be made arbitrary small as $s \to \infty$ ($\sim s^{-\delta}$ $\delta > 0$) and we have finally

$$T(s,t) = \sum_i \int_{C_i} \phi_\sigma(j,t)\, \eta_\sigma(j)\, s^j \frac{dj}{2\pi i}$$

C_i contours around singularities of $\phi_\sigma(j,t)$ in the complex j-plane.

What are these singularities?

Properties of reggeons.

In nonrelativistic theory the only singularities in j-plane are simple poles (Regge 1959) → Regge poles.

From two-particle unitarity one can prove (Gribov 1961)

$$T(j,t_+) = \frac{T(j,t_-)}{1 - 2i\rho(t_+)T(j,t_-)}$$

that possible singularities are moving poles at $j=\alpha_a(t)$. In this case

$$\varphi_\sigma(j,t) = \sum_a \frac{b_a(t)}{j-\alpha_a(t)}$$

$$T(s,t) = \sum_{\sigma,a} \eta_\sigma(\alpha_a(t))\,\tilde{b}_a(t)\left(\frac{s}{s_0}\right)^{\alpha_a(t)}$$

$$\tilde{b}_a(t) \equiv b_a(t)(s_0)^{\alpha_a(t)}$$

- It follows from t-channel unitarity that $T(j,t)$ can not have t-independent poles (fixed poles).
- Trajectory $\alpha(t)$ must have a branch point at $t=4m^2$ ($\alpha_a(t_+) \neq \alpha_a(t_-)$ for $t>4m^2$
- Below $t=4m^2$ $\alpha_a(t)$ is a real function of t. The residues are real functions of t.

- If there are many two-particle channels then from t-channel unitarity follows factorization of residues

$$b_a(t) = g_{13}(t)\, g_{24}(t)$$

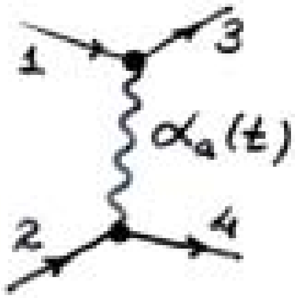

For particles with spins factorization holds for helicities $g_{ik} \to g_{\lambda_i \lambda_k}$

- Regge poles (as well as usual particles) have definite values of conserved quantum numbers: Parity P, isospin, G-parity (for light bosons), strangeness S, baryon number B,..

Bosonic and fermionic Regge poles.

Regge pole establish an important relation between high-energy behaviour of binary reactions and spectrum of particles and resonances.

When $\mathrm{Re}\,\alpha(t) = n$ (n-even for $\sigma = +$, n-odd for $\sigma = -$) and if $\mathrm{Im}\,\alpha(t) \ll 1$ the Regge pole exchange amplitude corresponds to exchange by a particle (resonance) with the same quantum numbers.

For fermionic trajectories $\sigma = (-1)^{J-\frac{1}{2}}$.

The well known bosonic trajectories:

ρ	$I=1,\ \sigma=-,\ P=-,\ G=+$		
ω	$I=0,\ \sigma=-,\ P=-,\ G=-$	$\sigma P=+1$	
f	$I=0,\ \sigma=+,\ P=+,\ G=+$	$\sigma G(-1)^I=+1$	
A_2	$I=1,\ \sigma=+,\ P=+,\ G=-$	$\alpha_i(0)\simeq 0.5$	
K^*	$I=\frac{1}{2},\ \sigma=-,\ P=-$	$\alpha_i(0)\simeq 0.3$	
K^{**}	$I=\frac{1}{2},\ \sigma=+,\ P=+$		
φ	$I=0,\ \sigma=-,\ P=-$	$\alpha_i(0)\simeq 0.1$	
f'	$I=0,\ \sigma=+,\ P=+$		
π	$I=1,\ \sigma=+,\ P=-,\ G=-$	$\sigma P=-1$	$\alpha_\pi(0)\simeq -0.02$
η	$I=0,\ \sigma=+,\ P=-,\ G=+$	$\sigma G(-1)^I=1$	$\alpha_\eta(0)\simeq -0.3$

Spectrum of mesons.

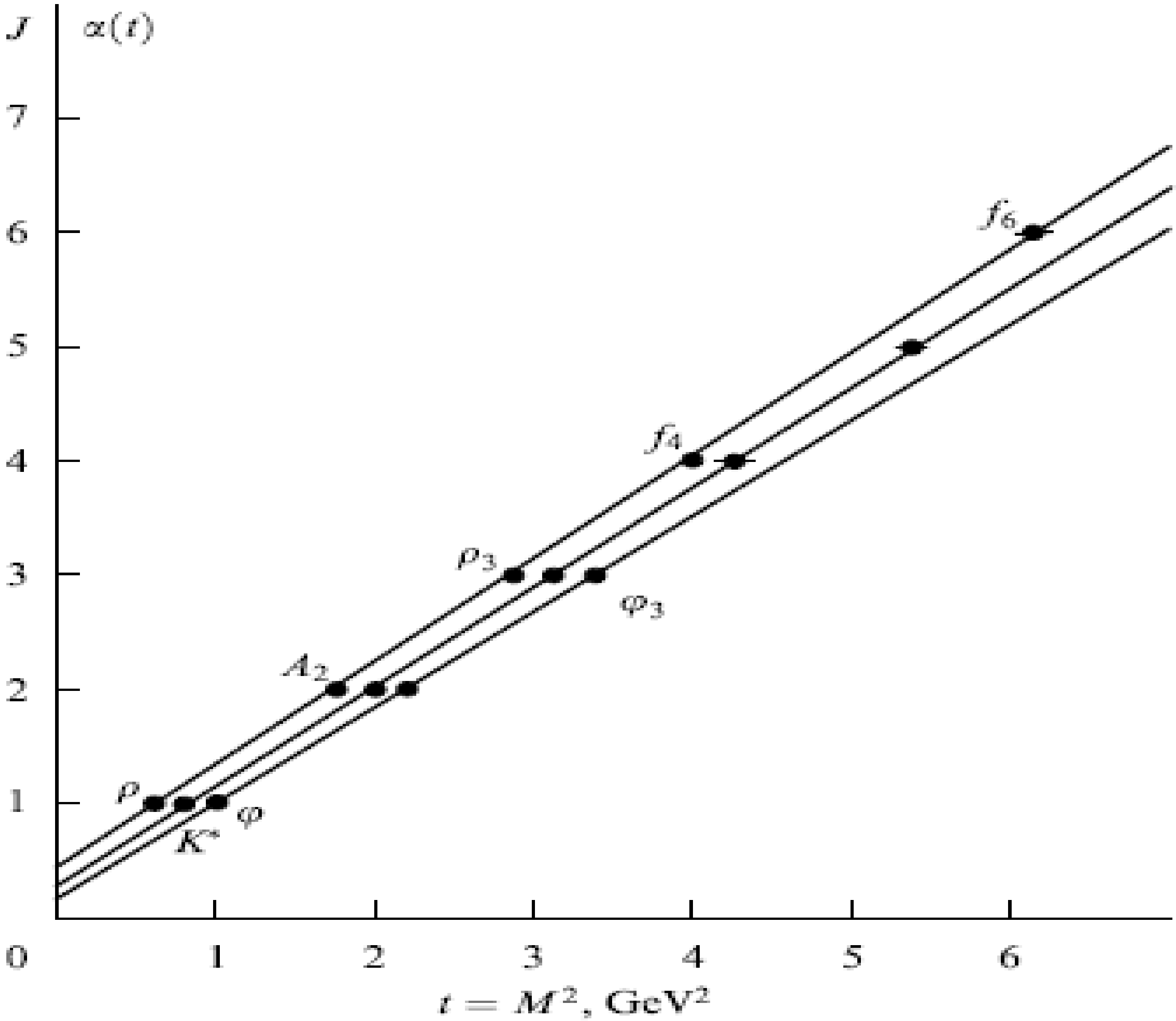

Linearity of the effective ρ-trajectory up to t ≈ -2 GeV^2 from $\pi^- p \rightarrow \pi^0 n$.

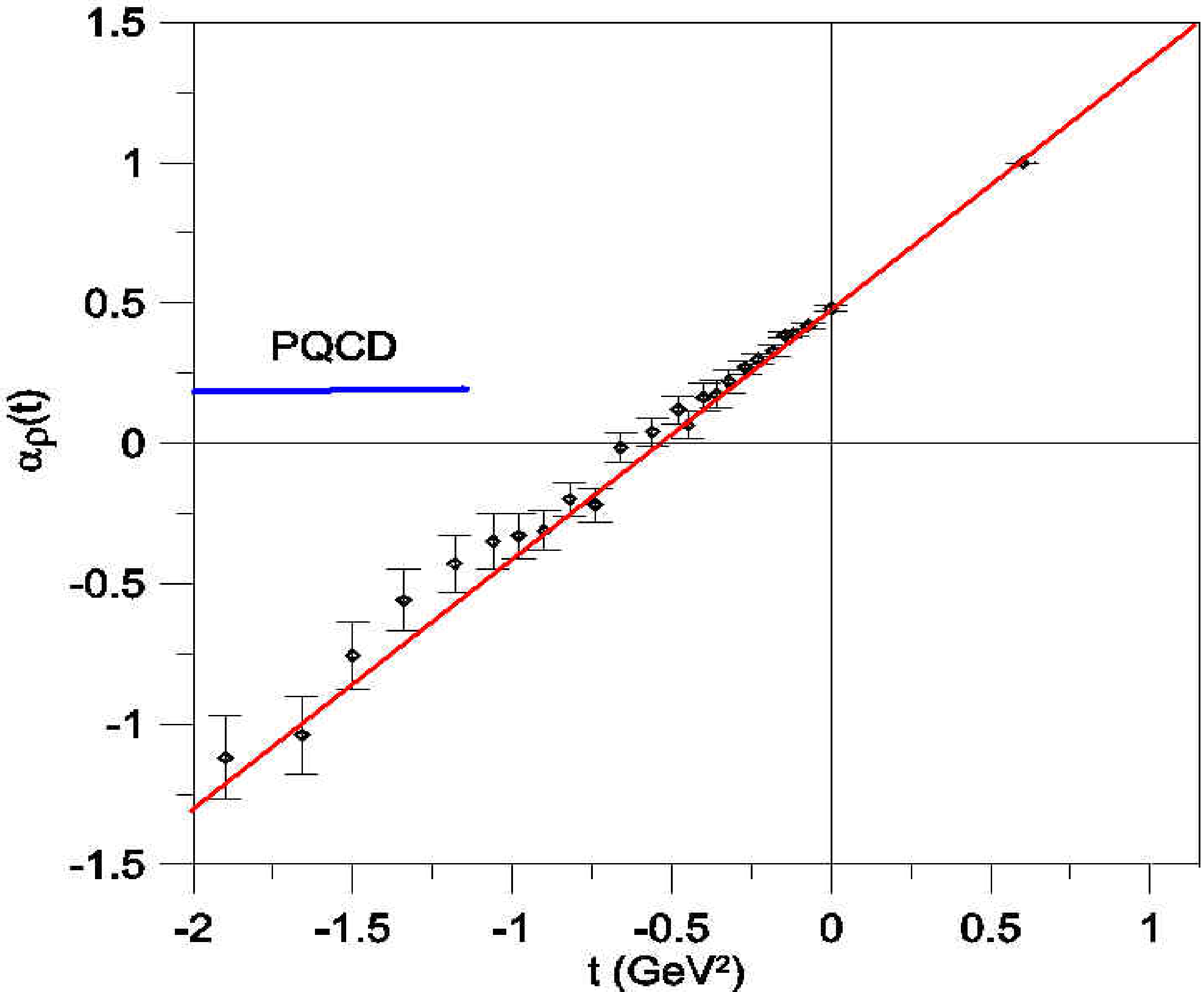

Spectrum of mesons

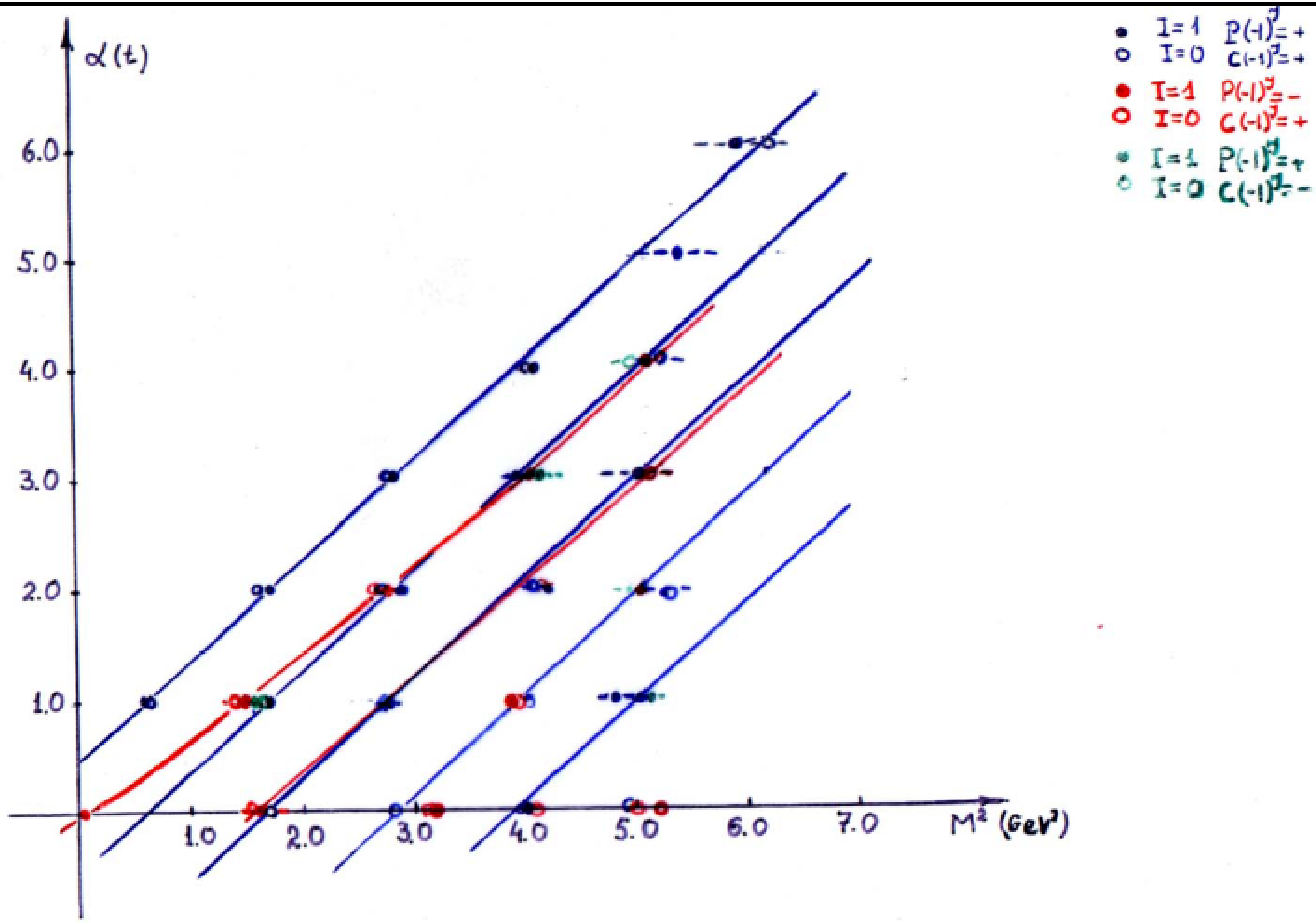

Spectrum of strange mesons.

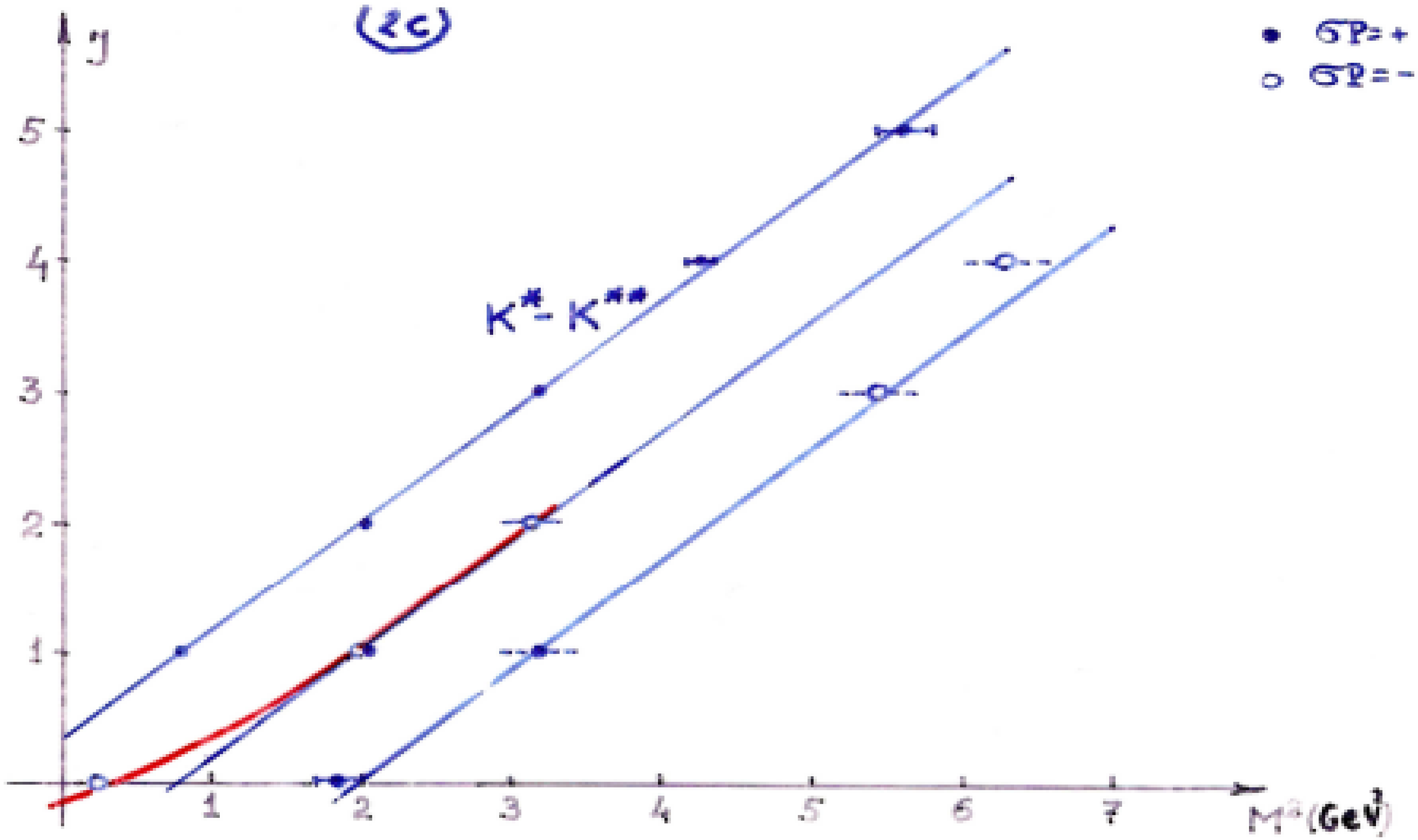

Spectrum of baryons.

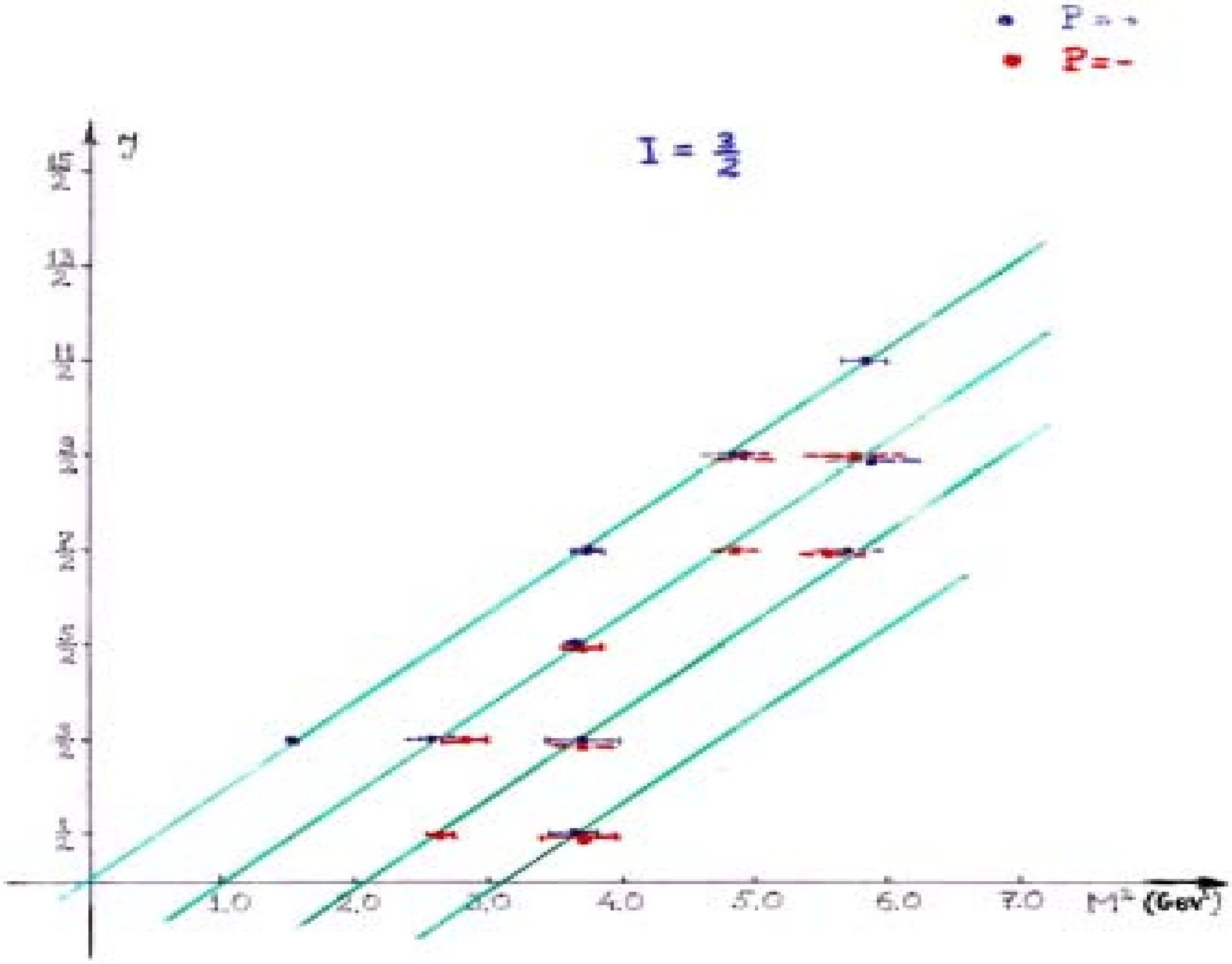

Spectrum of hadrons

Linear Regge trajectories with daughters shifted by integers.

$$\alpha(t) = \alpha(0) + \alpha' t$$

Isospin and exchange degeneracy.

Parity doublets on daughter trajectories.

These properties of spectrum naturally appear in the string picture of hadrons.

Pomeranchuk pole (pomeron).

In Regge pole model $\sigma^{\mathrm{tot}}(s) = \sum_k b_k(0)(s)^{\alpha_k(0)-1}$.

and poles discussed above with $\alpha_i(0) < 1$ give decreasing contributions to total cross sections. Experimentally

total cross sections increase as energy increases. To describe this behavior a

Special Regge pole – pomeron was introduced.

For $\alpha_P(0) = 1$ $\eta_P(0) = i$, i.e. P-contribution to

amplitude is purely imaginary.

Pomeron.

Pomeron has vacuum quantum numbers I=0, C=+, P=+, σ=+ and sometimes is called “vacuum” pole.

It automatically satisfies Pomeranchuk theorem.

For $\alpha_P(0) = 1$ $\quad \sigma^{(tot)} \to Const$ as $s \to \infty$

Both experiment and theory indicate that pomeron is “supercritical” : $\alpha_P(0) > 1$. Problems with unitarity are solved by Regge cuts (see below).

Regge poles in QCD.

Large distance phenomenon. Nonperturbative methods should be used.

- 1/N – expansion in QCD. H.t`Hooft, G.Veneziano

Expansion of amplitudes in terms of the small parameter 1/N, where $N=N_c \approx N_f$.

Diagrams are classified according to their topology.

The first term – planar diagrams.

Planar diagrams.

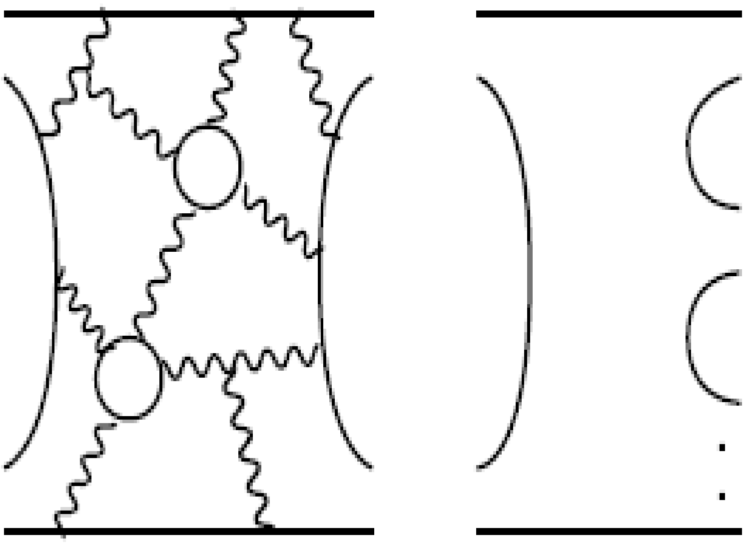

a) b)

Exchange by valence quarks in the t-channel.

At large energies they correspond to ρ,ω,f,.. exchanges.

Contributions to total cross sections decrease as $s^{(\alpha_R(0)-1)} \approx 1/\sqrt{s}$

Many consequences of planarity for reggeons.

In particular isospin and exchange degeneracy

Example of ππ-scattering. No planar diagrams

For π+π+ interaction and

$$\sigma^{(pl)}(\pi^+\pi^+) = \mathrm{Im}(T_f(s,0) - T_\rho(s,0)) = 0$$

From this follows an equality of intercepts

$$\alpha_f(0) = \alpha_\rho(0)$$

Using Kπ, KK-scattering and nonzero t prove:

$$\alpha_\rho(t) = \alpha_f(t) = \alpha_\omega(t) = \alpha_{A_2}(t)$$

$$\alpha_{K^*}(t) = \alpha_{K^{**}}(t) \qquad \alpha_\varphi(t) = \alpha_{f'}(t)$$

These results agree with experiment

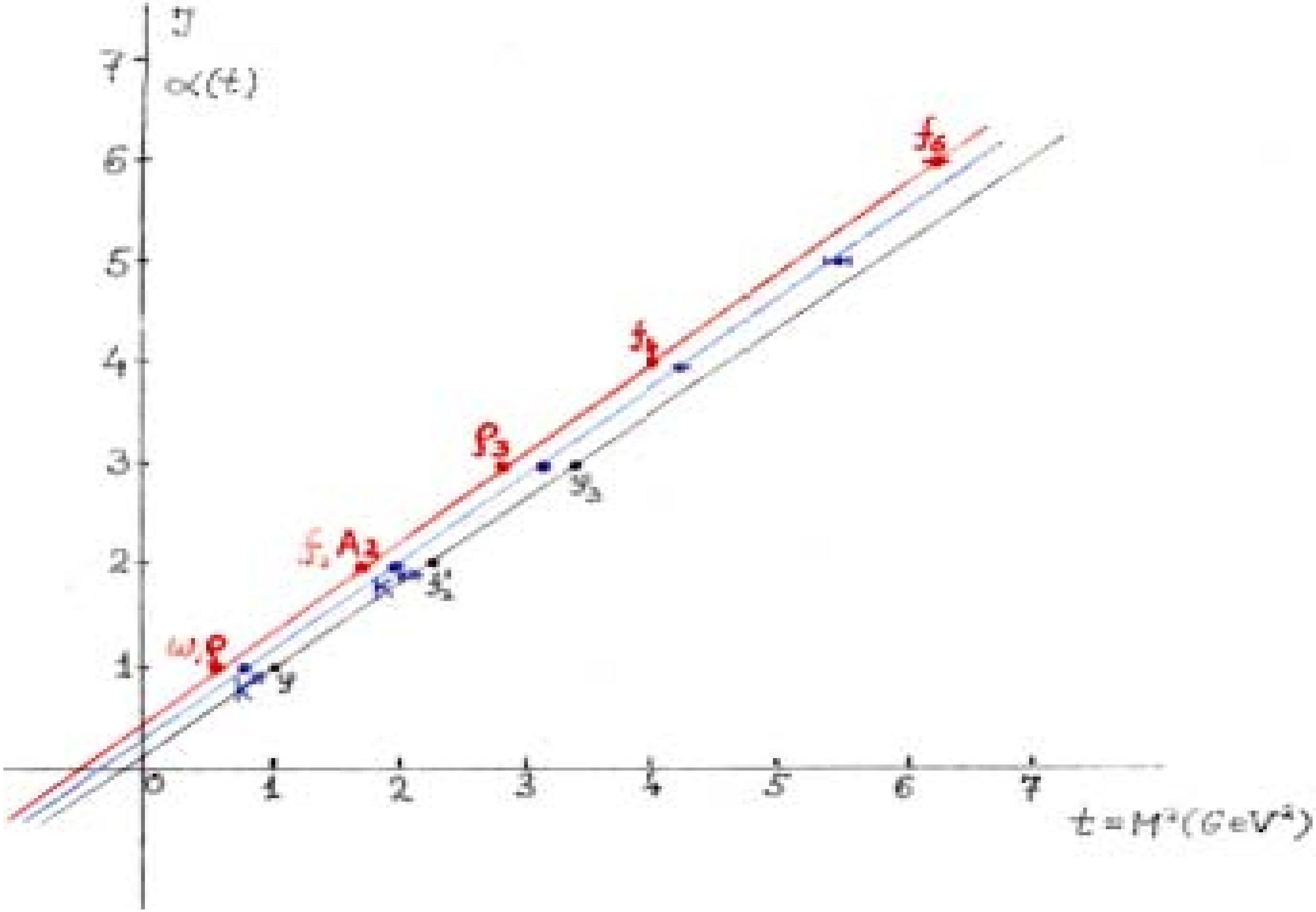

All vertices are expressed in terms of a single function g(t). From planarity of diagrams for reggeons and space-time picture of interaction: annihilation of valence quarks of colliding hadrons, formation and breaking of a color tube, it is possible to obtain many predictions for differences of total cross sections, masses of hadrons and widths of resonances in a good agreement with experiment.

1/N-expansion works well.

Calculation of Regge trajectories in QCD.

Difficult nonperturbative problem.

The method of Wilson loop path integral was used for calculation of $q\bar{q}$ and gg-states.

A.Yu.Dubin, A.K., Yu.A.Simonov

The main assumption is the minimal area low for Wilson loop at large distances

$$< W >= Z \exp(-\sigma S_{\min})$$

where σ is the string tension, $\sigma=\sigma_f$ for quarks and $\sigma=\sigma_{adj}=9/4\ \sigma_f$ for gluons.

Effective Hamiltonian

$$H = H_0 + \Delta H_s, \quad \Delta H_s = H_{SL} + H_{SS} + H_T$$

$$H_0 = \frac{p_r^2}{\mu(t)} + \mu(t) + \frac{L(L+1)}{r^2[\mu + 2\int_0^1 (\beta - \frac{1}{2})^2 \nu d\beta]} +$$

$$+ \int_0^1 \frac{\sigma_{adj}^2 d\beta}{2\nu(\beta,t)} r^2 + \frac{1}{2}\int_0^1 \nu(\beta,t) d\beta.$$

μ - effective quark (gluon) energy

v – energy density of the string.

The mass spectrum of H_0 with a good accuracy is described by a very simple formula

$$M^2 = 2\pi\sigma(L + 2n_r + C) \quad ;C \approx 1.55$$

Linear Regge trajectories with “daughters” like in string models

$$\alpha' = 1/2\pi\sigma$$

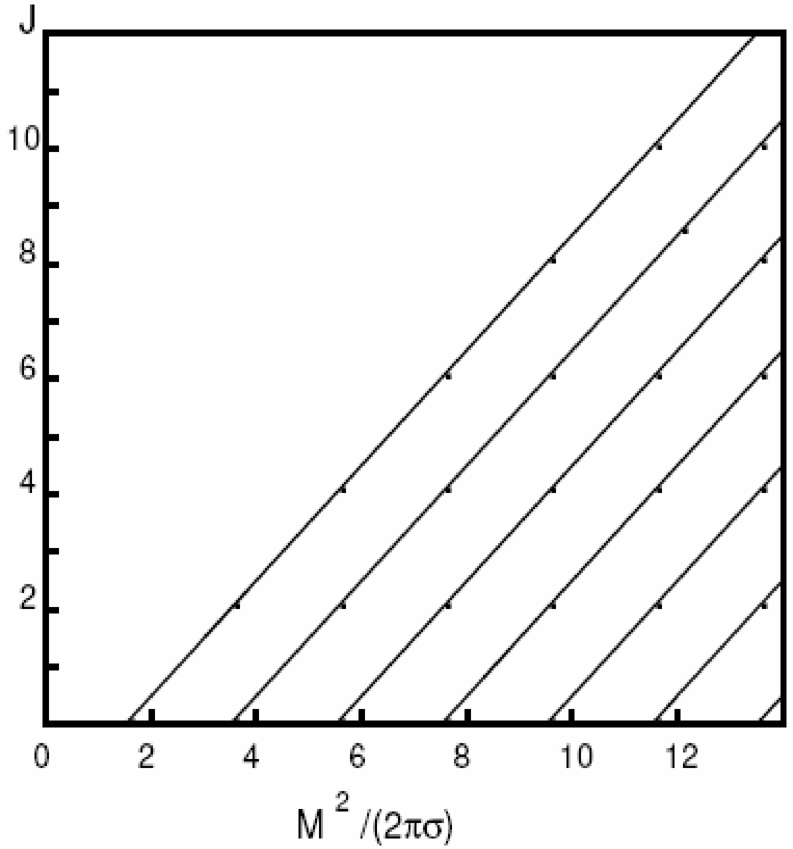

With account of spin effects, perturbative interactions and quark loops spectrum of hadrons is well described.

Pomeron in QCD

There are reasons to believe that Pomeron in QCD is related to gluonic exchanges in the t-channel.

The simplest 2-gluons exchange leads to

$$\alpha_P = 2S_g - 1 = 1$$

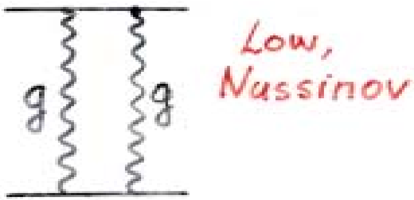

In QCD perturbation theory

The ladder-type diagrams are

Important – BFKL Pomeron.

reggeized gluon

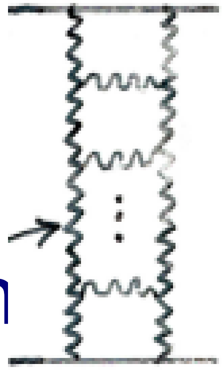

In LO

$$(\alpha_s \ln s)^n$$

$$\Delta \equiv \alpha_P(0) - 1 = \frac{12 \ln 2}{\pi} \alpha_s \approx 0.5$$

Leads to too fast increase of cross sections.

Large NLO corrections

$$\Delta = 0.15 \div 0.3$$

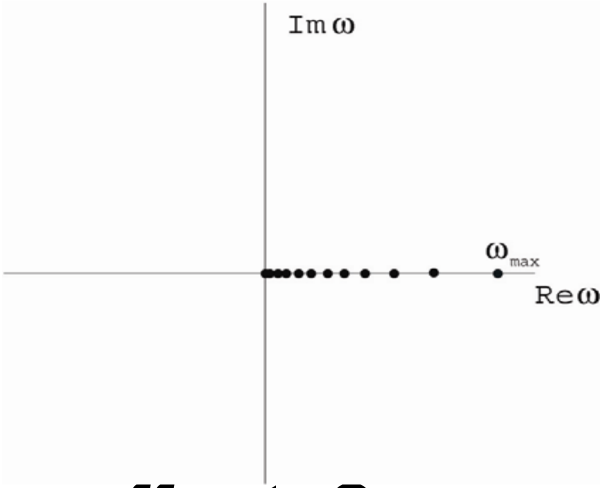

The leading pole is sensitive
 to soft physics.

What is the role of nonperturbative effects?

Are there glueballs on the Pomeron trajectory?

Pomeron and glueballs.

The spectrum of glueballs (gg-states) was calculated in the Wilson loop approach.

Comparison of calculated glueball masses (in GeV) with lattice data ($\sigma_f = 0.18$ GeV^2, $\alpha_s = 0.3$ ($\alpha_s = 0.2$ in parentheses))

J^{PC}	M_{theory} this work	M_{lat} [22]	[23]	[24]
0^{++}	(1.61) 1.41	1.53±0.10	1.53±0.04	1.52±0.13
2^{++}	(2.21) 2.30	2.13±0.12	2.20±0.07	2.12±0.15
0^{++*}	(2.72) 2.41	2.38±0.25	2.79±0.09	
2^{++*}	(3.13) 3.32	2.93±0.14	2.85±0.28	
0^{-+}	2.28	2.30±0.15	2.11±0.24	2.27±0.15
0^{-+*}	3.35	3.24±0.2		
2^{-+}	2.70	2.76±0.16	3.0±0.28	2.70±0.19
2^{-+*}	3.73	3.46±0.21		

Pomeron trajectory and mixing with reggeons.

The leading glueball trajectory

$$\alpha_P^{(np)}(t) = -C + \alpha_P' t + 2 \leftarrow \text{ due to spin of gluons}$$

$$\alpha_P^{(np)}(0) \approx 0.5$$

Confining forces decrease intercept of gg singularity from the born value α=1.

In the small t region bare gg and $q\bar{q}$ - trajectories cross and mixing is important.

Mixing between 3 bare Regge trajectories

with vacuum quantum numbers: P,f and f’.

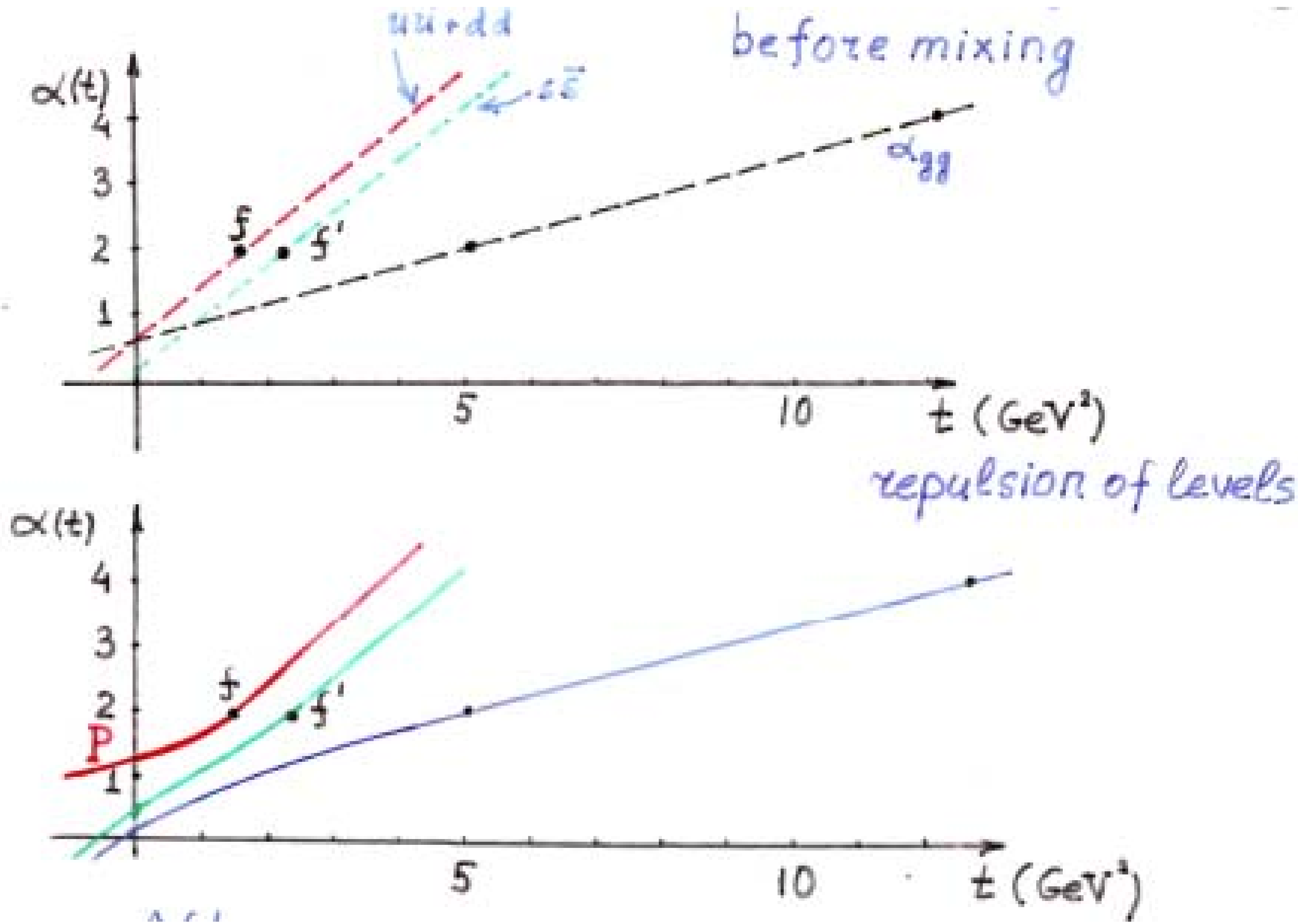

uu+dd
before mixing
$s\bar{s}$
$\alpha(t)$
4
3
2
1
f
f'
α_{gg}
5
10
t (GeV²)
repulsion of levels
$\alpha(t)$
4
3
2
1
P
f
f'
5
10
t (GeV²)

After account of mixing and small distance perturbative dynamics

$$\alpha_P(0) = 1.15 \div 1.25$$

Note that physical pomeron contains both soft and hard effects.

Very rich physics of the Pomeron:

Confinement and glueballs, quark-gluon mixing, semihard interactions.

Pomeron in 1/N-expansion.

In 1/N-expansion the Pomeron corresponds to the cylinder-type diagrams.

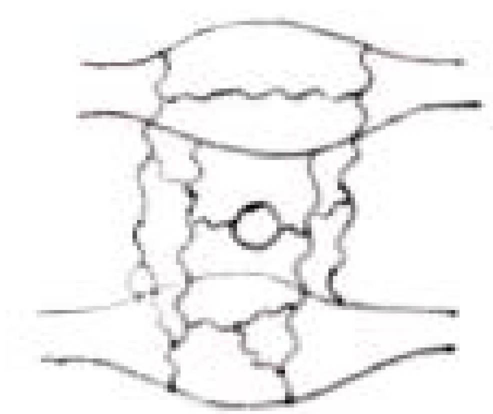

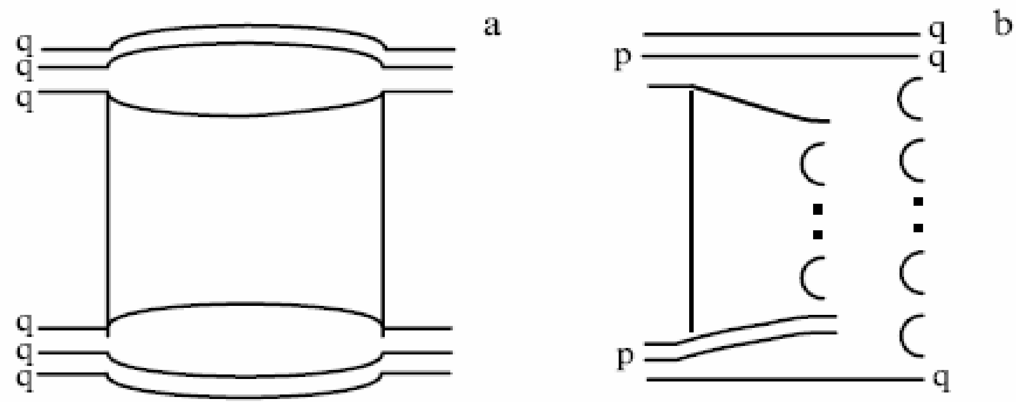

$$T_{pl} \sim 1/N \qquad T_{cyl} \sim 1/N^2$$

$$T_{n_b,n_h} \sim \left(\frac{1}{N}\right)^{n_b+2n_h}$$

n_b - number of boundaries,

n_h – number of holes

Lecture 3
Reggeon calculus and multiparticle production

Impact parameter picture of Regge-exchange

At very high energies amplitudes of binary reactions are concentrated in the region of very small momentum transfer

$$|t| \sim 1/\alpha' \ln\frac{s}{s_0} \,. \quad \left[T(s,t) \sim \left(\frac{s}{s_0}\right)^{\alpha(0)+\alpha' t} \sim \left(\frac{s}{s_0}\right)^{\alpha(0)} \exp\left(\alpha' t \ln\frac{s}{s_0}\right) \right]$$

In this region it can be parametrized in the form

$$M^a(s,t) = \frac{T^a(s,t)}{8\pi s} \,; \qquad \alpha_a(t) = \alpha_a(0) + \alpha'_a \cdot t$$

$$\bar{b}^a(t) = \bar{b}^a(0) \exp\left(R_a^2 \cdot t\right) ; \quad \eta(\alpha_a(t)) = e^{-\frac{i\pi}{2}\alpha_a(t)} \times \begin{cases} -\dfrac{1}{\sin\frac{\pi\alpha_a}{2}} ; & \sigma = + \\ -\dfrac{i}{\cos\frac{\pi\alpha_a}{2}} ; & \sigma = - \end{cases}$$

$$M^a(s,t) = b^a(0)\, \eta(\alpha_a(0)) \exp\left[\lambda^a(s)\, t\right] \cdot \left(\frac{s}{s_0}\right)^{\alpha_a(0)-1}$$

$$\lambda^a(s) = R_a^2 + \alpha_a'\left(\ln\frac{s}{s_0} - i\frac{\pi}{2}\right)$$

The amplitude in the b-space has the form

$$f^a(s,b) = \int M^a(s,b)\, e^{-i\vec{q}\vec{b}} \frac{d^2q}{2\pi} =$$

$$= \frac{b^a(0)\,\eta(\alpha_a(0))}{2\cdot\lambda^a(s)}\left(\frac{s}{s_0}\right)^{\alpha_a(0)-1} \exp\left(-\frac{b^2}{4\lambda^a(s)}\right)$$

Radius of interaction increases as $\sqrt{\alpha' \ln\frac{s}{s_0}}$

as $s \to \infty$.

s-channel picture of reggeons.

Regge poles contribute to imaginary parts of two-body amplitudes. Unitarity relates $\mathrm{Im}\, T_{12\to34}(s,t)$ to contributions of multiparticle intermediate states in the s-channel

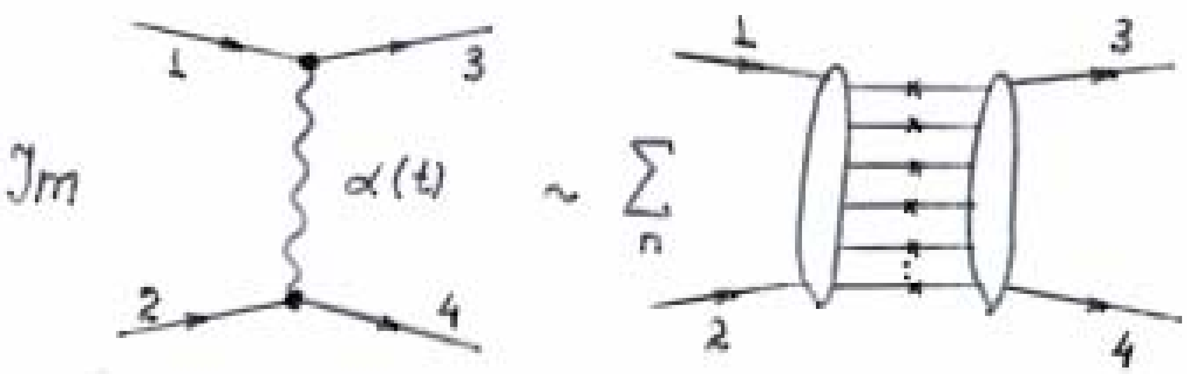

What are these states for reggeons?

Multiperipheral final states.

$\pi\pi \to n\pi$

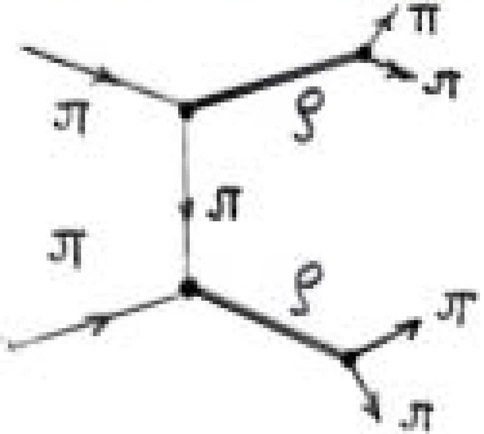

For $s \gg m_\rho^2$

$\sigma \sim \frac{1}{s^2}$

Space-time picture in the lab. frame

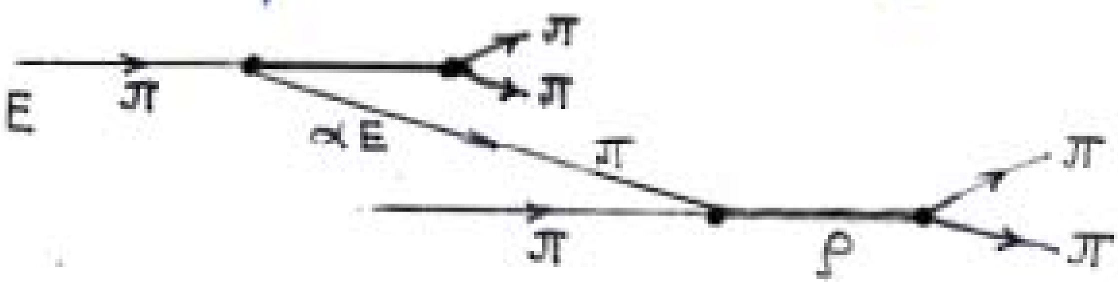

$\alpha \lesssim 1$

$\alpha E \cdot m_\pi \simeq m_\rho^2$

For fixed α this is impossible at large E

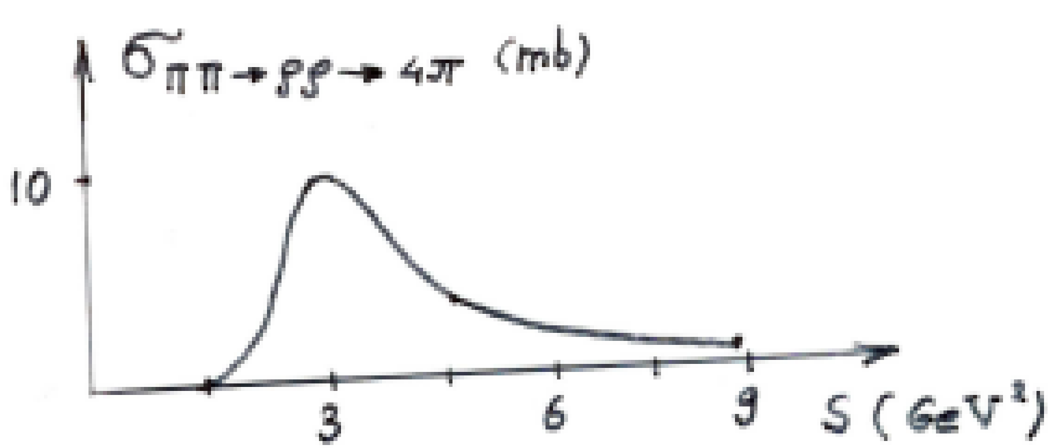

It is possible to decrease pion energy by emitting many ρ-mesons

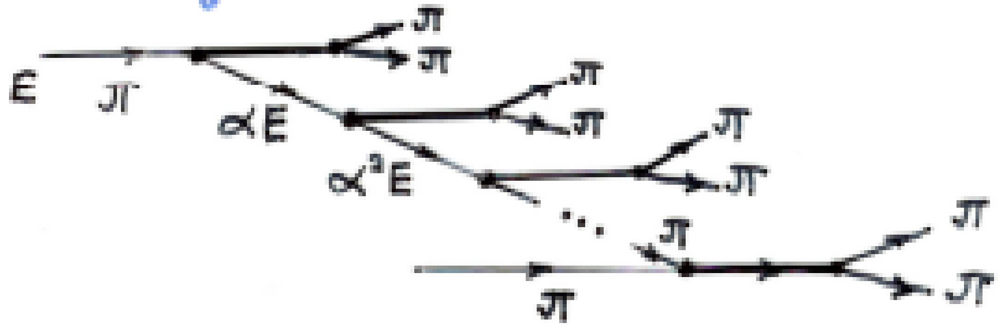

$$\alpha^n E m_\pi \approx m_\rho^2$$

Production of many pions

Multiperipheral mode
AFS (1962)

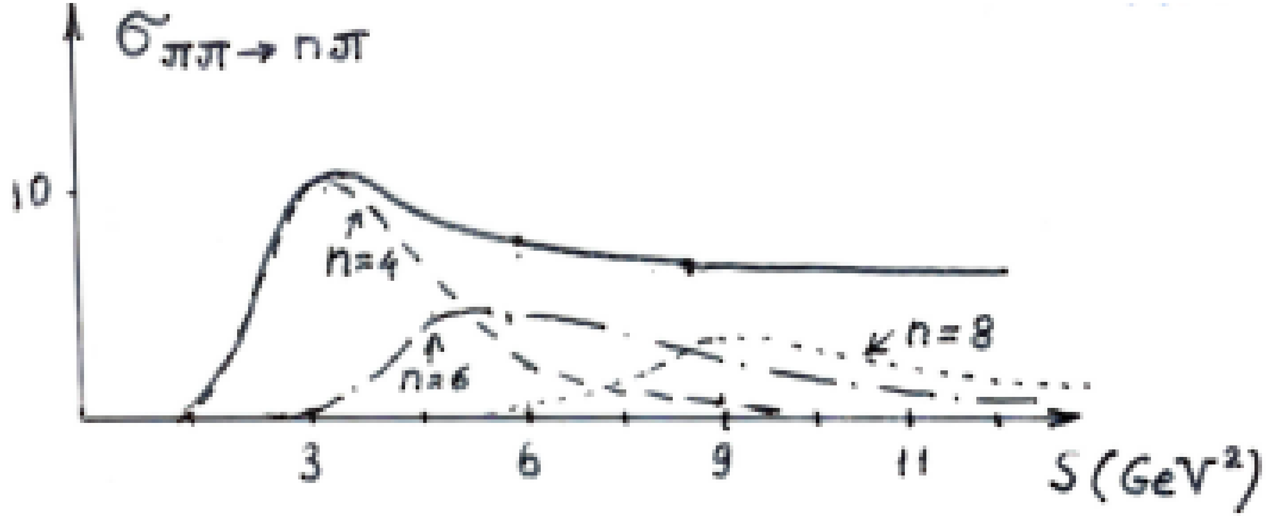

So $\sigma^{in} = \sum_n \sigma_n$ can be nearly const with energy

$$\langle n \rangle \approx \ln\frac{1}{\alpha} \cdot \ln\frac{E \cdot m_\pi}{m_\rho^2}$$

Average multiplicity increases logarithmically with energy.

In the impact parameter space each step has a finite size $\bar{b} \sim 1/m_\pi$. These two-dimensional vectors $\vec{b}_i$ add independently. – random walk in $\vec{b}$-space. (41)

$$\overline{R}^2 \equiv \overline{\vec{b}^2} \approx \frac{\bar{n}}{m_\pi^2} \sim \frac{\ln \frac{s}{m_\rho^2}}{m_\pi^2}$$

This is the origin of the growth with energy of the radius of interaction in the Regge-model.

The time of developement of the multiperipheral fluctuation is large ($\sim E$)

$$\tau_i \sim \frac{1}{m_\rho} E_i$$

Summation of m.-p. diagrams leads to Regge-behaviour for two-body amplitudes

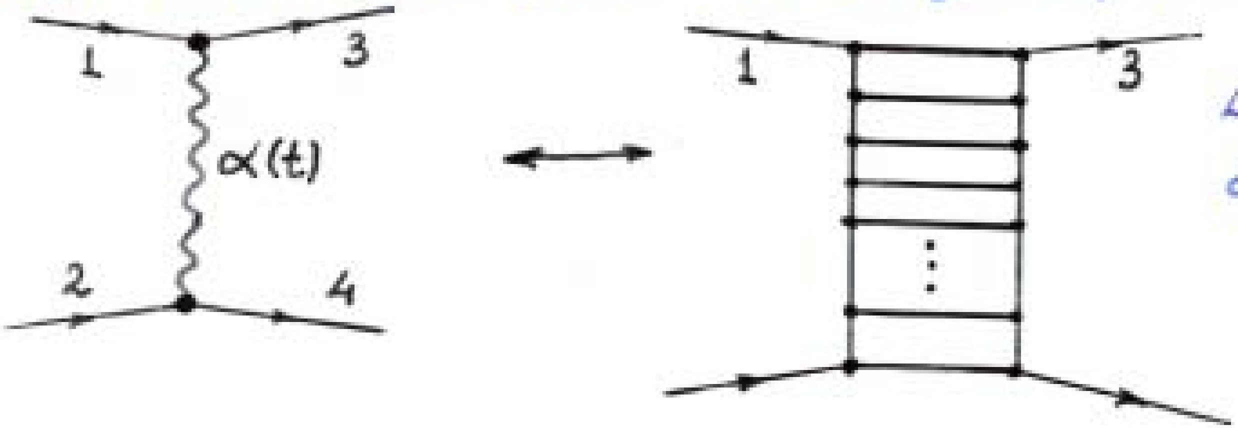

Ladder type diagrams

In the multiperipheral model hadronic final states have the following properties.

a) Short range correlations in rapidity.

$\left(y = \ln \frac{E + p_{\parallel}}{m_{\perp}}\right)$. Particles separated by many steps of the m.-p. process are uncorrelated.

Inclusive processes.

$$a + b \to c_1 + c_2 + \ldots + c_n + X$$

Single particle inclusive cross section

$$a + b \to c + X$$

$$F^c = E^c \frac{d^3\sigma}{d^3 p_c}$$ invariant cros section

It depends on $y_a - y_c,\ y_c - y_b,\ p_{\perp c}^2$

$$\rho^c = \frac{F^c}{\sigma^{in}}$$ — mean number of particles in the unit of phase space

$\rho^c E^c$ — energy carried by particles c

Sum rules from conservation laws.

Energy conservation:

$$\sum_c \int \rho^c d^3p_c = E^a + E^b$$

Conservation of charge Q

$$\sum_c \int \rho^c Q^c \frac{d^3p_c}{E_c} = Q^a + Q^b$$

Double inclusive cross section $a + b \to c_1 + c_2 + X$

$$E^{c_1} E^{c_2} \frac{d^6\sigma}{d^3p_{c_1} d^3p_{c_2}}$$

$$C(y_1^{c_1}, y_2^{c_2}, p_{\perp c_1}^2, p_{\perp c_2}^2) = \frac{d^6\sigma}{\sigma^{in} dy_1^{c_1} dy_2^{c_2} d^2p_{\perp c_1} d^2p_{\perp c_2}} - \rho_{c_1} \cdot \rho_{c_2}$$

in m.p. model decreases $\sim \exp[-\lambda|y_1 - y_2|]$ for large $y_1 - y_2$.

The property **a)** leads to many other consequences. In particular all ρ^c are independent of $y_i - y_k$ $(i, k = a, b, c)$ if $y_i - y_k \gg 1$. For example at high energies $(y_a - y_b \gg 1)$ in the fragmentation region of the particle a

$(y_a - y_c \sim 1)$

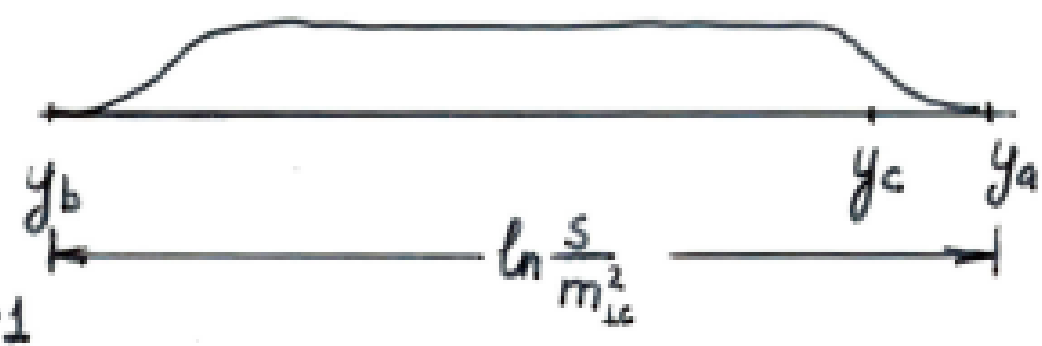

and

$y_c - y_b \approx y_a - y_b \gg 1$

the density ρ^c depends only on $y_a - y_c$, $p_{\perp c}^2$

b) $$\rho^c = \varphi(y_a - y_c, p_\perp^2)$$

This is equivalent to the Feynman scaling

$$\rho^c = \varphi(x_F, p_\perp^2) \quad ; \quad x_F = \frac{2p_{\parallel c}}{\sqrt{s}} \approx \exp[-(y_a - y_c)]$$

c) In the central rapidity region

$$y_a - y_c \gg 1 \quad , \quad y_c - y_b \gg 1$$

ρ^c depends only on $p_{\perp c}^2$

$$\rho^c = \varphi(p_\perp^2)$$

– flat rapidity distributions.

d) Average number of produced particles

$\langle n_c \rangle$ increases logarithmically with s

$$\langle n_c \rangle = \int \rho^c(y_c, p_{\perp c}^2)\, d^2 p_{\perp c}\, dy_c \sim \ln \frac{s}{m_c^2}$$

e) Fast decrease of distributions with $p_\perp$.

The form of $\varphi(p_{\perp c}^2, y_c)$ depends on the model.

f) Multiplicity distributions have a Poisson-type behaviour

$$\langle n^2 \rangle - \langle n \rangle^2 \simeq c \langle n \rangle$$

If $y_a - y_c \gg 1$, $y_c - y_b \gg 1$ we obtain diagrams of the double Regge limit

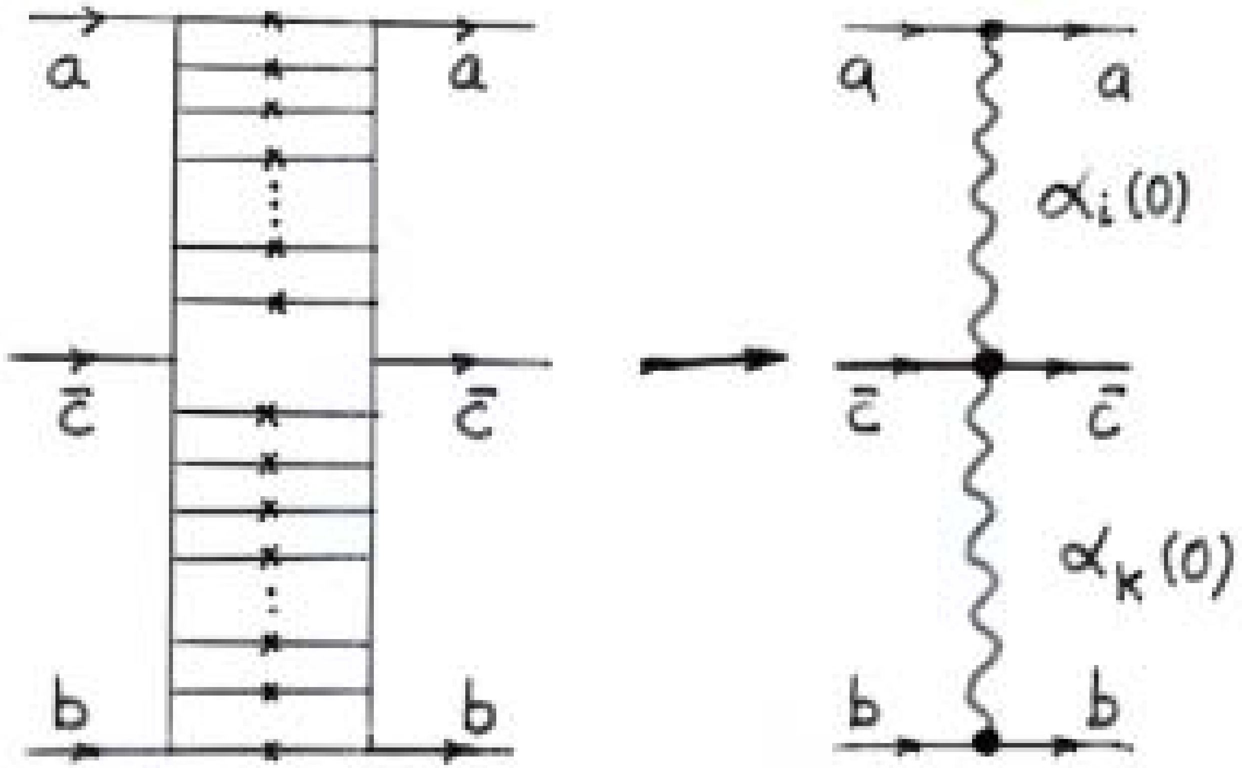

Diffractive production of hadrons in Regge theory.

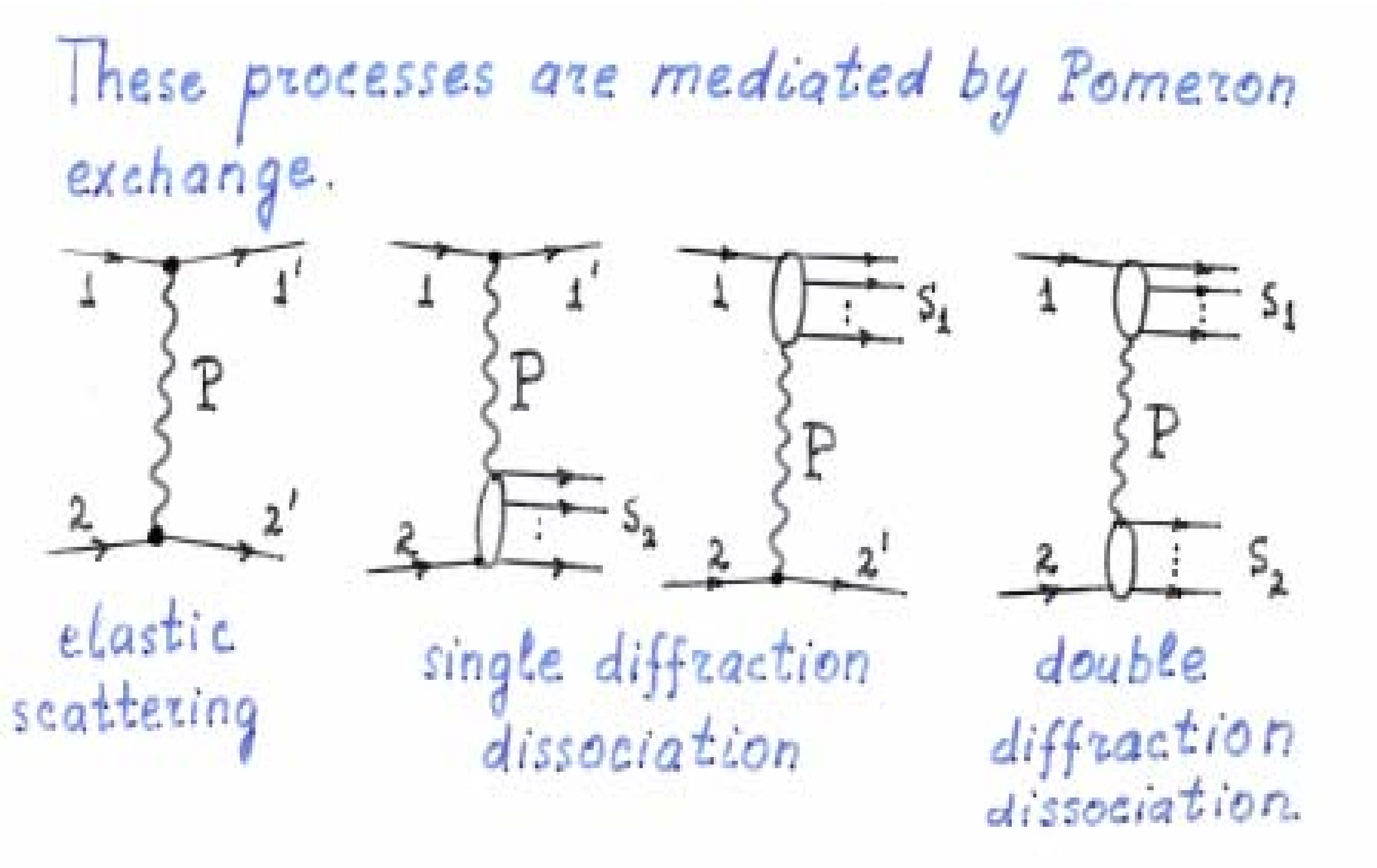

Kinematics.

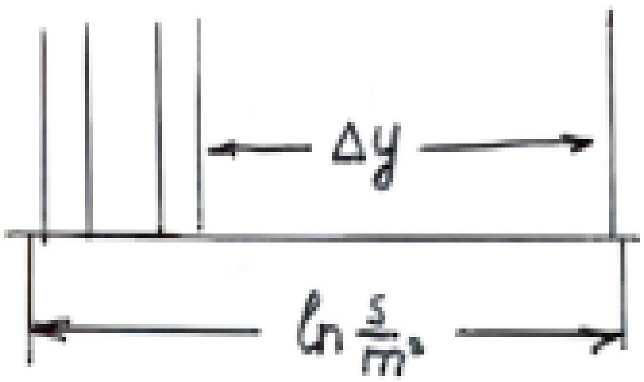

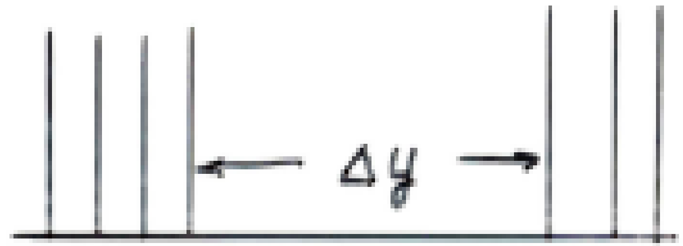

Events with large rapidity gaps $(\Delta y \gg 1)$

$s_2 \ll s$ $\quad (1 - x_F) \approx \dfrac{s_2 - m_2^2 - t}{s}$; $\quad t \approx -p_{\perp 1'}^2$

t - fixed

$$\Delta y \approx \ln\left(\frac{1}{1-x_F}\right)$$

$1 - x_F \equiv x_{\mathbb{P}}$

Cross section for inclusive single diffraction dissociation

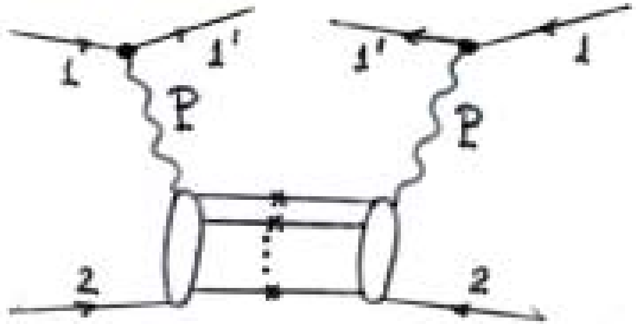

$$T(s, s_2, t, \tau_n) = g_{11}^{P}(t) V_n^{Pb}(s_2, t, \tau_n) \times \left(\frac{s}{s_2}\right)^{\alpha_P(t)} \eta(\alpha_P(t))$$

$$s_2 \frac{d^2\sigma}{ds_2\, dt} = \frac{s_2}{s} x \frac{d^2\sigma}{dx\, dp_\perp^2} = \pi \frac{s_2}{s} E \frac{d^3\sigma}{d^3p} =$$

$$= \frac{(g_{11}^{P}(t))^2}{16\pi} \left|G_P(\xi', t)\right|^2 \sigma_{P2}^{(tot)}(s_2, t) \qquad (*)$$

$$G_P(\xi', t) = \eta(\alpha_P(t)) \exp\left[(\alpha_P(t) - 1)\xi'\right]$$

$$\xi' \equiv \ln \frac{s}{s_2} \approx \Delta y$$

$$\sigma^{(tot)}_{P2}(s_2,t) \equiv \frac{1}{2 s_2} \sum_n \left| V_n(s_1, t, \tau_n) \right|^2 \frac{d\tau_n}{\pi}$$

Note that this is "unphysical" cross-section and it is defined by relation (*)

It has usual Regge behavior for large s_2

$$\sigma^{(tot)}_{P2}(s_2,t) = \sum_k g^k_{22}(0)\, r^{\alpha_k}_{PP}(t) \left(\frac{s_2}{s_0}\right)^{\alpha_k(0)-1}$$

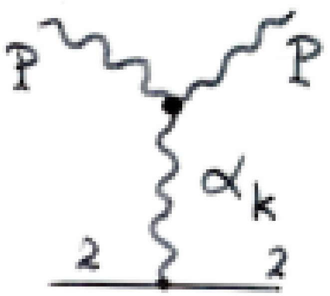

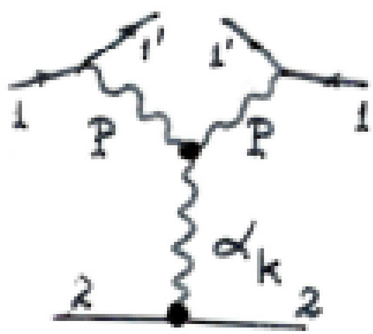

Triple-Regge diagram

Inclusive cross section has the form

$$F^{1'} = \sum_k G_{\mathbb{P}\mathbb{P}k}(t)\,(1-x)^{\alpha_k(0)-2\alpha_{\mathbb{P}}(t)} \left(\frac{s}{s_0}\right)^{\alpha_k(0)-1}$$

For arbitrary reggeons

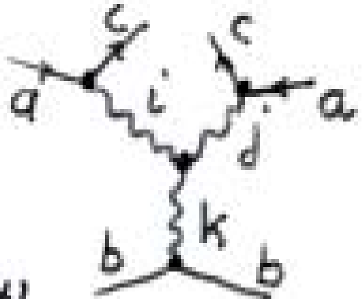

$$F^{c} = \sum_{i,j,k} G_{ijk}(t)\,(1-x)^{\alpha_k(0)-\alpha_i(t)-\alpha_j(t)} \times \left(\frac{s}{s_0}\right)^{\alpha_k(0)-1}$$

$\mathbb{P}$ exchange leads to increase of $F^{c} \sim \frac{1}{1-x}$ as $x \to 1$

Regge cuts and their properties.

From 2-particle unitarity in the t-channel

– **moving (Regge) poles**

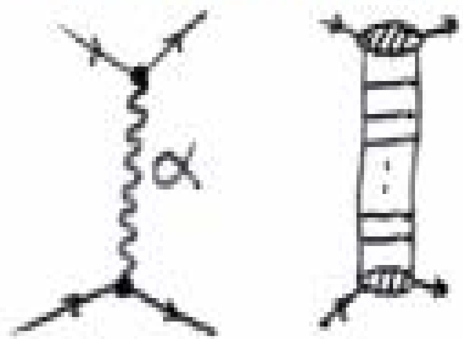

From many-particle unitarity (in the t-channel)

– **moving branch points**

due to exchange by several Regge poles.

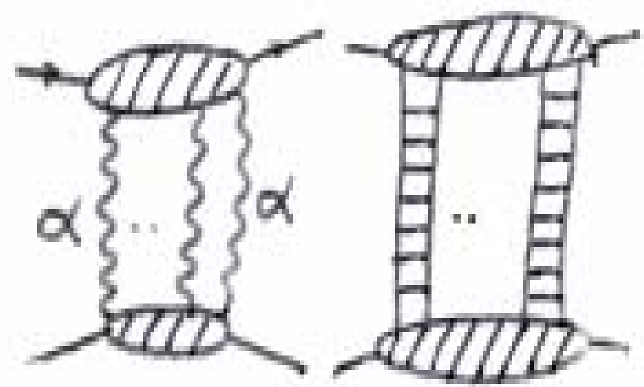

The simplest diagrams

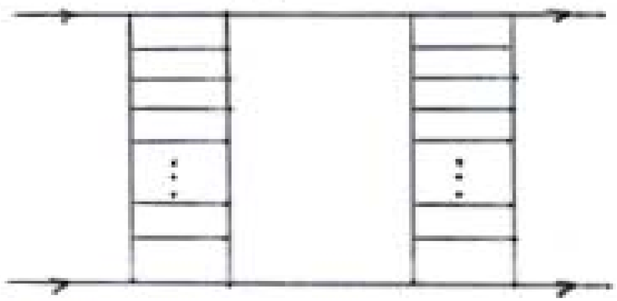

AFS-type diagram = 0 as $s \to \infty$

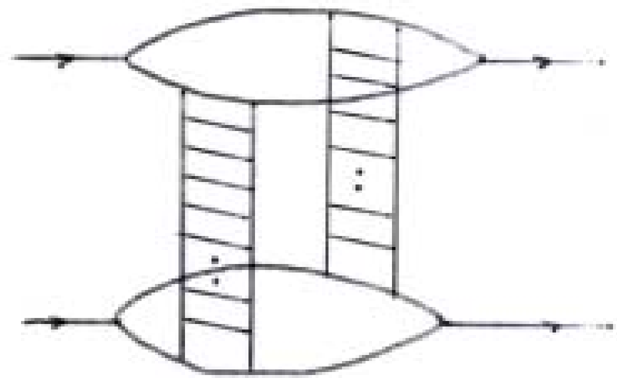

Mandelstam-type diagram

They correspond to different space-time pictures of the process

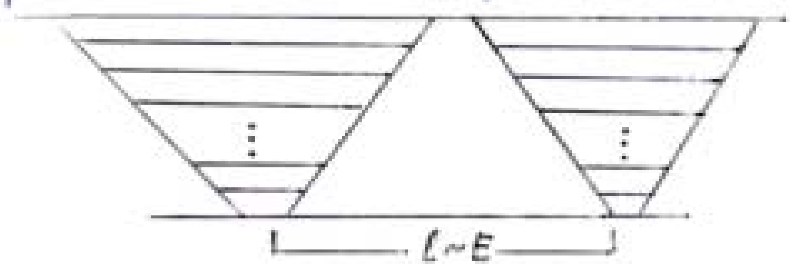

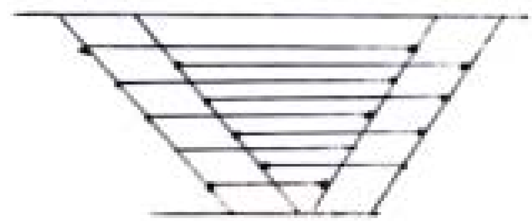

Successive interactions take too long time to exist at high energies.

The position of the singularity connected to an exchange by n Pomerons

$$\alpha_{nP}(t) = n\alpha_P\left(\frac{t}{n^2}\right) - n + 1$$

at $t=0$ $\quad \alpha_{nP}(0) = n(\alpha_P(0)-1)+1 = n\Delta+1$

For supercritical Pomeron $(\Delta>0)$ all nP-cuts should be taken into account.

From the point of view of $1/N$-expansion nP-exchange corresponds to sets of diagrams with $n-1$ "handles"

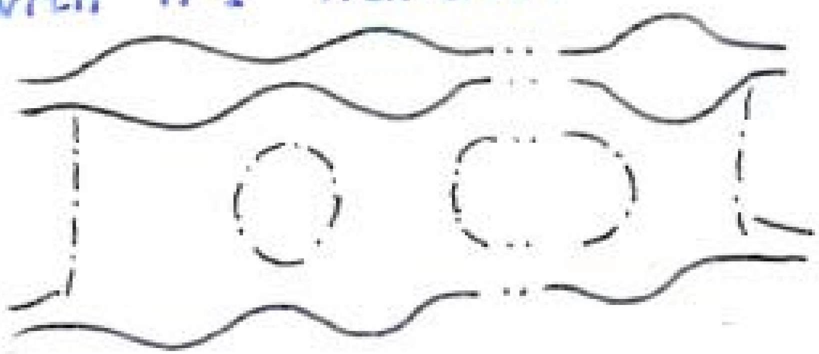

Exchange by N-cylinders $\sim \left(\frac{1}{N^2}\right)^n$

Gribov`s method of evaluation of moving cuts contributions.

Consider as an example PP-cut

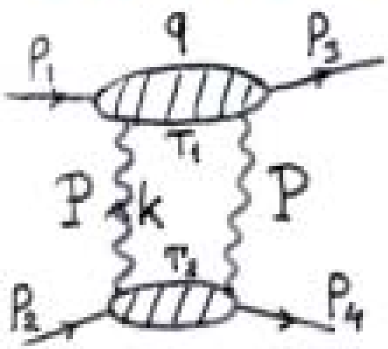

$$T^{(2)}(s,t) = \left(\frac{-i}{2!(2\pi)^4}\right)\int d^4k\, \eta_P(k^2)\,\eta_P(q-k)^2 \times \left(\frac{s}{s_0}\right)^{\alpha_P(k^2)+\alpha_P((k-q)}\cdot T_1(s_1, k^2, (q-k)^2, q^2)\cdot T_2$$

$q = p_3 - p_1$

change variables from $k_0, k_z \to$

$$s_1 = (p_1+k)^2, \quad s_2 = (p_2-k)^2$$

$$s_1 = m_1^2 + k^2 + \sqrt{s}(k_0 - k_z)\;;\; s_2 = m_2^2 + k^2 - \sqrt{s}(k_0 + k_z)$$

$$T^{(2)}(s,t) = \frac{(-i)}{2!(2\pi)^4 2s} \int_0^\infty d^2k_\perp \int_C ds_1 ds_2\, \eta_P(k^2)\, \eta_P(q-k)^2 \times$$

$$\times \left(\frac{s}{s_0}\right)^{\alpha_P(k^2)+\alpha_P((k-q)^2)} T_1 \cdot T_2$$

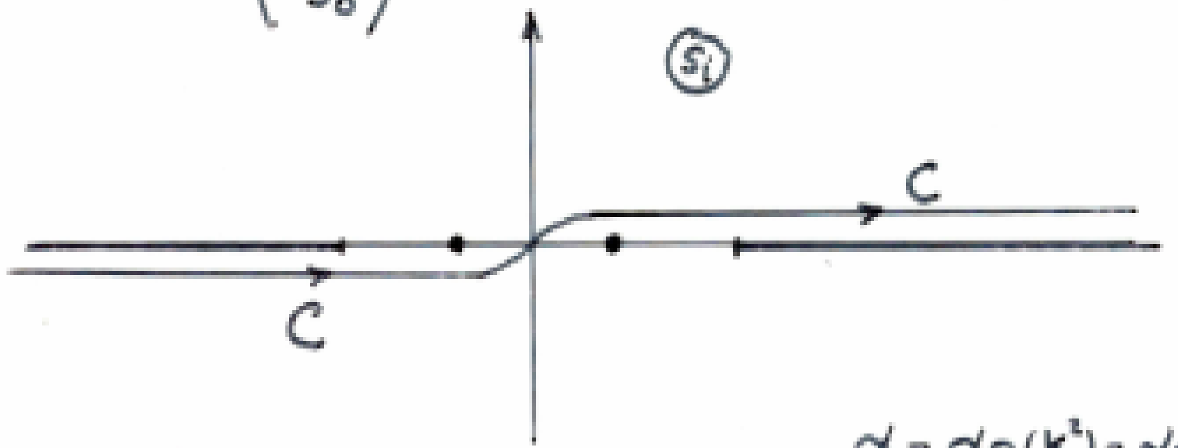

For large s_i: $\quad T_i \sim (s_i)^{\alpha - \alpha_P(k^2) - \alpha_P((k-q)^2)} < \frac{1}{s_i}$

if $\alpha < 1 + 2\Delta$

In this case integrals in s_i are convergent and it is possible to deform $C \to C'$

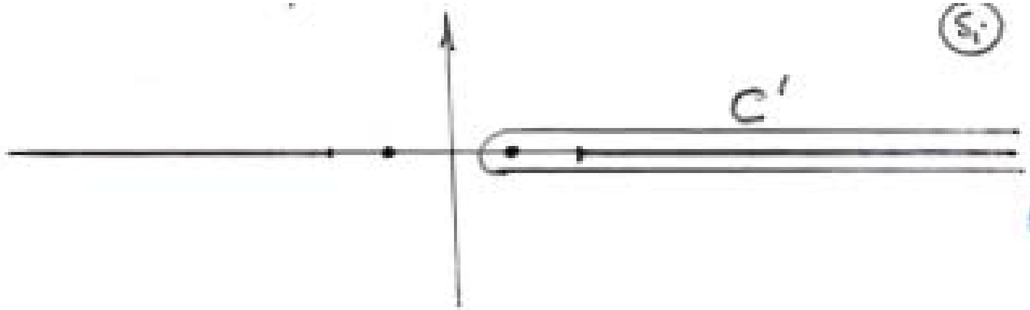

AFS diagram leads to 0 as it does not have left hand singularities

$$\frac{T^{(2)}}{8\pi s} = \frac{i}{2!}\int \frac{d^2 k_\perp}{\pi}\,\frac{\eta_P(k_\perp^2)\left(\frac{s}{s_0}\right)^{\alpha_P(k_\perp^2)-1}}{8\pi s_0}\cdot\frac{\eta_P((\vec q_\perp-\vec k_\perp)^2)\left(\frac{s}{s_0}\right)^{\alpha_P((\vec q-\vec k_\perp)^2)-1}}{8\pi s_0}\cdot$$

$$\times\, N_1 \cdot N_2$$

$$N_k^{(2)} = \frac{1}{2\pi i}\int_{C'} ds_k\, T_k = s_0\, g_k(k_\perp^2)\, g_k((\vec k-\vec q_\perp)^2) + \frac{1}{\pi}\,\mathrm{Im}\, T_k$$

$$\mathrm{Im}\, T_k = \frac{1}{2}\sum_n T_{kP\to n}(s_k, k_\perp^2, \tau_n)\, T^*_{kP\to n}(s_k, (\vec{q}-\vec{k}_\perp)^2 \tau_n)$$

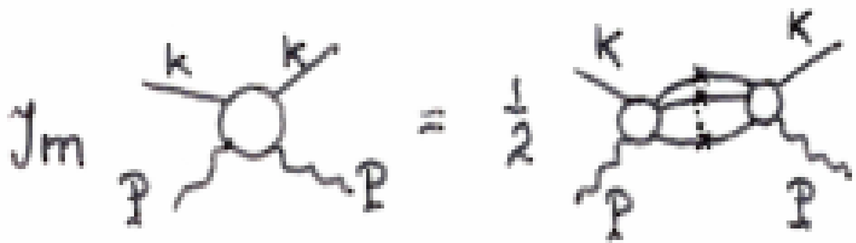

Unitarity condition for P-particle scattering amplitude

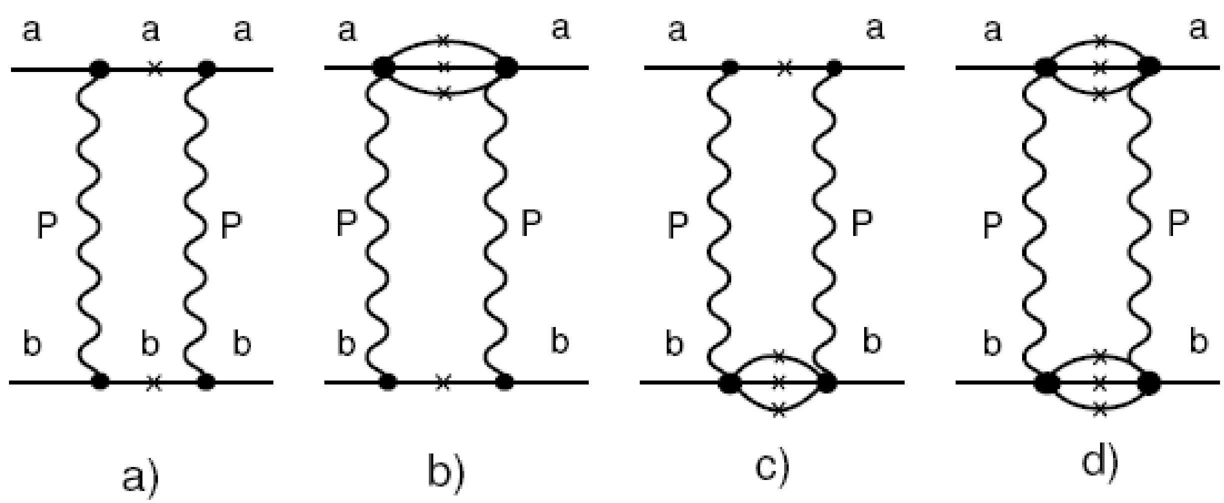

For forward elastic amplitude

$$\frac{\mathrm{Im}\, T^{(2)}(s,0)}{s} \equiv \sigma^{(2)}(s,0) \simeq -\sigma_{P}^{DIF} = -\left(\sigma_{P}^{el} + \sigma_{P}^{SD} + \sigma_{P}^{DD}\right)$$

For pole contributions

$$M^{(2)} = \frac{T^{(2)}}{8\pi s} = \frac{i}{2!}\int M^{(1)}(s,k_\perp^2)\, M^{(1)}(s,(\vec{q}-\vec{k}_\perp)^2)\,\frac{d^2k_\perp}{\pi}$$

Same method can be used for n-Pomeron exchange amplitudes.

$$M^{(n)}(s,t) = \frac{(i)^{n-1}}{n!} \int N_1^{(n)}(\vec{q}_{i\perp})\, N_2^{(n)}(\vec{q}_{i\perp}) \left(\frac{s}{s_0}\right)^{\alpha_{1P}+\alpha_{2P}+\dots+\alpha_{nP}-n} \times$$

$$\times \quad \frac{\eta_P(q_{1\perp}^2)}{8\pi s_0} \cdot \dots \cdot \frac{\eta_P(q_{n\perp}^2)}{8\pi s_0} \frac{d^2 q_{1\perp}}{\pi} \dots \frac{d^2 q_{n-1\perp}}{\pi}$$

$$N_k^{(n)}(\vec{q}_{i\perp}) = \int_{C'} \dots \int T_k^{(n)}(\vec{q}_{i\perp}, s_{k1}, \dots, s_{k(n-1)}) \frac{ds_{k1}}{2\pi i} \dots \frac{ds_{k(n-1)}}{2\pi i}$$

can be expressed as multiple discontinuity of $T_K^{(n)}$ on the right hand cut.

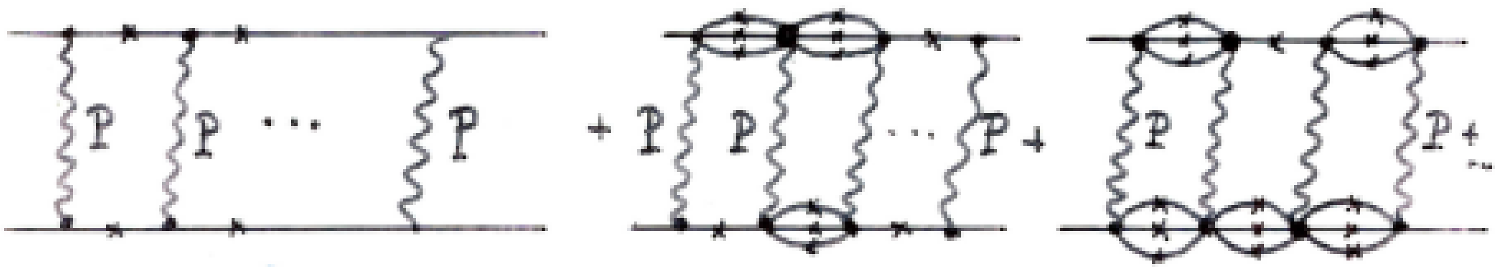

The diagrams with elastic rescatterings only

$$N_1^{(n)} N_2^{(n)} = b_p(q_{1\perp}^2) \dots b_p(q_{n\perp}^2)$$

$$M^{(n)} = \frac{(2i)^{n-1}}{n!} \int M_p^{(1)}(s,\vec{q}_{1\perp}^{\,2}) \dots M_p^{(1)}(s,\vec{q}_{n\perp}^{\,2}) \frac{d^2 q_{1\perp} \dots d^2 q_{n\perp}}{(2\pi)^{n-1}} \delta\left(\vec{q} - \sum_{i=1}^{n} q_{i\perp}\right)$$

$$M = \sum_n M^{(n)}$$

can be written in the closed form in the impact parameter space

Eikonal approximation.

$$f(s,b)=\int M(s,\vec{q}^2)e^{-i\vec{q}\vec{b}}\frac{d^2q}{2\pi}$$

$$f^{(n)}(s,b)=\int M^{(n)}(s,\vec{q}^2)e^{-i\vec{q}\vec{b}}\frac{d^2q}{2\pi}=\frac{(2i\delta_P(s,b))^n}{2i\cdot n!}$$

$$\delta_P(s,b)=\int M_P^{(1)}(s,q^2)e^{-i\vec{q}\vec{b}}\frac{d^2q}{2\pi}$$

$$f(s,b)=\frac{e^{2i\delta_P(s,b)}-1}{2i}$$

$$\mathrm{Im}\,\delta_P(s,0)\sim\left(\frac{s}{s_0}\right)^{\Delta}\exp\left(-\frac{b^2}{\lambda_P(s)}\right)=\exp\left(-\frac{b^2}{\lambda_P(s)}+\Delta\ln\frac{s}{s_0}\right)$$

$$R^2(s)=\lambda_P(s)\Delta\ln\left(\frac{s}{s_0}\right)\simeq\alpha_P'\Delta\ln^2\left(\frac{s}{s_0}\right)$$

Account of low-mass diffraction.

For resonances in intermediate states δ_P is a matrix in the space of diffractive states: multi-channel eikonal.

"Quasieikonal" approximation:

$$f(s,b) = \frac{e^{2i\delta_P(s,b)\cdot C} - 1}{2iC}\,; \quad C = 1 + \frac{\sigma_{in}^{D}}{\sigma^{(el)}} > 1$$

corresponds to maximum inelastic diffraction consistent with unitarity.

AGK-cutting rules.

What are multiparticle configurations in the s-channel, which correspond to moving cuts contributions?

All possible “cuttings” should give ImT

$$\delta_s T = \frac{1}{i}\left(T(s+i\varepsilon) - T(s-i\varepsilon)\right) = 2\,\mathrm{Im}\,T$$

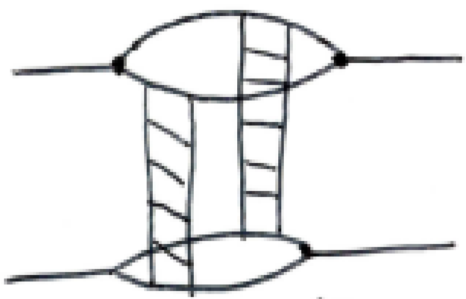

$T^{(2)}$

3 possibilities

a) Diffractive cutting (between Pomerons)

$$\delta_s T_0^{(2)}$$

positive contr.

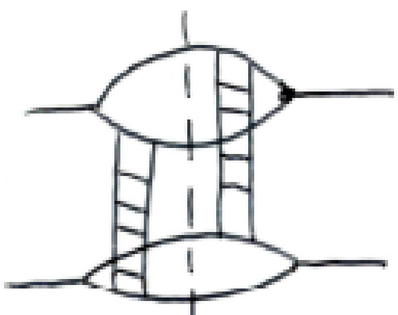

b) Cutting through one of Pomerons

$\delta_s T_1^{(2)}$

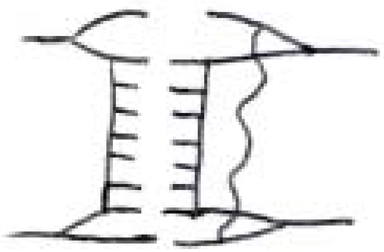

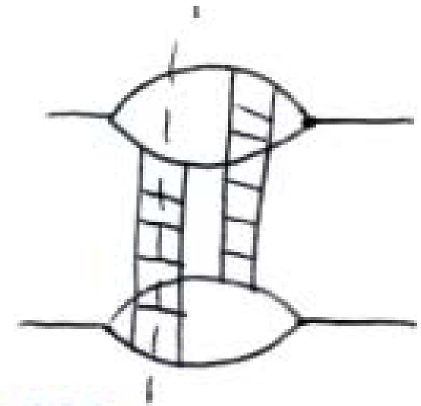

interference diagram -
- negative contr.

c) Cutting of both reggeons.

$\delta_s T_2^{(2)}$

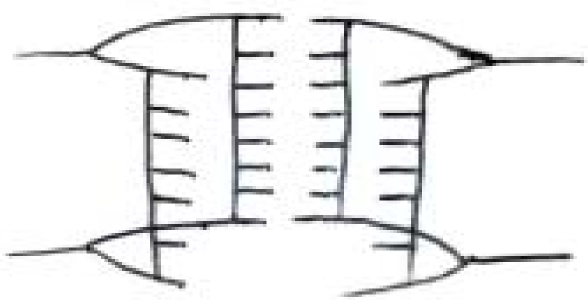

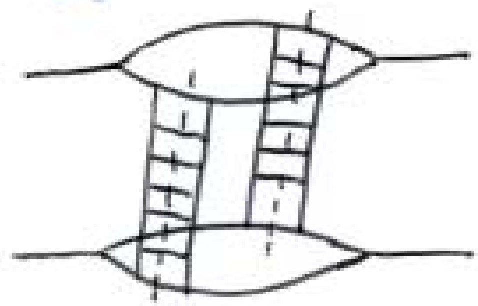

Positive contribution

$$\frac{T^{(2)}_{(s,0)}}{8\pi s} = \frac{-i}{(8\pi s_0)^2}\int \frac{d^2k_\perp}{\pi}\; i\,G_{\alpha_1}(s,k_\perp^2)\, i\,G_{\alpha_2}(s,k_\perp^2)\times$$
$$\times\, N_1 \cdot N_2$$

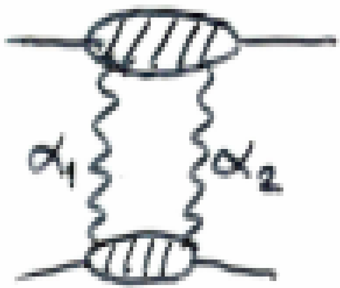

$$G_{\alpha_i} = \eta(\alpha_i)\left(\frac{s}{s_0}\right)^{\alpha_i(k_\perp^2)-1}$$

$N_{1(2)}$ - are real functions

AGK result:

$$\delta_s T_0^{(2)}(s,0) \sim \int d^2k_\perp 2\left(\mathrm{Re}\, G_{\alpha_1} \mathrm{Re}\, G_{\alpha_2} + \mathrm{Im}\, G_{\alpha_1} \cdot \mathrm{Im}\, G_{\alpha_2}\right) N_1 N_2$$

$$\delta_s T_1^{(2)}(s,0) \sim \int d^2k_\perp \left(-8\, \mathrm{Im}\, G_{\alpha_1} \cdot \mathrm{Im}\, G_{\alpha_2}\right) \cdot N_1 \cdot N_2$$

$$\delta_s T_2^{(2)}(s,0) \sim \int d^2k_\perp \left(4\, \mathrm{Im}\, G_{\alpha_1} \cdot \mathrm{Im}\, G_{\alpha_2}\right) \cdot N_1 \cdot N_2$$

For $\mathbb{P}\mathbb{P}$-exchange $(\mathrm{Re}\, G_{\mathbb{P}} \ll \mathrm{Im}\, G_{\mathbb{P}})$

$$\mathrm{Im}\, T^{(2)}_{\mathbb{P}\mathbb{P}}(s,0) \equiv - A^{(2)}_{\mathbb{P}\mathbb{P}}$$

$$\mathrm{Im}\, T^{(2)}_{0}(s,0) = A^{(2)}_{\mathbb{P}\mathbb{P}}$$

$$\mathrm{Im}\, T^{(2)}_{1}(s,0) = -4 A^{(2)}_{\mathbb{P}\mathbb{P}}$$

$$\mathrm{Im}\, T^{(2)}_{2}(s,0) = 2 A^{(2)}_{\mathbb{P}\mathbb{P}}$$

$$\mathrm{Im}\, T^{(2)}_{\mathbb{P}\mathbb{P}} = \sum_{\mu} \mathrm{Im}\, T^{(2)}_{\mu}$$

In general case of ν- Pomeron exchange with μ- Pomerons cut:

$$\delta_s T_\mu^{(\nu)} \sim (-1)^{\nu-\mu} C_\nu^\mu \prod_{\beta=1}^{\nu} (2 \, Im \, G_{P\beta})$$

$$C_\nu^\mu = \frac{\nu!}{\mu!(\nu-\mu)!} \qquad (\mu \neq 0)$$

$$\delta_s T_0^{(\nu)} \sim (-1)^\nu \prod_{\beta=1}^{\nu} (2 \, Im \, G_{P\beta}) + 2 \, Im \left[-i \prod_{\beta=1}^{\nu} (i \, G_{P\beta}) \right]$$

It satisfies the condition

$$\delta_s T^{(\nu)} = \sum_{\mu=0}^{\nu} \delta_s T_\mu^{(\nu)}$$

$$\sum_{\mu=0}^{\nu} \mu \cdot \left(\delta_s T_\mu^{(\nu)}\right) = 0 \qquad \left(\sum_{\mu=1}^{\nu} (-1)^\mu \mu \, C_\nu^\mu = 0 \right)$$

$$\sum_{\mu=2}^{\nu} \mu \cdot (\mu - 1) \left(\delta_s T_\mu^{(\nu)}\right) = 0$$

...

They lead to cancellations for inclusive spectra

For example for single particle inclusive spectra contributions of different diagrams $\sim \mu$.

Diffraction ($\mu = 0$) gives zero contribution for $x_F \simeq 0$

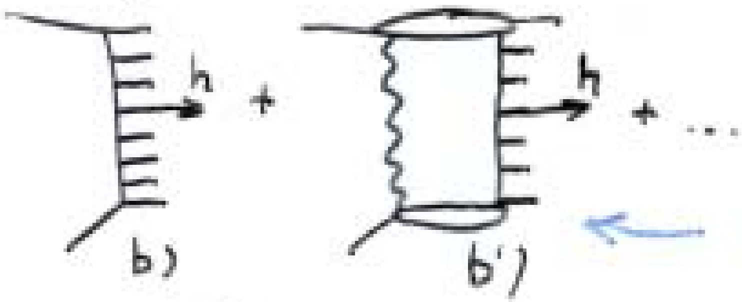

$\leftarrow n(y)\,(-4)\,A^{(2)}_{\mathbb{P}\mathbb{P}}$

AGK cancellation

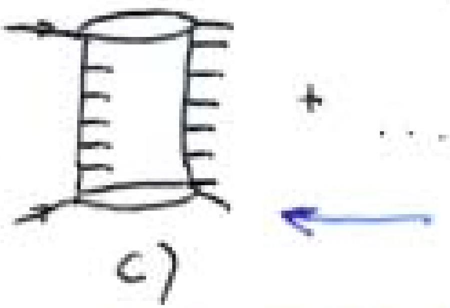

$\leftarrow 2n(y)\,(+2)\,A^{(2)}_{\mathbb{P}\mathbb{P}}$

Thus only the contribution of the diagram of $\mathbb{P}$-cutting (b) is left.

Thus AGK-cutting rules allow to predict properties of multiparticle production if contributions of rescattering to $\sigma^{(tot)}_{(s)}$ are known.

In the eikonal model

$$\sigma_k(s,b) = \frac{\left(4\,\mathrm{Im}\,\delta_2(s,b)\right)^k}{4\cdot k!} \exp\left[-4\,\mathrm{Im}\,\delta_2(s,b)\right] \qquad k \geq 1$$

k-cut Pomerons + any number of uncut

Multiparticle production and topological expansion.

Cuttings of many pomerons in 1/N- expansion correspond to multi-chain configurations

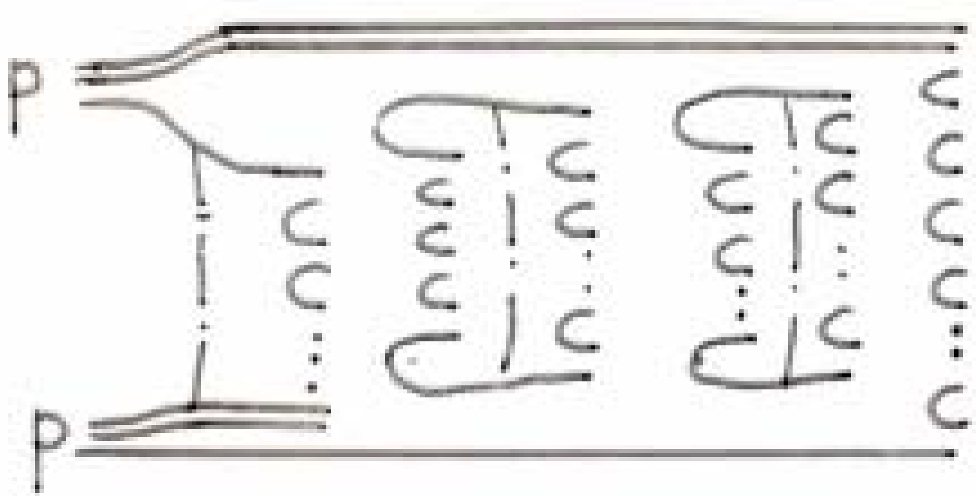

Extra chains due to sea-quarks or gluons in colliding hadrons

Quark-Gluon Strings Model.

Models of multi-particle production, based on reggeon calculus, 1/N-expansion and string dynamics:

Dual Parton Model (DPM) – Orsay,

Quark-Gluon Strings Model (QGSM) – ITEP

AGK-cutting rules determine the weights of 2k-chains configurations.

Rapidity and multiplicity distributions of final hadrons in chains can be determined theoretically.

Inclusive spectra

$$\frac{d\sigma^h}{dy} = \sum_{k=0}^{\infty} \sigma_k(\xi)\, \varphi_k^h(\xi, y) \quad ; \qquad \xi \equiv \ln \frac{s}{s_0}$$

σ_k cross section for 2k chains production

Multiplicity distribution (k=0 - diffraction)

$$\sigma_n(\xi) = \sum_{k=0}^{\infty} \sigma_k(\xi)\, W_n^k(\bar{n}_k(\xi))$$

Consider as an example $pp \to hX$

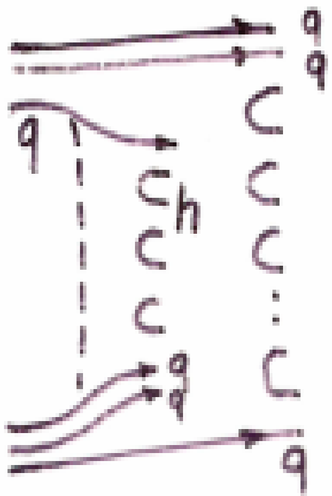

In the fragmentation region

$$\frac{x}{\sigma_2}\frac{d\sigma_2^h}{dx} = \int_x^1 dx_1\, f_p^{q(2)}(x_1)\, D_q^h\left(\frac{x}{x_1}\right)\frac{x}{x_1} +$$

+ contrib. from second chain

$x = 2p_\parallel/\sqrt{s} \equiv x_F$

$f_p^{q(2)}(x_1)$ determines how energy is devided between q and qq-chains

$$f_p^{qq(2)}(x_1) = f_p^{q(2)}(1-x_1)$$

For arbitrary configurations with both valence and "sea"-chains

$$\varphi_k^h(\xi, x) = a^h \Big\{ F_{qq}^{h(k)}(x_+) F_q^{h(k)}(x_-) + F_{qq}^{h(k)}(x_-) F_q^{h(k)}(x_+) +$$

$$+ 2(k-1) F_{q_{sea}}^{h(k)}(x_+) F_{q_{sea}}^{h(k)}(x_-) \Big\}$$

$$x_\pm = \frac{1}{2}\left(\sqrt{x^2 + \frac{4\bar{m}_\perp^2}{s}} \pm x\right) \quad ; \qquad x_+ = \exp(y - y_{max}^h)$$

$$F_i^{h(k)}(x) = \int_x^1 dx_1 \, f_p^{i(k)}(x_1) \, \tilde{D}\left(\frac{x}{x_1}\right) \frac{x}{x_1} \quad ; \qquad i = q, qq, q_{sea}$$

From analysis of planar diagrams :

$$f_p^{q(1)}(x) = \begin{cases} C_1 x^{-\alpha_R(0)} , & x \to 0 \\ C_2 (1-x)^{\alpha_R(0) - 2\alpha_N(0)} , & x \to 1 \end{cases}$$

$$\alpha_R(0) = 0.5 \quad , \quad \alpha_N(0) = -0.5$$

Interpolation formulas for $f_p^{i(k)}(x)$

e.g. $$f_p^{u_v(k)}(x_1) = C_k^{u_v} x_1^{-\alpha_R(0)} (1-x_1)^{\alpha_R(0) - 2\alpha_N(0) + (k-1)}$$

$C_k^{u_v}$ determined from normalization cond.

Inclusive spectra of different hadrons are determined by the fragmentation functions $D_i^h(z)$. From planar diagrams:

$$z D_u^{\pi^+}(z) = \begin{cases} a^{\pi} & , \quad z \to 0 \\ c^{\pi^+}(1-z)^{-\alpha_R+\lambda} & , \quad z \to 1 \end{cases}$$

$$z D_u^{\pi^-}(z) = \begin{cases} a^{\pi} & , \quad z \to 0 \\ c^{\pi^-}(1-z)^{-\alpha_R+\lambda+1} & , \quad z \to 1 \end{cases}$$

$2(1-\alpha_R(0))$

$\lambda = 2\alpha_R' \cdot \overline{p_{\perp\pi}^2} \approx 0.5$, $\alpha_R \equiv \alpha_R(0) = 0.5$

$\left(\tilde{D}_i^h(z) \equiv D_i^h(z)/a^h \right)$

Interpolation formulas for $D_i^h(z)$

e.g.

$$z D_u^{\pi^+}(z) = a^{\pi}(1-z)^{-\alpha_R+\lambda}$$

$$z D_u^{\pi^-}(z) = a^{\pi}(1-z)^{-\alpha_R+\lambda+1}$$

$$z D_u^{K^+}(z) = a^{K}(1-z)^{-\alpha_\psi(0)+\lambda_K} \cdot (1+b_K z) \; ; \quad \alpha_\psi(0) \simeq 0$$

$$z D_u^{\bar{D}^0}(z) = a^{D}(1-z)^{-\alpha_\psi(0)+\lambda_D} \cdot (1+b_D z)$$

Constants a^{π}, a^{K}, b_K can be determined theoretically.

$$a^{\pi} = 0.44$$

$$a^{K}/a^{\pi} \simeq 0.12$$

Constraints due to energy-momentum, S, B, Q,.. conservation allow one to fix parameters in many cases.

No free parameters!

The model has correct double ($x \rightarrow 0$) and triple ($x \rightarrow 1$) Regge limits.

Multiplicity distribution for a single cut Pomeron is of Poisson-type. Summary distribution is much broader.

Comparison with experiment.

Parameters of the model are determined from the data on $\sigma^{(tot)}(s)$ and $d\sigma^{(el)}/dt$

Δ=0.12÷014

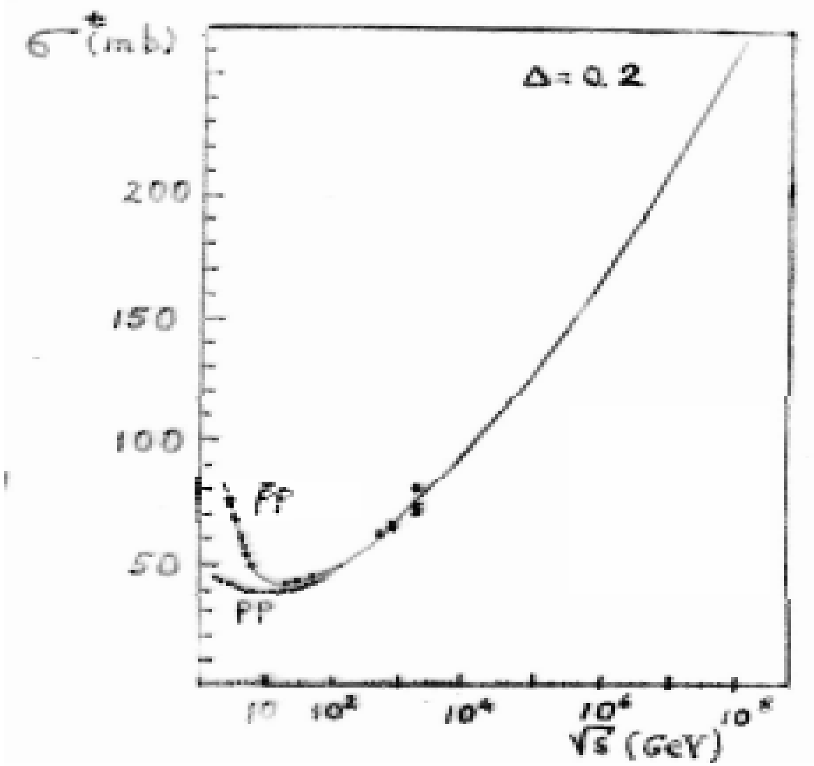

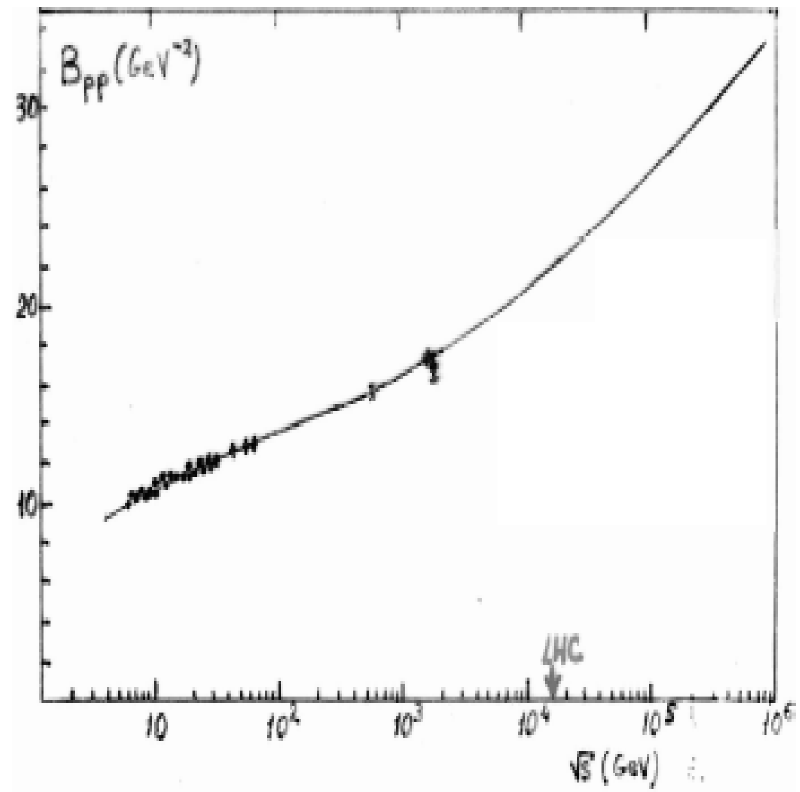

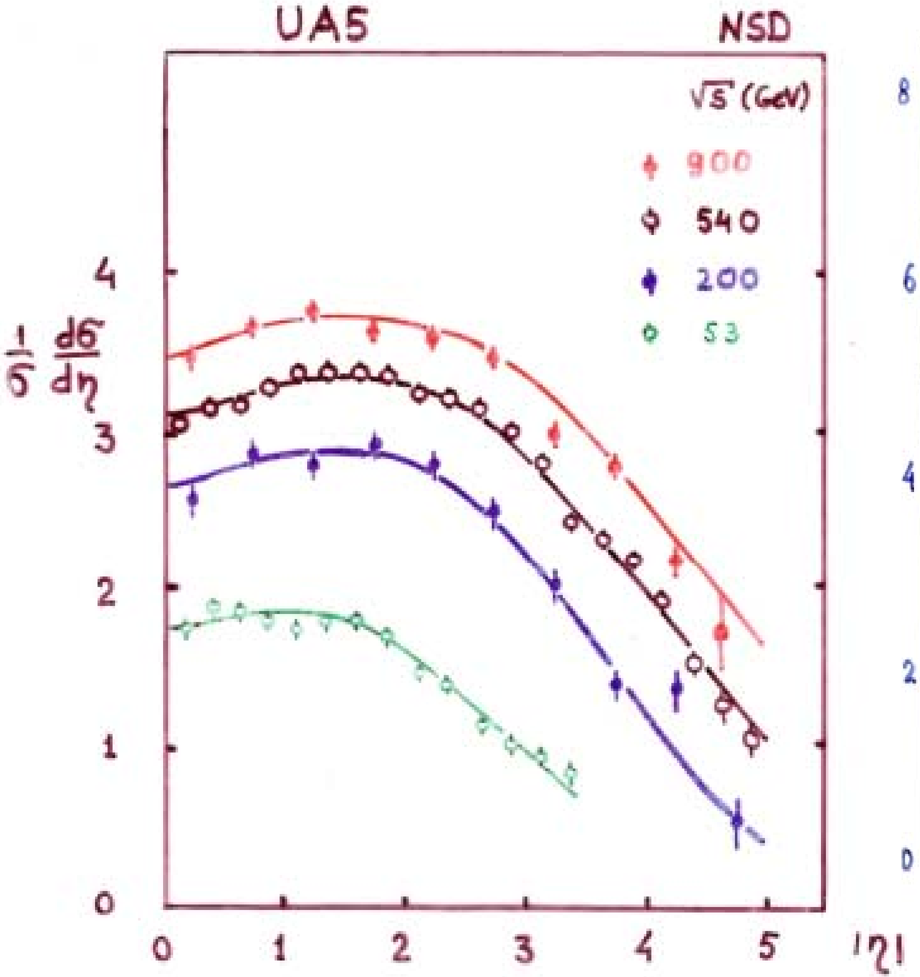

UA5
NSD
$\frac{1}{\sigma}\frac{d\sigma}{d\eta}$
$\sqrt{s}$ (GeV)
900
540
200
53
$|\eta|$

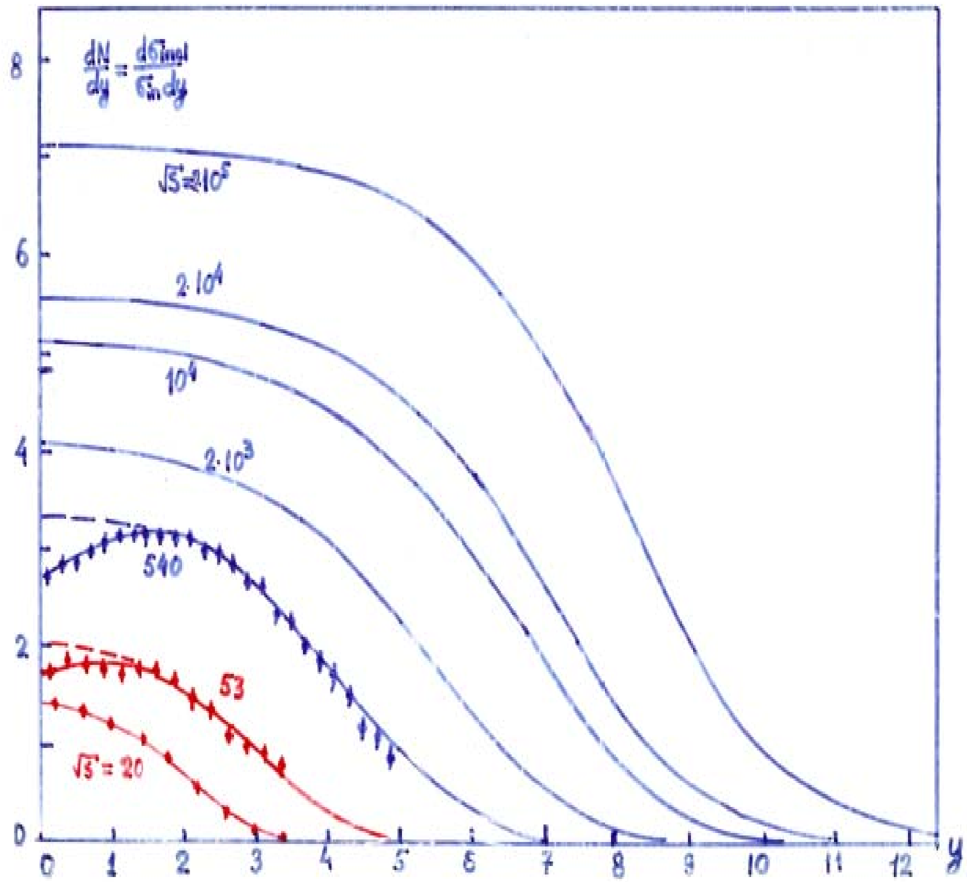

$\frac{dN}{dy} = \frac{d\sigma_{inel}}{\sigma_{in} dy}$
$\sqrt{s}=2\cdot10^5$
$2\cdot10^4$
10^4
$2\cdot10^3$
540
53
$\sqrt{s}=20$
y

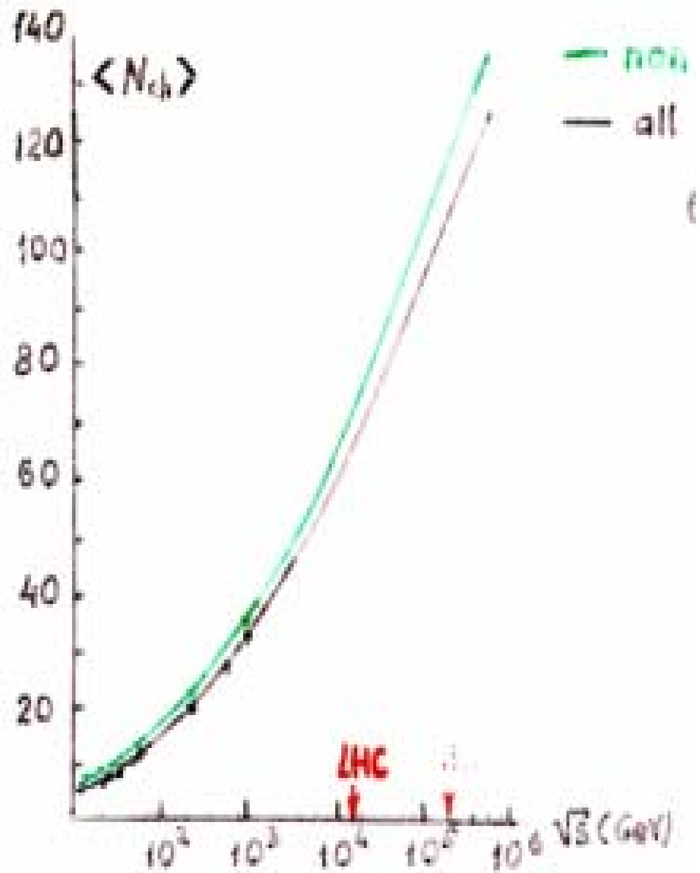

⟨N_ch⟩
non
all
LHC
√s (GeV)

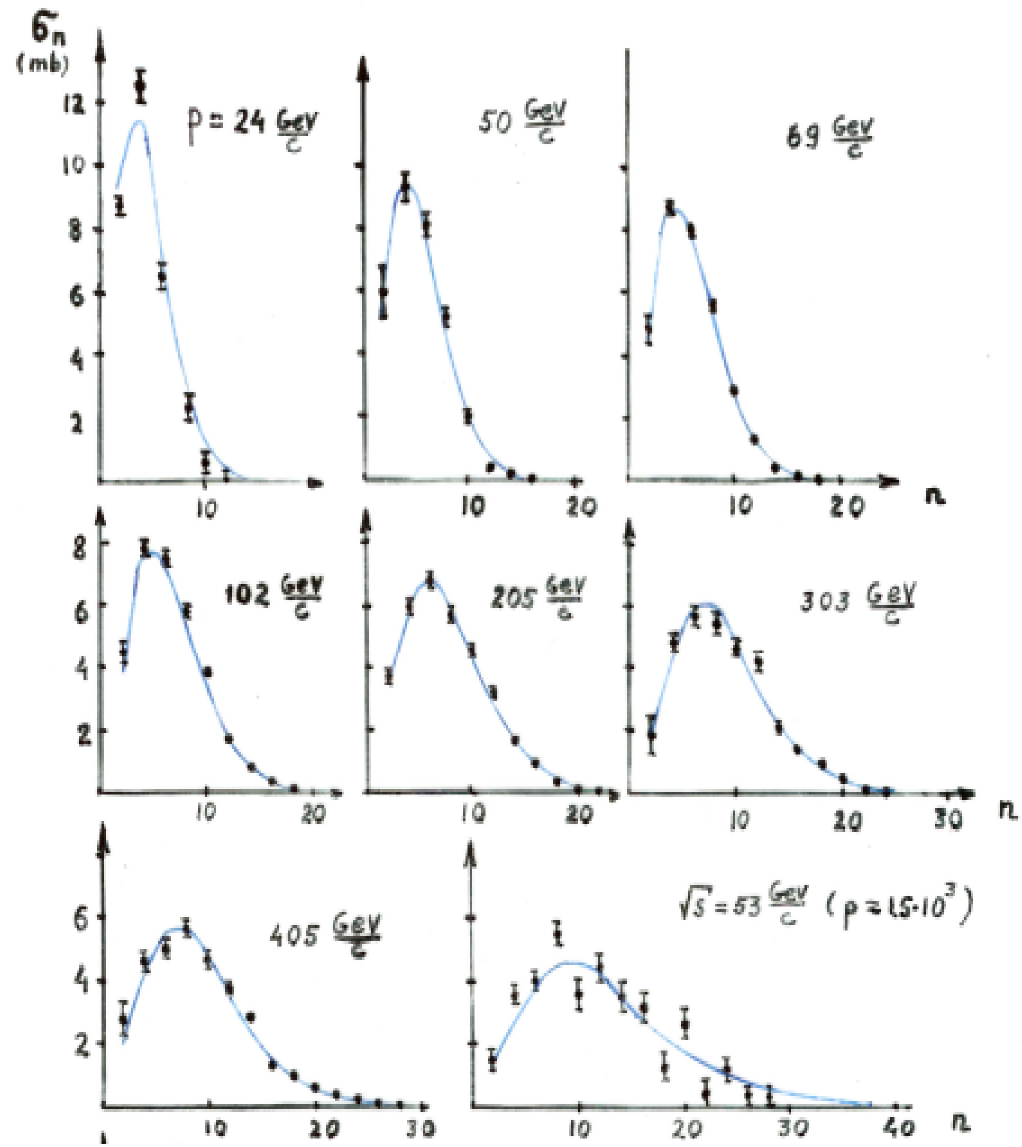

σ_n (mb)
p = 24 GeV/c
50 GeV/c
69 GeV/c
102 GeV/c
205 GeV/c
303 GeV/c
405 GeV/c
√s = 53 GeV/c (p ≈ 1.5·10³)
n

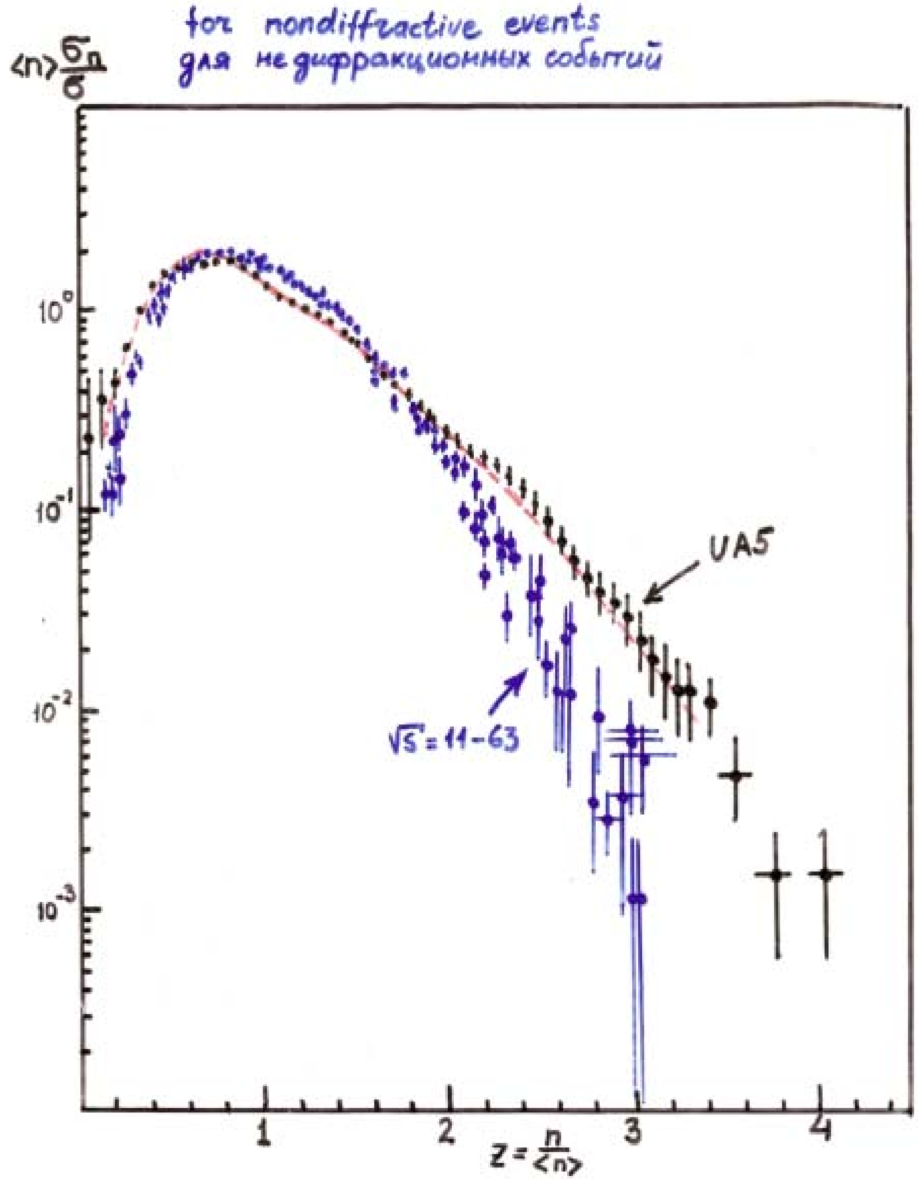

for nondiffractive events
для недифракционных событий
$\langle n \rangle \frac{\sigma_n}{\sigma}$
10⁰
10⁻¹
10⁻²
10⁻³
UA5
√s = 11-63
1
2
3
4
$z = \frac{n}{\langle n \rangle}$

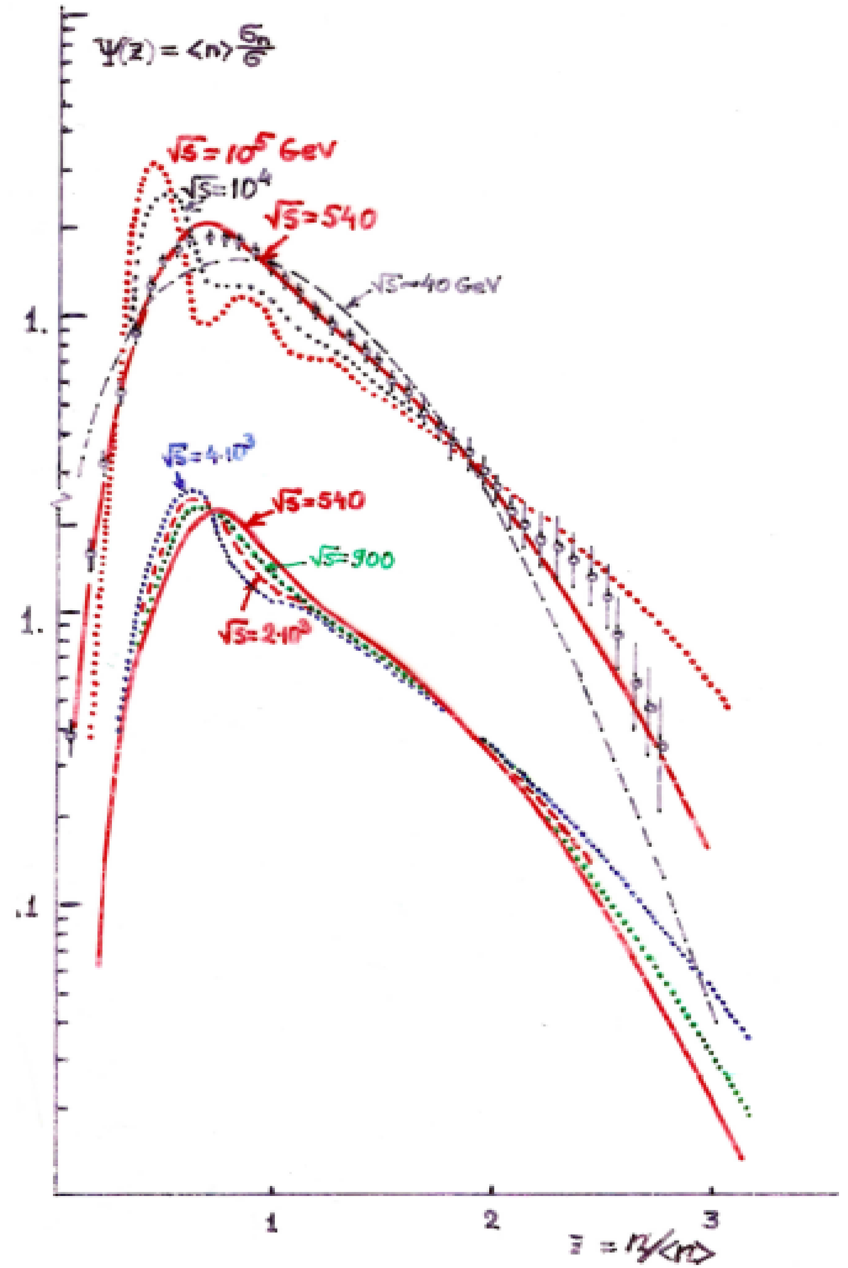

$\Psi(z) = \langle n \rangle \frac{\sigma_n}{\sigma}$
√s = 10⁵ GeV
√s = 10⁴
√s = 540
√s → 40 GeV
1.
√s = 4·10³
√s = 540
√s = 900
√s = 2·10³
1.
.1
1
2
3
z = n/⟨n⟩

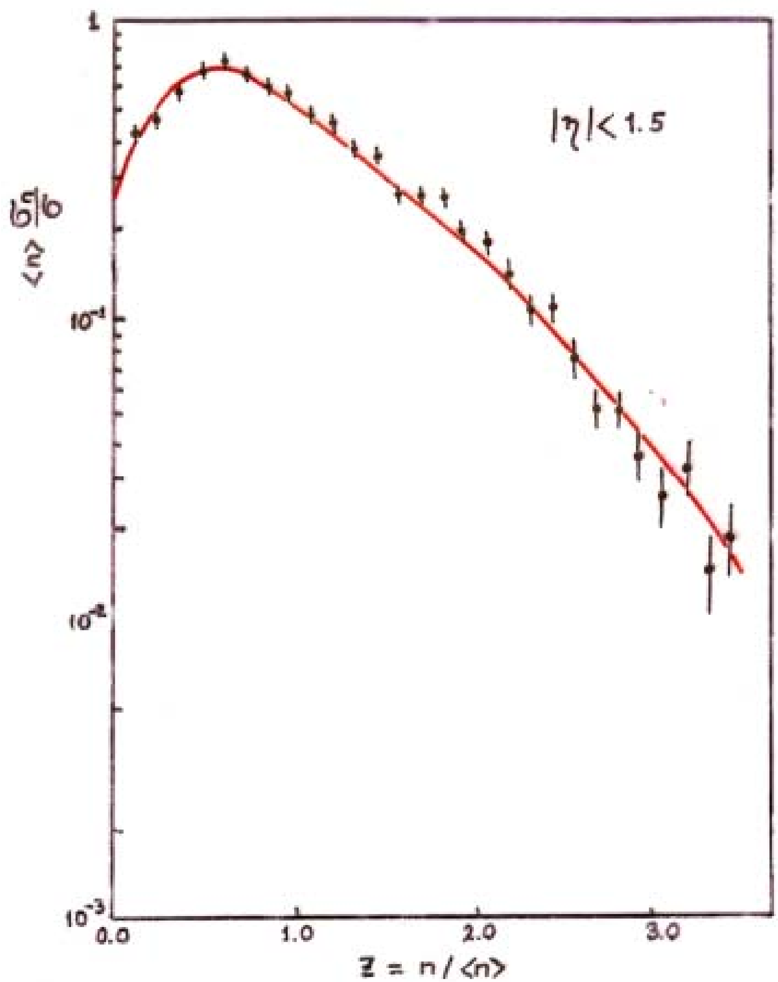

$|\eta| < 1.5$
$\langle n \rangle \frac{\sigma_n}{\sigma}$
$z = n/\langle n \rangle$

$pp \to \pi^+(\pi^-)X$

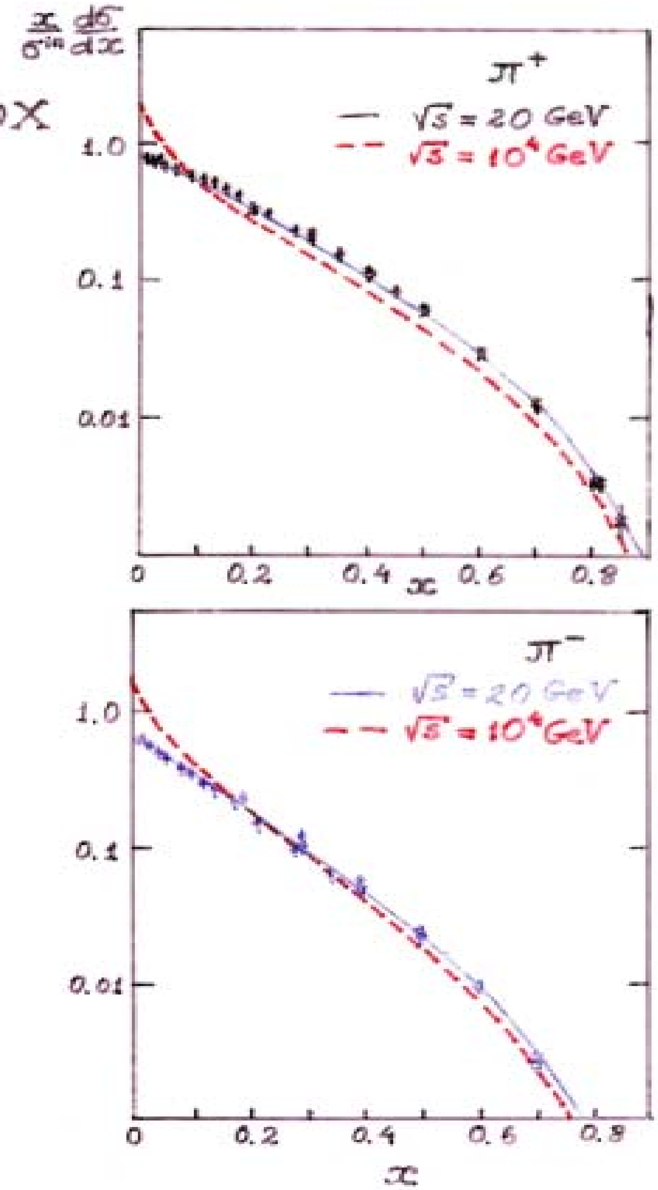

$\frac{x}{\sigma^{in}} \frac{d\sigma}{dx}$
π^+
$\sqrt{s} = 20$ GeV
$\sqrt{s} = 10^4$ GeV
π^-
$\sqrt{s} = 20$ GeV
$\sqrt{s} = 10^4$ GeV
x

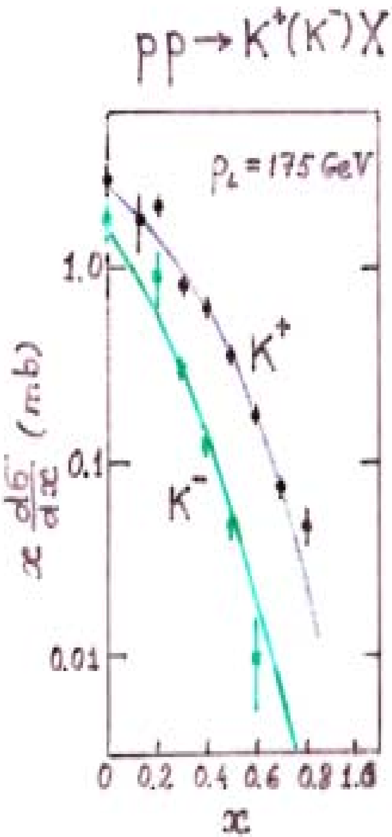
pp → K+(K-)X
pL = 175 GeV
K+
K-
x dσ/dx (mb)
1.0
0.1
0.01
0 0.2 0.4 0.6 0.8 1.0
x

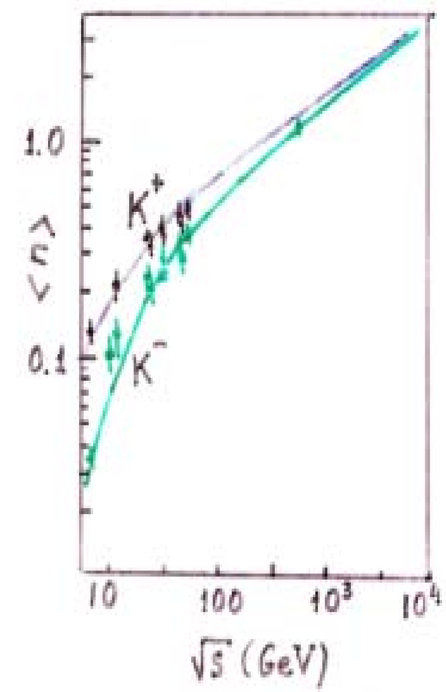
<n>
1.0
0.1
K+
K-
10 100 10³ 10⁴
√s (GeV)

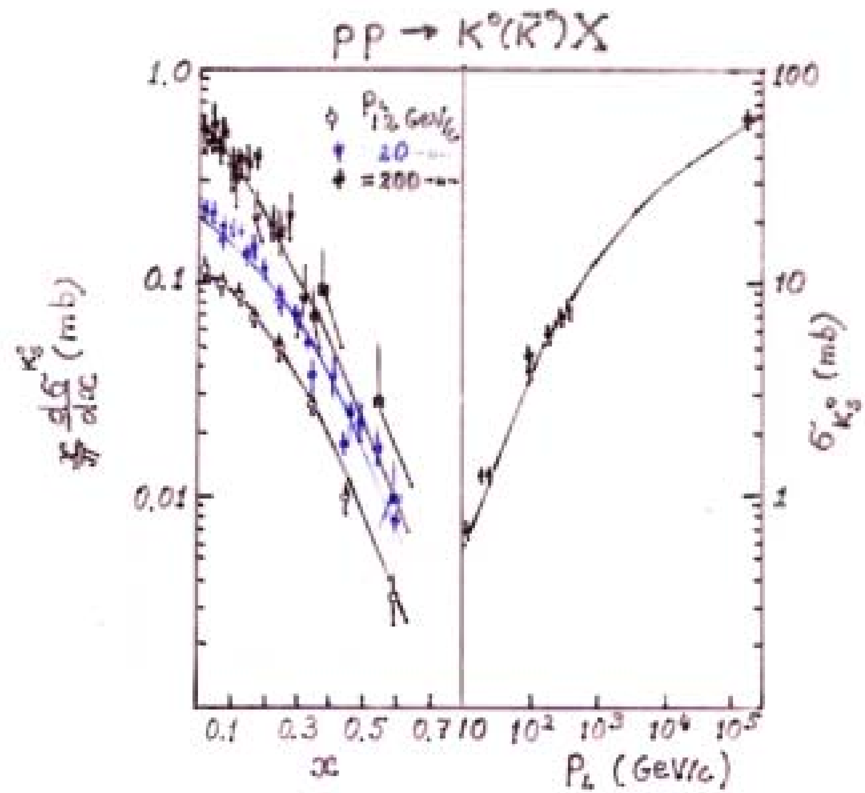
pp → K°(K̄°)X
1.0
0.1
0.01
x dσ/dx (mb)
0.1 0.3 0.5 0.7
x
10 10² 10³ 10⁴ 10⁵
PL (GeV/c)
100
10
1
σ K°s (mb)
=200

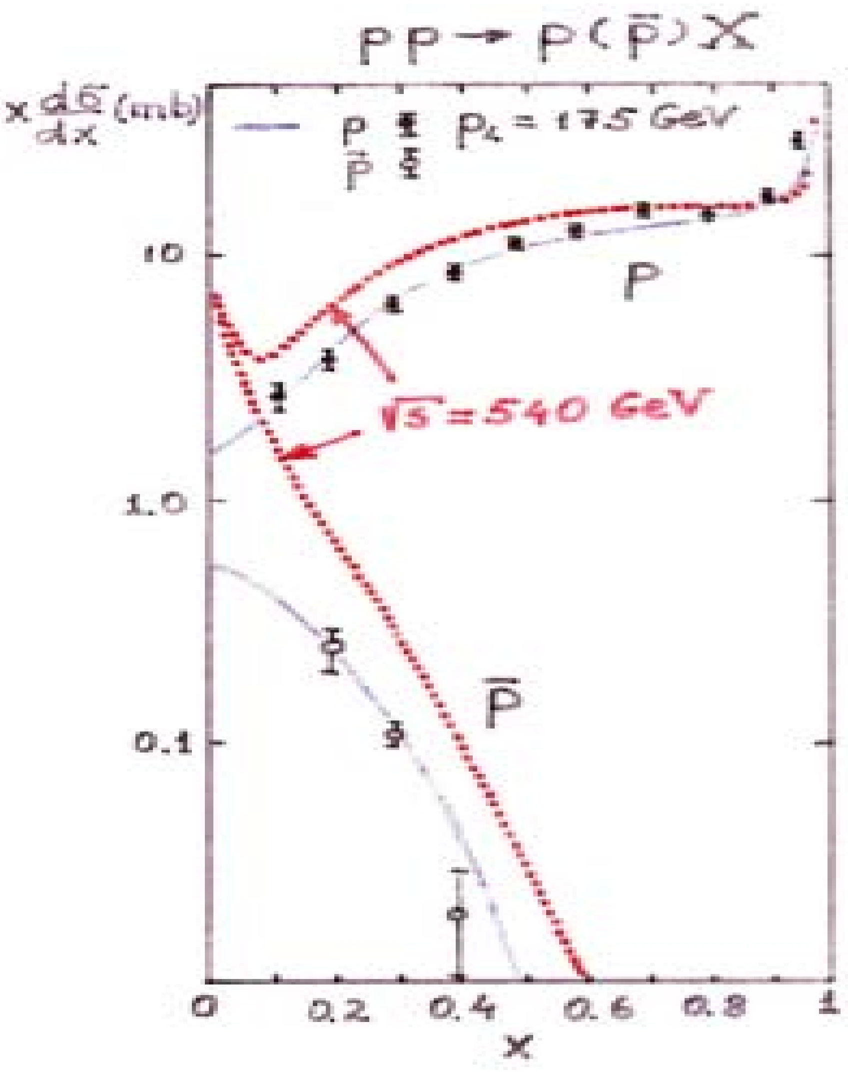
PP → P(P̄)X
x dσ/dx (mb)
P P̄ P_L = 175 GeV
√s = 540 GeV
P
P̄
10
1.0
0.1
0
0.2
0.4
0.6
0.8
1
x

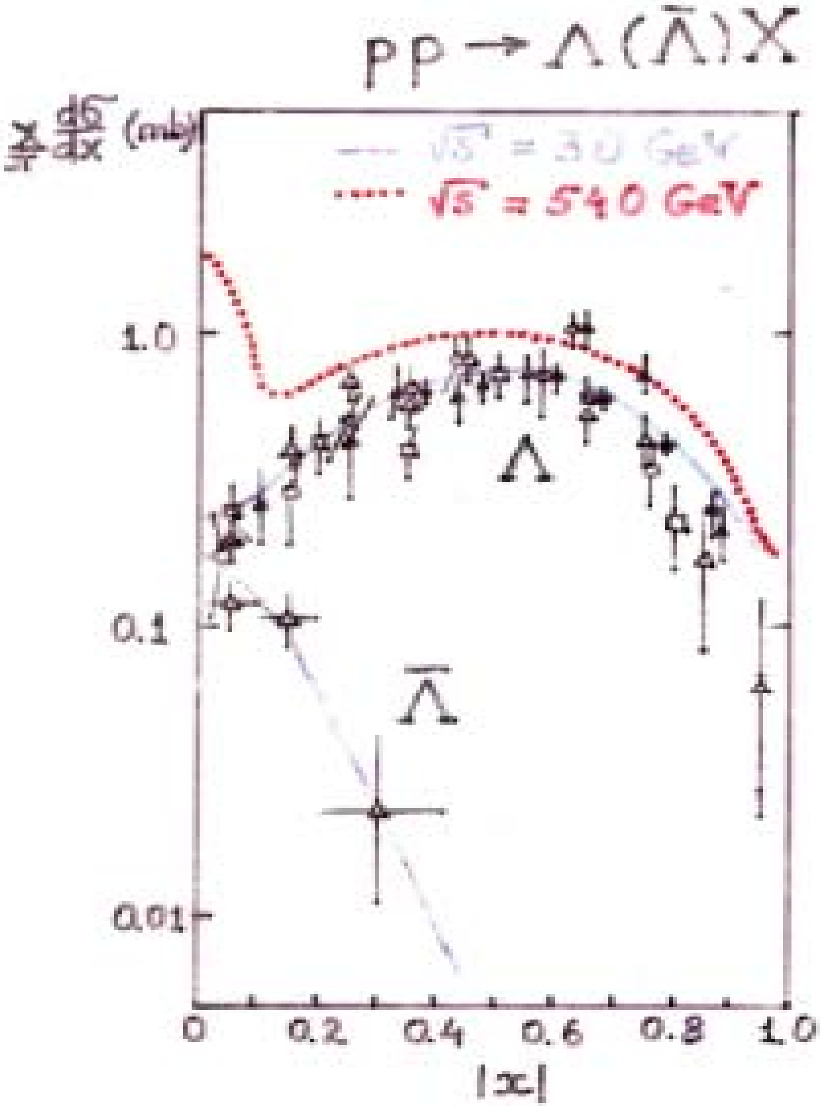
PP → Λ(Λ̄)X
x dσ/dx (mb)
√s = 30 GeV
√s = 540 GeV
Λ
Λ̄
1.0
0.1
0.01
0
0.2
0.4
0.6
0.8
1.0
|x|

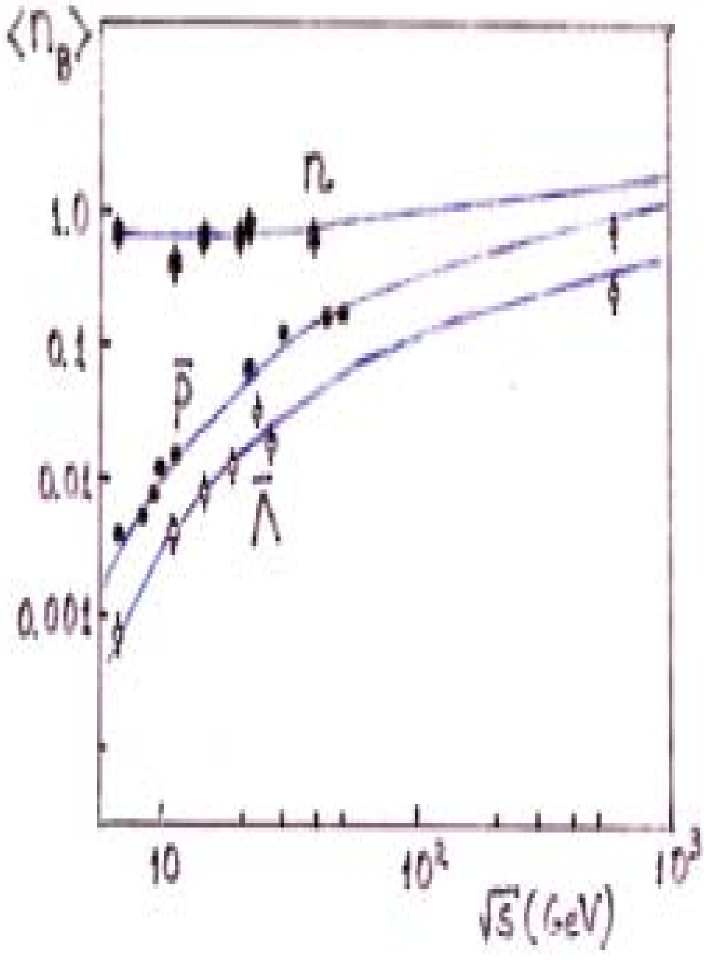

⟨n_B⟩
1.0
0.1
0.01
0.001
n
p̄
Λ̄
10
10²
10³
√s (GeV)

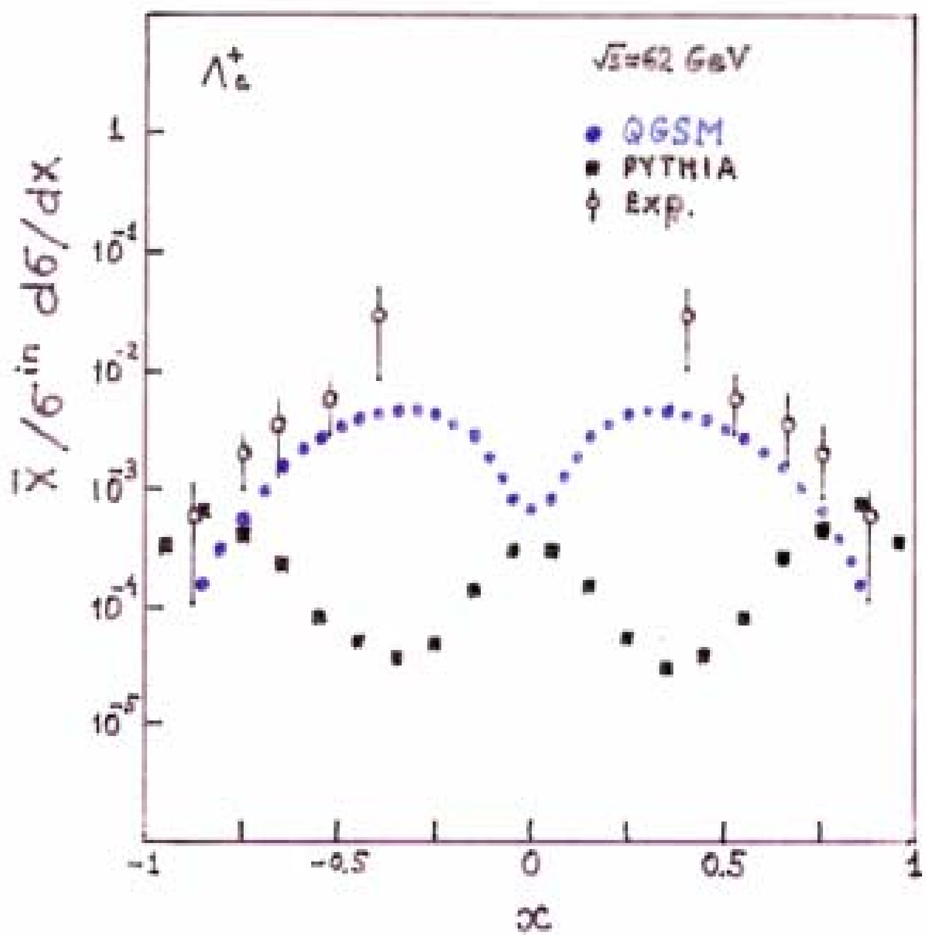

Λc+
√s=62 GeV
QGSM
PYTHIA
Exp.
x/σin dσ/dx
1
10⁻¹
10⁻²
10⁻³
10⁻⁴
10⁻⁵
-1
-0.5
0
0.5
1
x

QGSM gives a unified description of:

$$\sigma^{(tot)}_{hp}(s), \quad \frac{d\sigma^{(el)}}{dt}, \quad E\frac{d^3\sigma}{d^3p}$$

for $\pi^{\pm}, K^{\pm}, K^0(\bar{K}^0), p, \bar{p}, \Lambda, \bar{\Lambda}, ..$

$\sigma_n(s)$, correlations,…

Substantial deviations from predictions of the model at superhigh energies would indicate to a new physics.

Lecture 3
Hadronic physics at LHC

Small x-physics and “saturation” problem.

Fast increase of the structure function F2

in deepinelastic scattering as x→0 ($x = \frac{Q^2}{W^2+Q^2}$).

$$\sigma^{(tot)}_{\gamma^* p}(W^2, Q^2) = \frac{4\pi\alpha_{e.m.}}{Q^2}\, F_2(x, Q^2)$$

This fast increase should be stopped by unitarity effects.

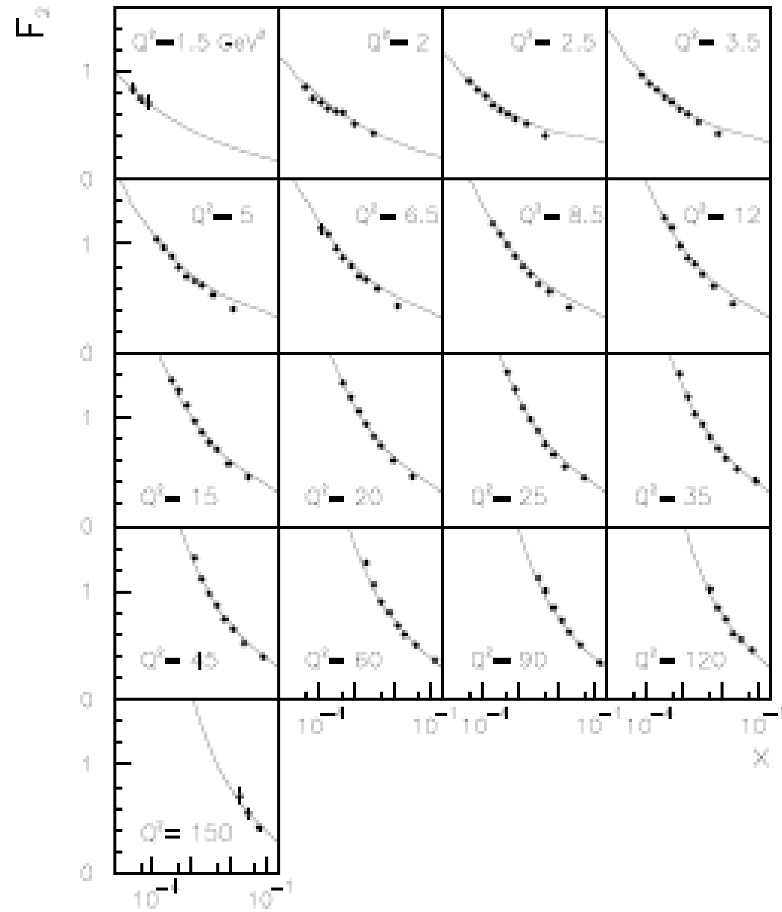

“Saturation” problem.

From DIS data distributions of quarks and gluons are extracted.

- H1+ZEUS combined NLO DGLAP fit yields impressive precision

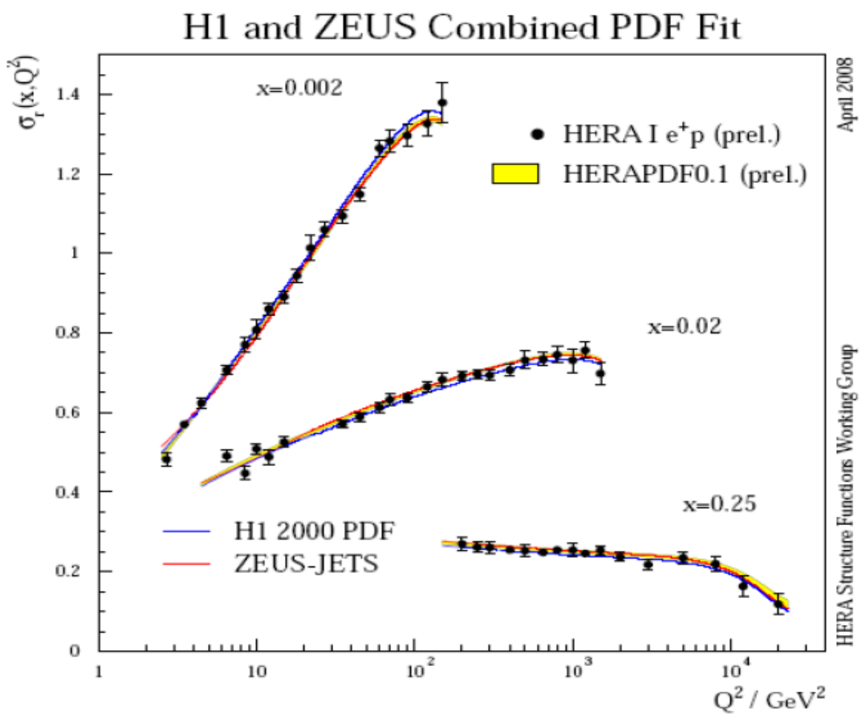

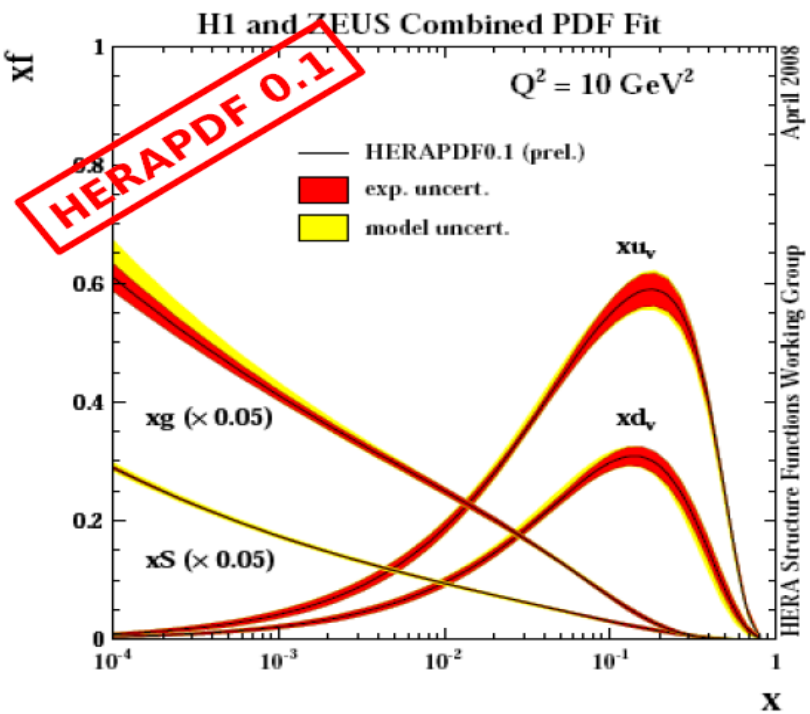

Just based on HERA-I NC&CC data sets
→ more to come!

“Saturation” problem.

It is reasonable to assume that at very small x the increase of parton densities will be stopped and “saturation” will be achieved.

It is important to determine the border of the saturation region $Q_s(x)$.

“Color glass condensate” in PQCD.

L.Mc Lerran et.al.

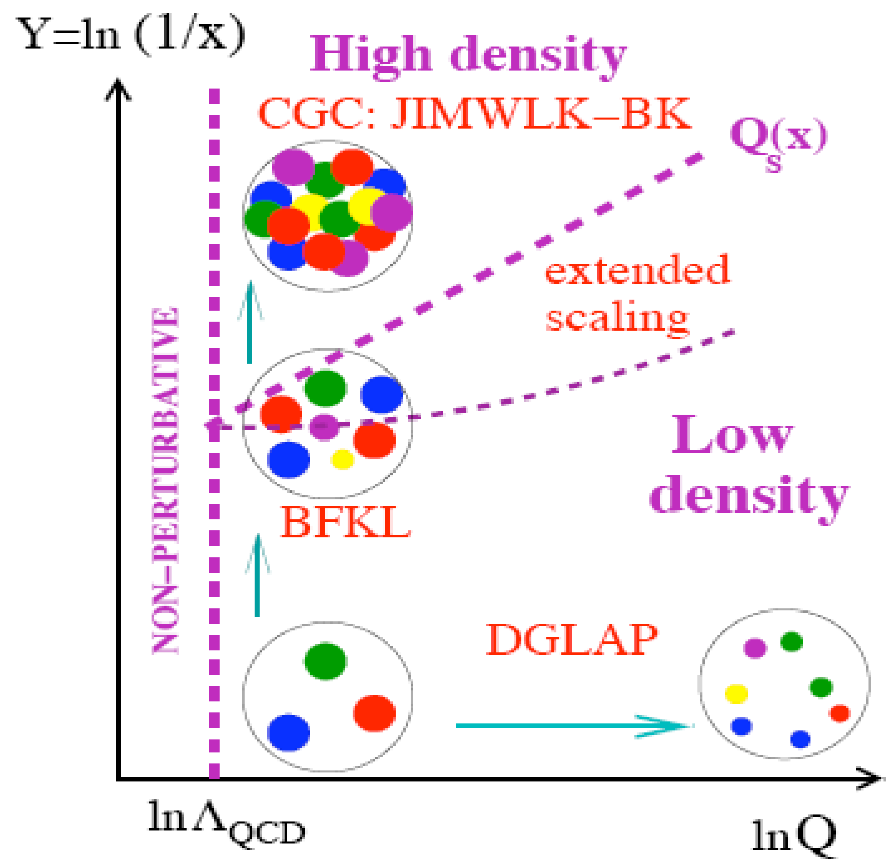

“Saturation” problem.

Saturation is achieved earlier for nuclei, where densities of partons are higher (by $A^{1/3}$ at fixed impact parameter).

This phenomenon is very general and in reggeon theory is due to multi-pomeron contributions. In the reggeon calculus approach it is possible to describe F_2 in a broad region of Q^2 starting from $Q^2=0$.

CFKS

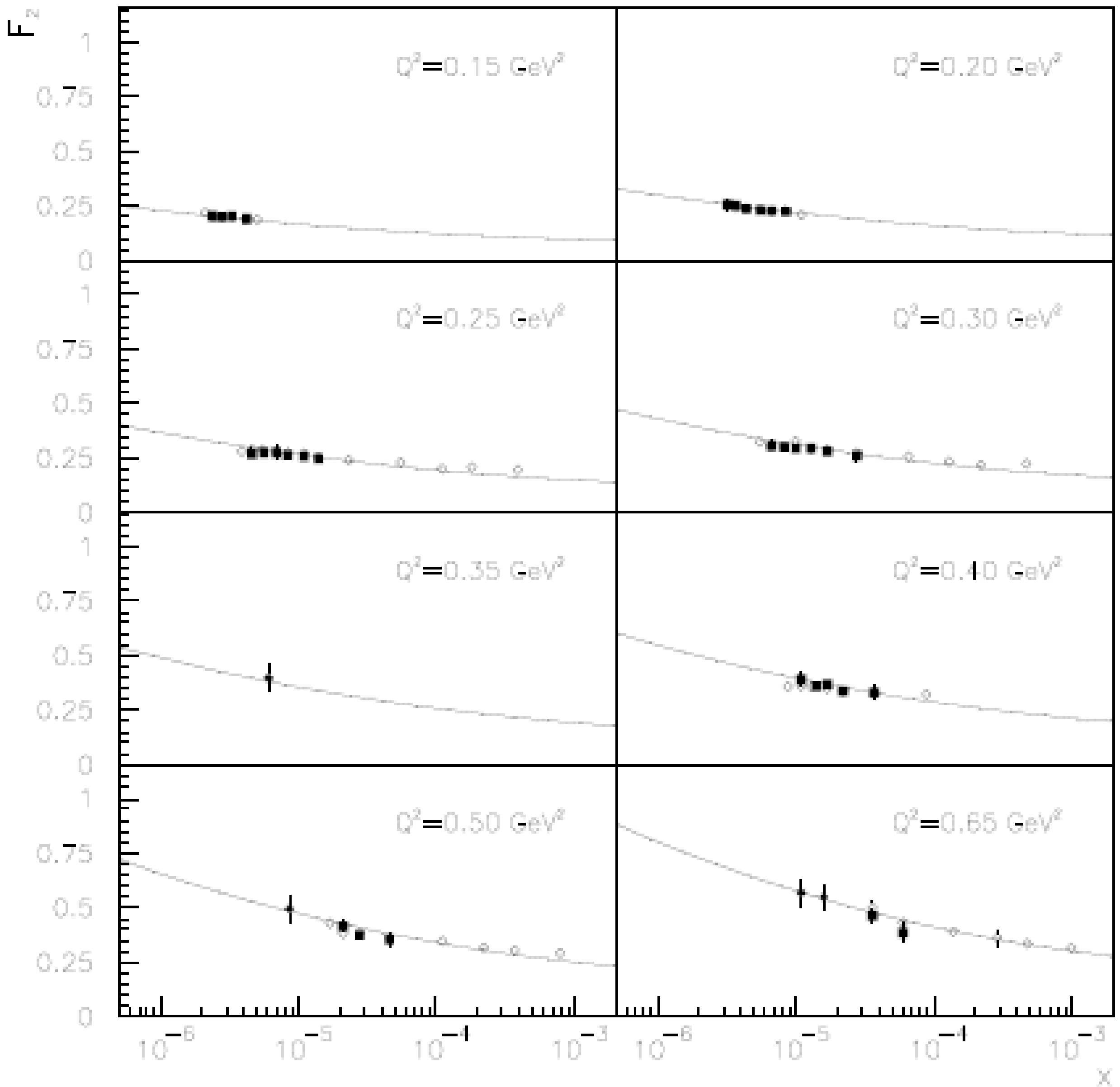

F_2
Q^2=0.15 GeV^2
Q^2=0.20 GeV^2
Q^2=0.25 GeV^2
Q^2=0.30 GeV^2
Q^2=0.35 GeV^2
Q^2=0.40 GeV^2
Q^2=0.50 GeV^2
Q^2=0.65 GeV^2
0
0.25
0.5
0.75
1
10^{-6}
10^{-5}
10^{-4}
10^{-3}
x

Interactions of pomerons.

Shadowing effects for partons as x→0 are especially important at superhigh energies (LHC, cosmic rays) as

$$x_1 x_2 = \frac{M^2}{s}.$$

This problem is closely related to existence of large-mass diffraction and to interactions between pomerons (“enhanced diagrams”).

Large mass diffraction and "enhanced" diagrams.

For large masses $M^2 \gg 1\ \mathrm{GeV}^2$

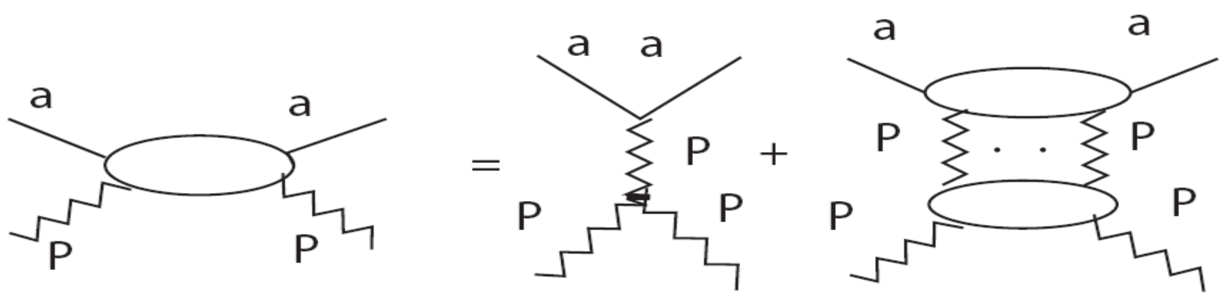

Triple-pomeron and n→2 pomeron vertices. In general there are n→m P vertices g_m^n

In eikonal approximation $g_m^n = C g^{n+m}$

This is natural from point of view of t-channel unitarity.

Relation of diffraction to pomeron interactions

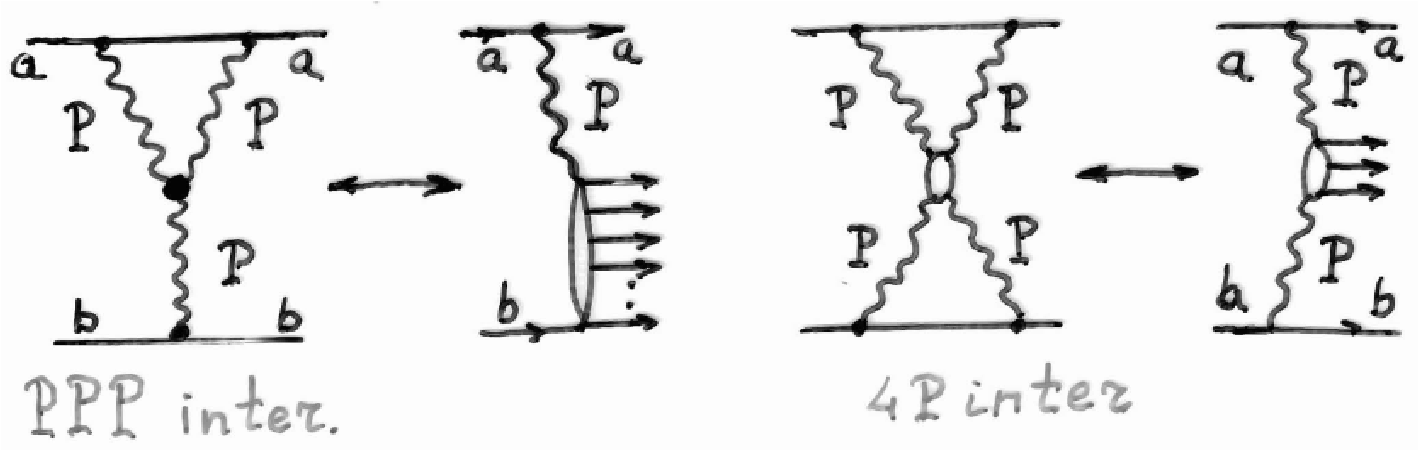

In 1/N-expansion correspond to the diagrams

Different approaches to the theory of interacting pomerons.

Theory of supercritical pomeron with triple-pomeron interactions is studied since 70-ies D.Amati et al (1976)

It is not clear that such theory is consistent with s and t-channel unitarity.

Partonic interpretation indicates that 4P-interaction is necessary for consistency.

K.Boreskov (2001)

S.Bondarenko et al (2006)

Different approaches to the theory of interacting pomerons.

Summation of all enhanced diagrams

with $g_m^n = Cg^{n+m}$ has been performed by

A.K., K.Ter-Martirosyan, L.Ponomarev (KT-MP) (1986).

Good description of pp

total cross section, elastic scattering

and σ_{SD} with Δ=0.2. Correct predictions of single diffraction dissociation cross section

for Tevatron.

Diffractive processes and exclusive Higgs production.

Note a substantial increase of Δ compared to Δ_{eff}. Triple-pomeron coupling is about 3 times larger than the effective one.

Important role of limitations on rapidity gaps $\delta y > y_0$.

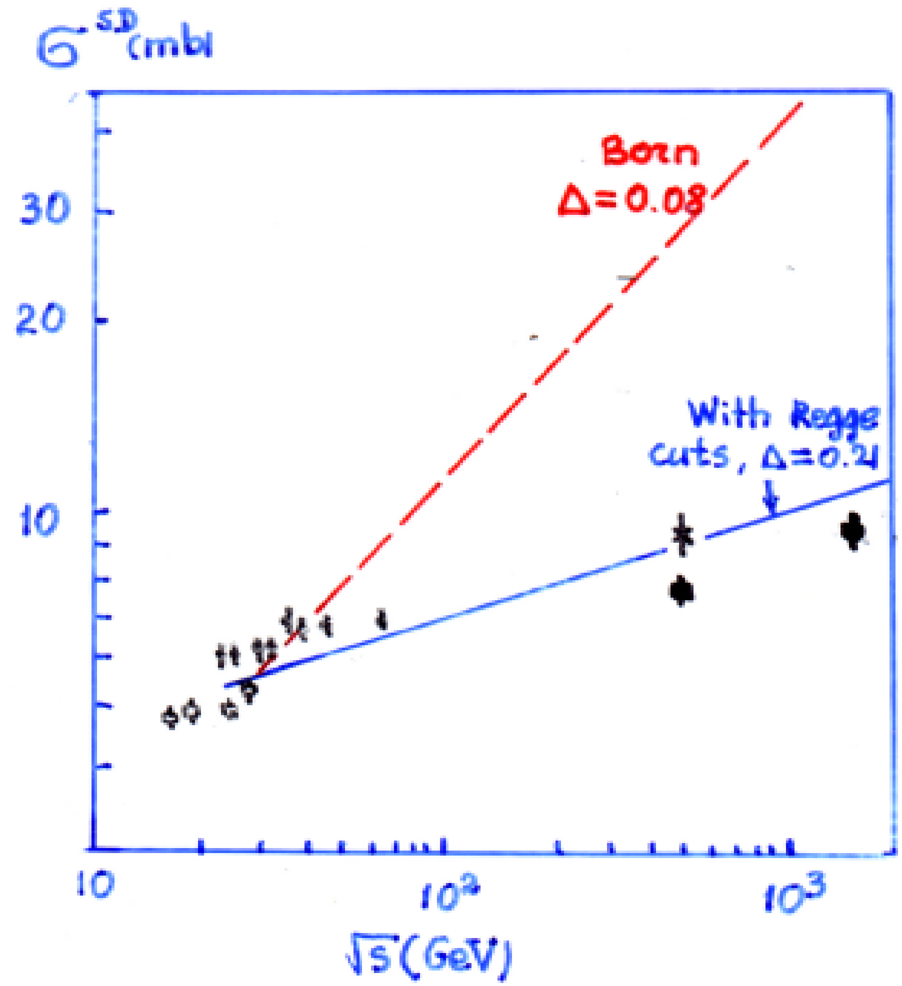

Description of large mass diffractive production.

Detailed description of large mass diffractive production with account of multi-pomeron exchanges in a simplified model

M.Poghosyan et al (2007)

Single diffraction

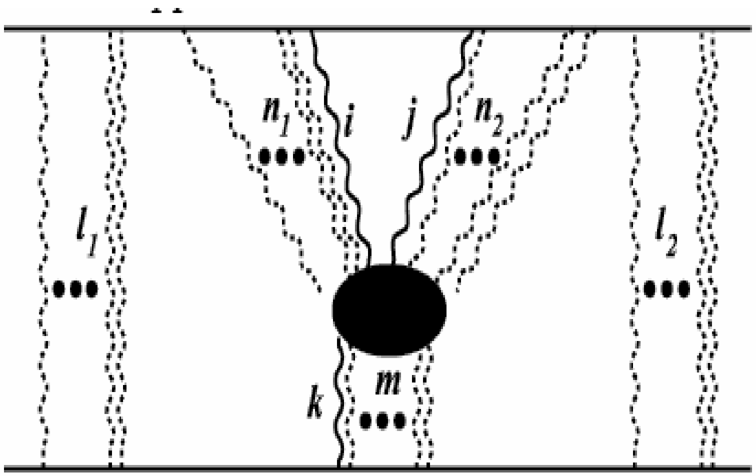

Double diffraction

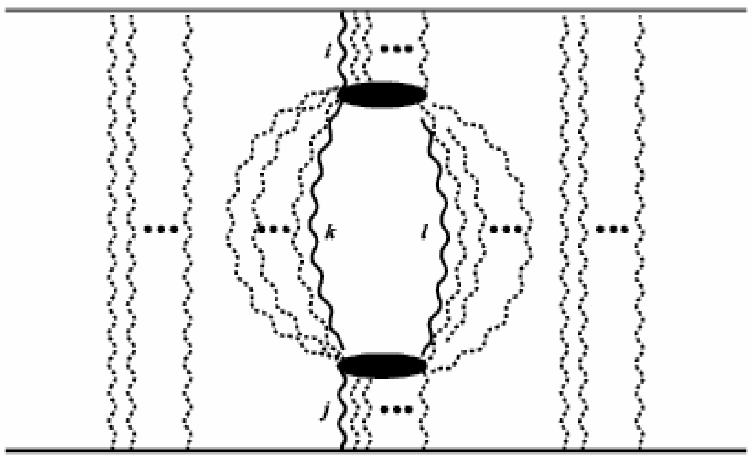

P, R-exchanges are taken into account

Description of data on single DD

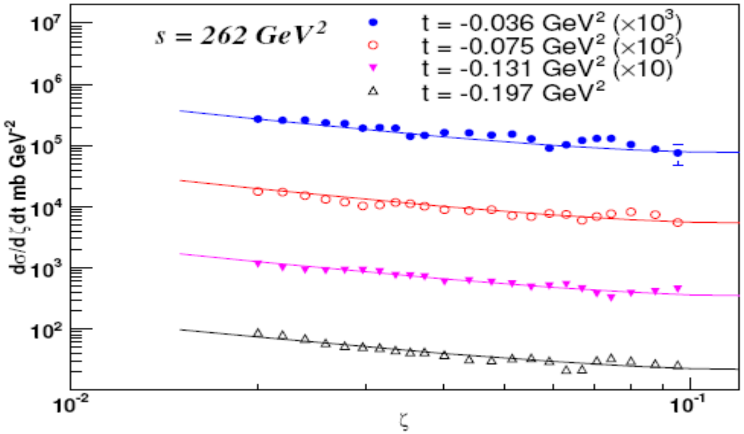

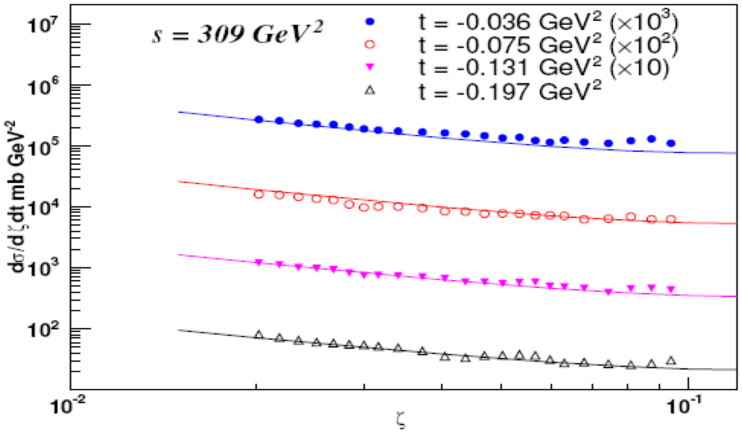

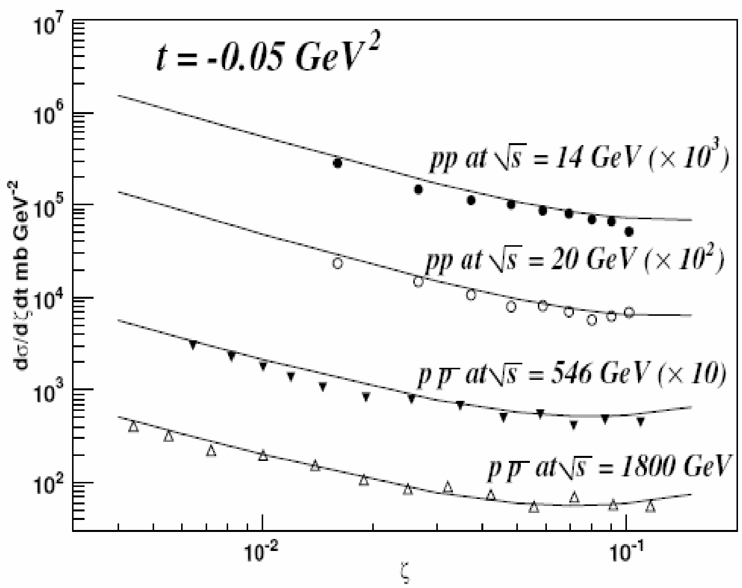

Description of data on double diffraction production.

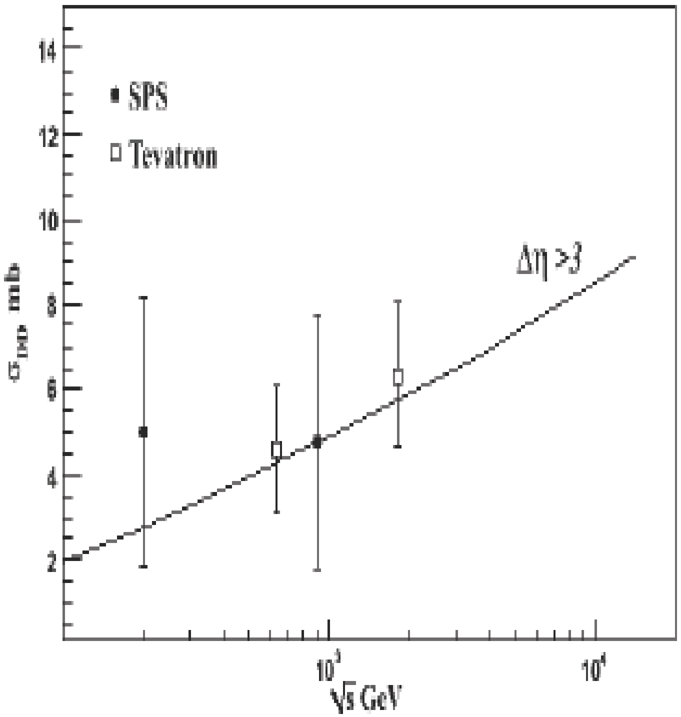

Double diffraction				
$\sqrt{s}$ *GeV*	Kinematic region	Data *mb*	Model *mb*	Experiment
200	$\Delta\eta > 2.5$	3.5 ± 2.2	4.0 ± 0.14	UA5
630	$\Delta\eta > 3$	$4.58 \pm 0.02 \pm 1.5$	4.1 ± 0.15	CDF
900	$\Delta\eta > 2.5$	4 ± 2.5	6.39 ± 0.23	UA5
1800	$\Delta\eta > 3$	$6.32 \pm 0.03 \pm 1.7$	5.73 ± 0.22	CDF

Hard diffraction.

Regge pole approximation for hard diffraction

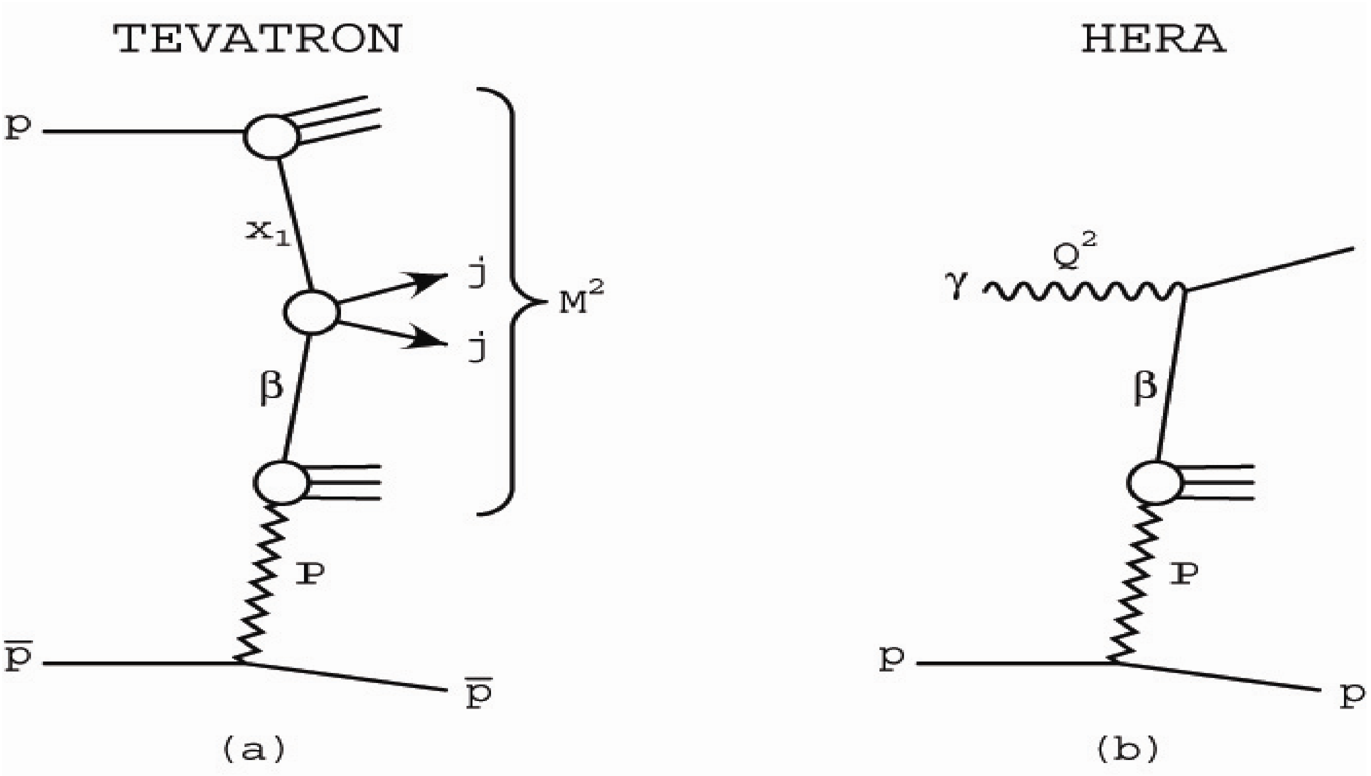

Unitarity effects for hard diffractive processes.

Both Regge and QCD factorizations of the lowest order diagrams are strongly broken due to multipomeron exchanges (unitarity effects).

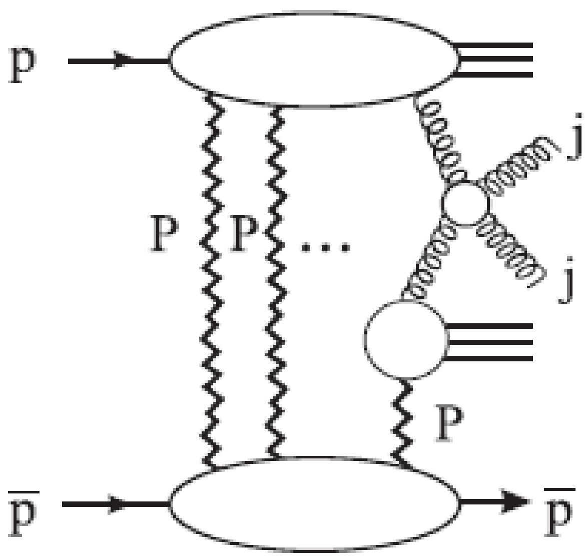

Same effects for double gap configurations.

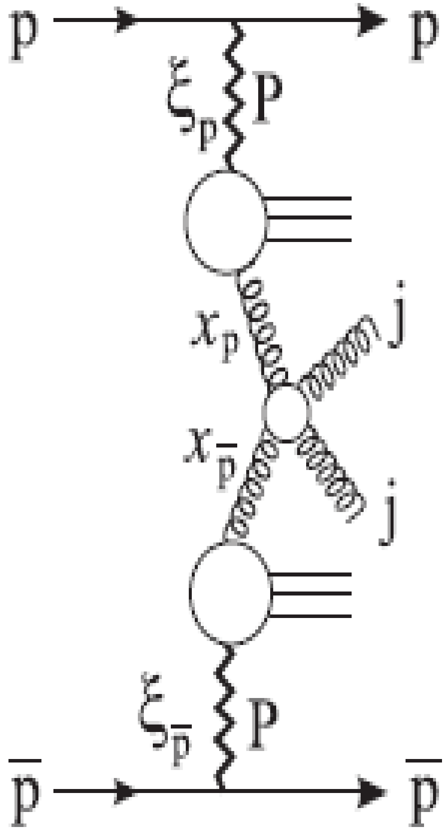

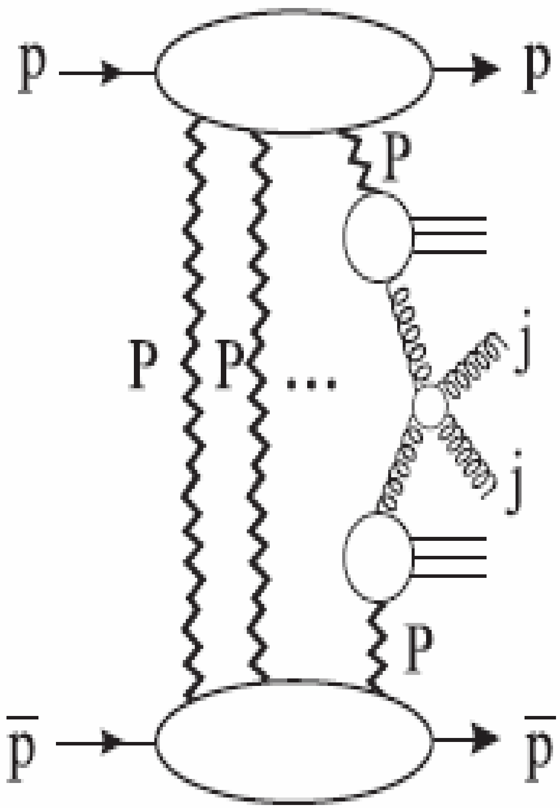

DPE Higgs production.

Central exclusive production of a Higgs boson at very high energies.

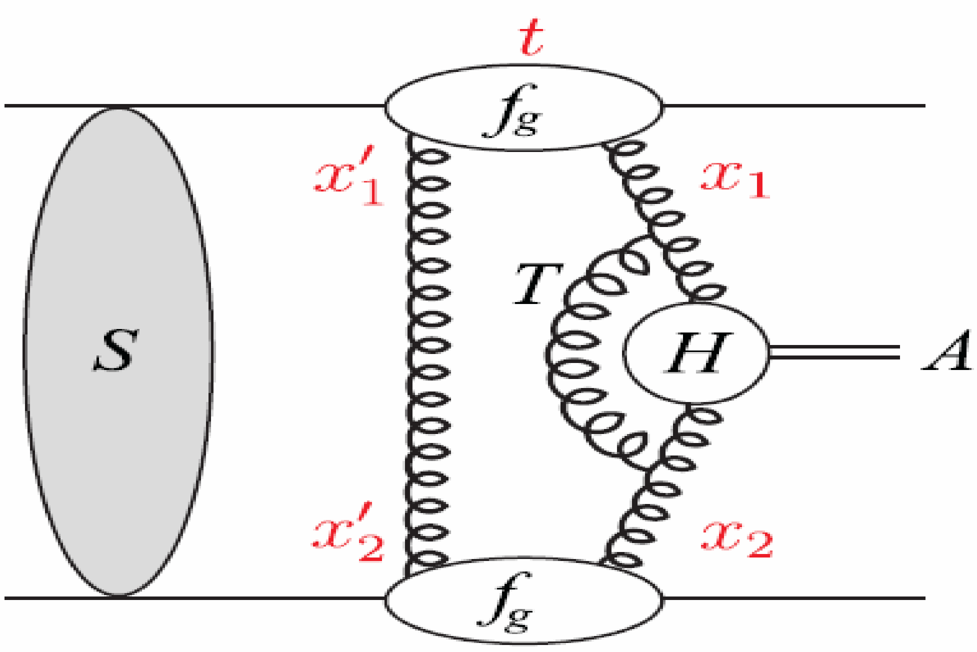

Why?

- Excellent mass resolution ~3 GeV
- Spin-parity analyser

  Possibility to investigate CP structure of Higgs system
- Reduced backgrounds

Higgs production at LHC

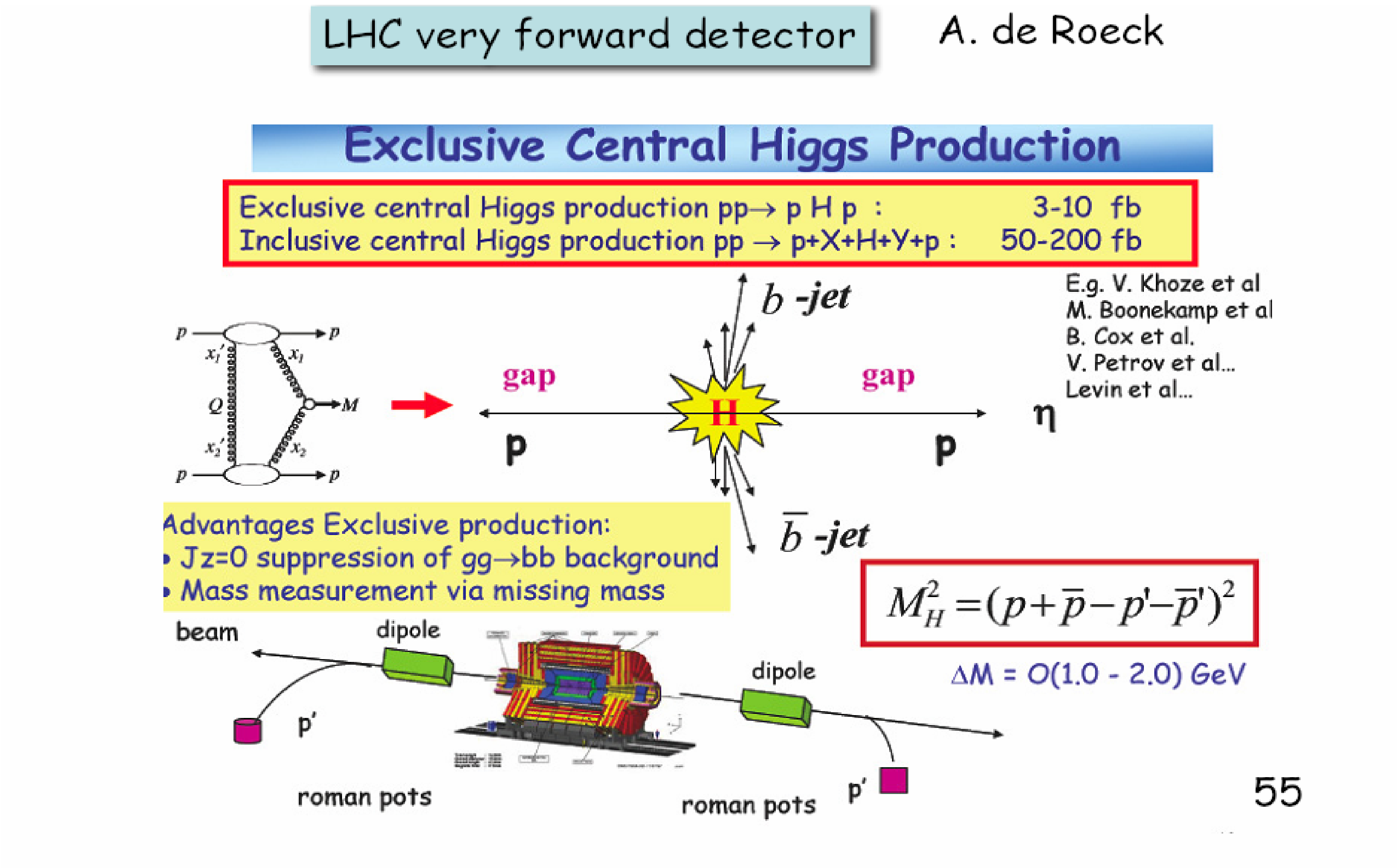

Survival probability.

A value of suppression of cross section of diffractive production process compared to the "born" (Regge pole exchange) approximation is often called "survival probability" - S^2.

In the eikonal approximation:

$$S^2 = \frac{\int |\mathcal{M}(s,b)|^2 e^{-\Omega(b)} d^2b}{\int |\mathcal{M}(s,b)|^2 d^2b},$$

$$\Omega(b) \equiv -4i\delta_P(s,b)$$

$e^{-\Omega(b)}$ -probability not to produce particles (to fill the gap)

Consequences of unitarity effects.

Generalization to several channels is straightforward.

Strong suppression of inelastic diffraction in the region of small b,

where Ω»1. Inelastic diffraction occur at the periphery of interaction region, where nonperturbative effects are essential.

Suppression in diffractive Higgs production.

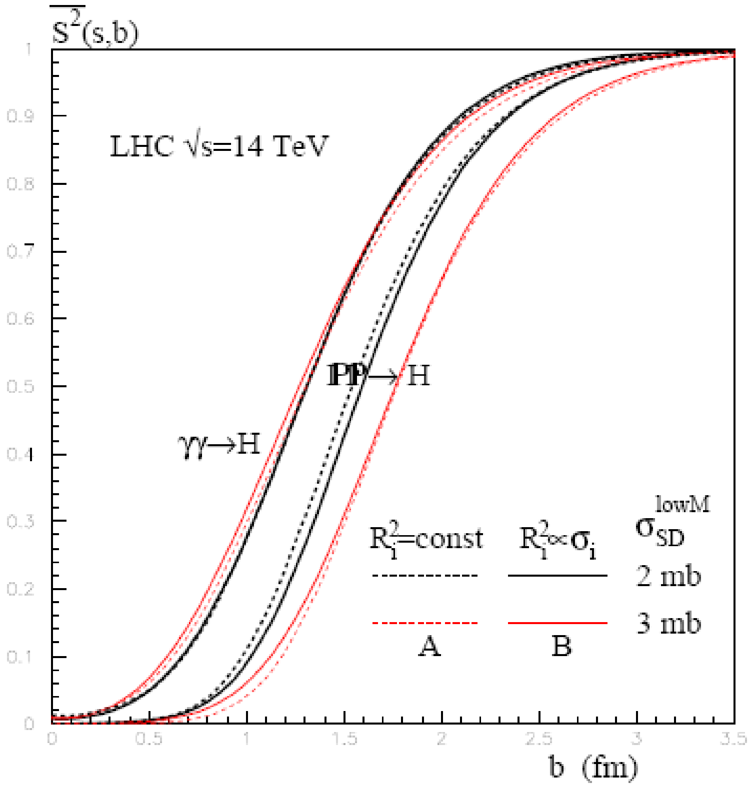

From V.Khoze, A.Martin, M.Ryskin (KMR) (2007)

Double pomeron Higgs production at LHC is effective for b > 1fm.

Suppression for different processes is not universal.

Suppression of diffractive dijets at Tevatron.

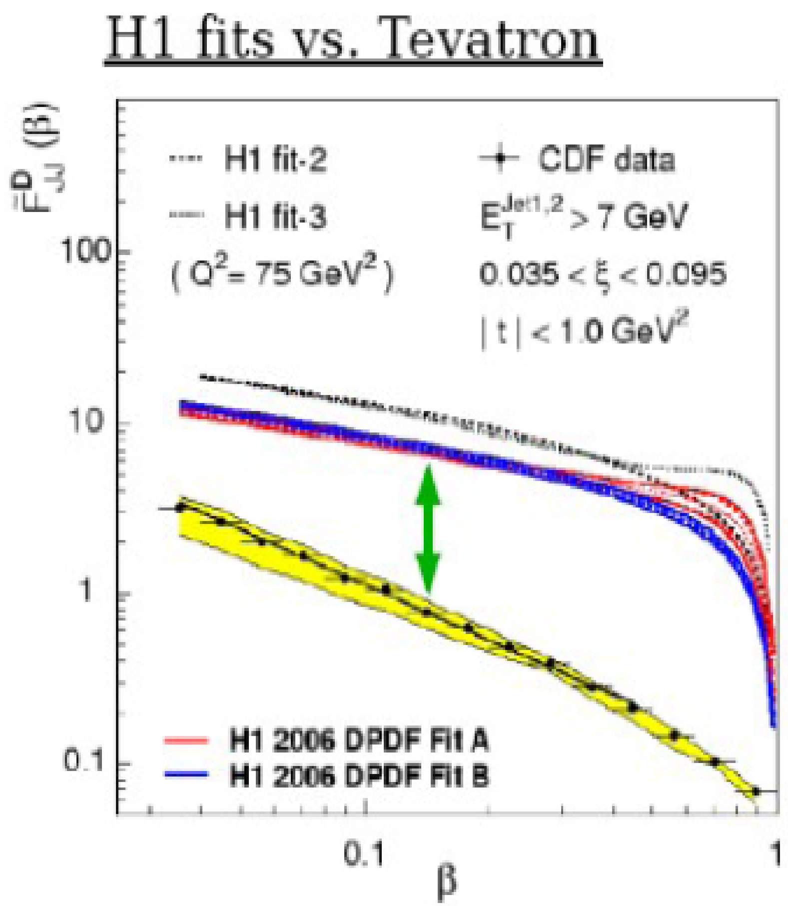

Suppression in hadronic interactions is due to multipomeron exchanges.

V.Khoze et al (KKMR)

describe CDF data in multi-channel eikonal model.

Important for Higgs production at LHC.

Role of diagrams with interactions of Pomerons.

How large are extra shadowing effects due to pomeron interactions?

a) Small for H due to threshold effects.

KKMR (2001)

b) Can be substantial.

PQCD estimate by

J.Bartels et al (2006)

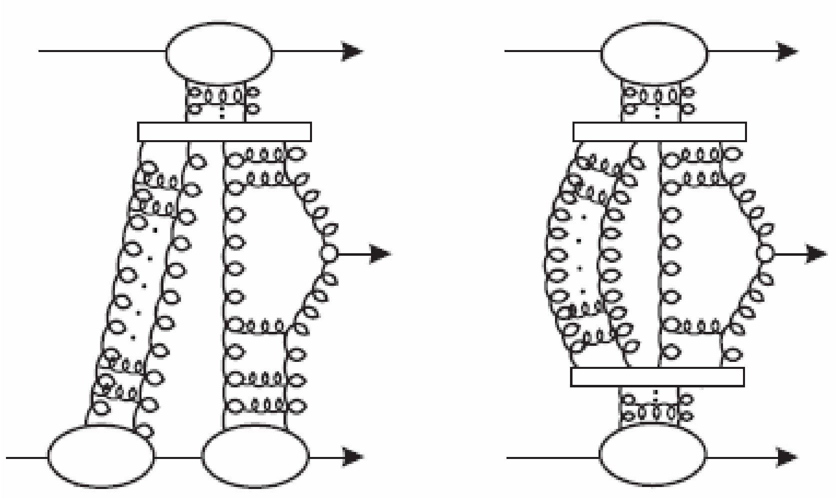

Recent calculations of rapidity gap survival.

Durham group KMR (2007) approach

Multi-P vertices $$g_m^n = Cnmg^{n+m}$$

Different approach by Tel-Aviv group

E.Gotsman, E.Levin,U.Maor,J.S.Miller (2008)(GLM)

Motivated by PQCD pomeron, only diagrams with triple-pomeron interaction are considered (besides 2-channel eikonal).

For pp σtot, dσel/dt, σSD, σDD are described. Δ=0.33

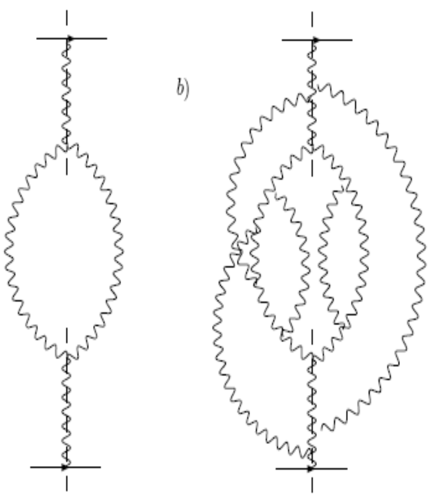

Role of enhanced diagrams.

Recent calculation of

S^2_{enh} by KMR (2008).

Threshold effects play an important role.

S^2_{enh} can be essential for soft processes.

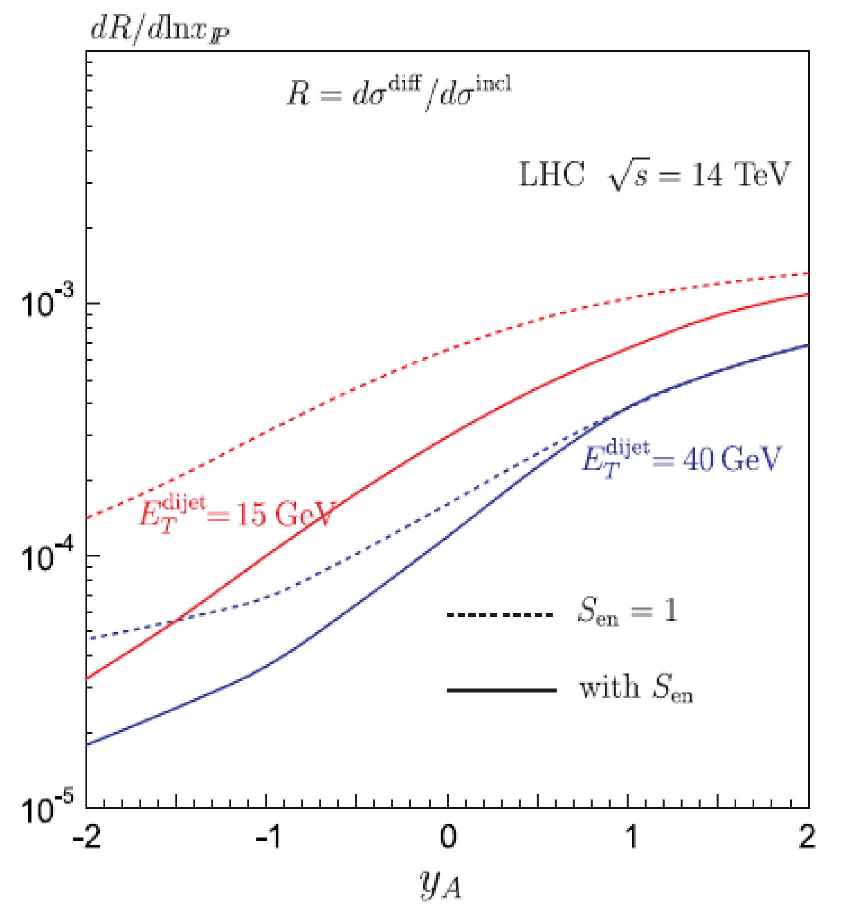

Bounds on S^2_{enh} from experiment.

From analysis of CDF data on diffractive dijets one can conclude that effects due to enhanced diagrams do not exceed 50%.

Same conclusion follows from analysis of HERA data on spectra of leading neutrons.

KKMR (2006)

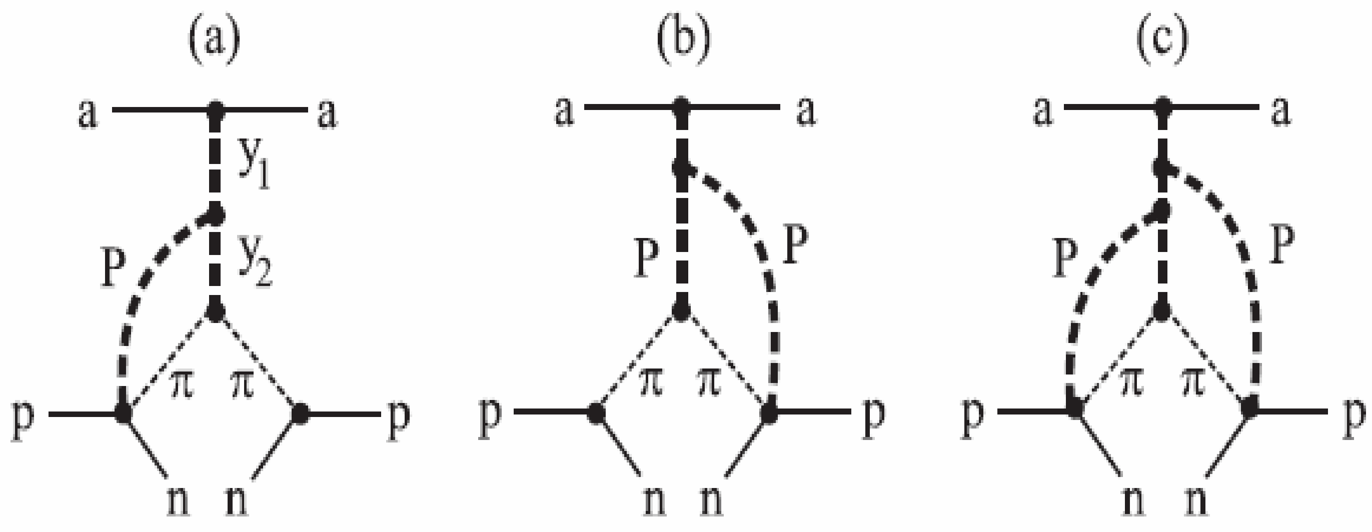

Bounds on S^2_{enh} from experiment.

Most direct test of

the role of enhanced

diagrams in DPE

exchange is provided

by the data on central, exclusive diffractive double jet production at Tevatron

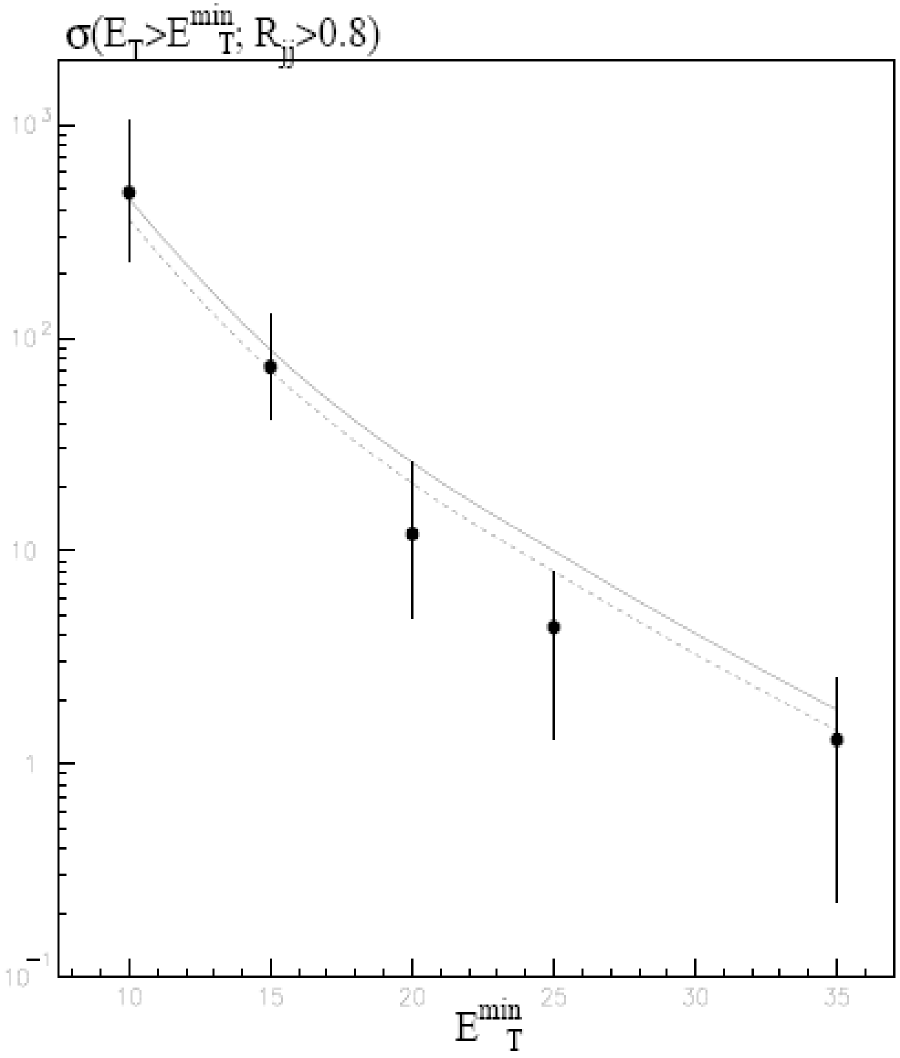

Predictions for LHC.

Qualitative predictions:

a) $\sigma^{(tot)}(s) \sim \ln^2 \frac{s}{s_0}$ as $s \to \infty$

b) Diffractive slope $B(s) \sim \ln^2 \frac{s}{s_0}$

c) $\langle n(s) \rangle \sim s^{\Delta} / \ln \frac{s}{s_0}$ without Pomeron interactions

$\langle n(s) \rangle \sim \ln^3 \frac{s}{s_0}$ with account of P-interac.

d) $\left.\frac{d\sigma}{dy}\right|_{y=0} \sim s^{\Delta}$

$\ln^4 \frac{s}{s_0}$ (with P-interactions)

Qualitative predictions.

e) Multiplicity distributions

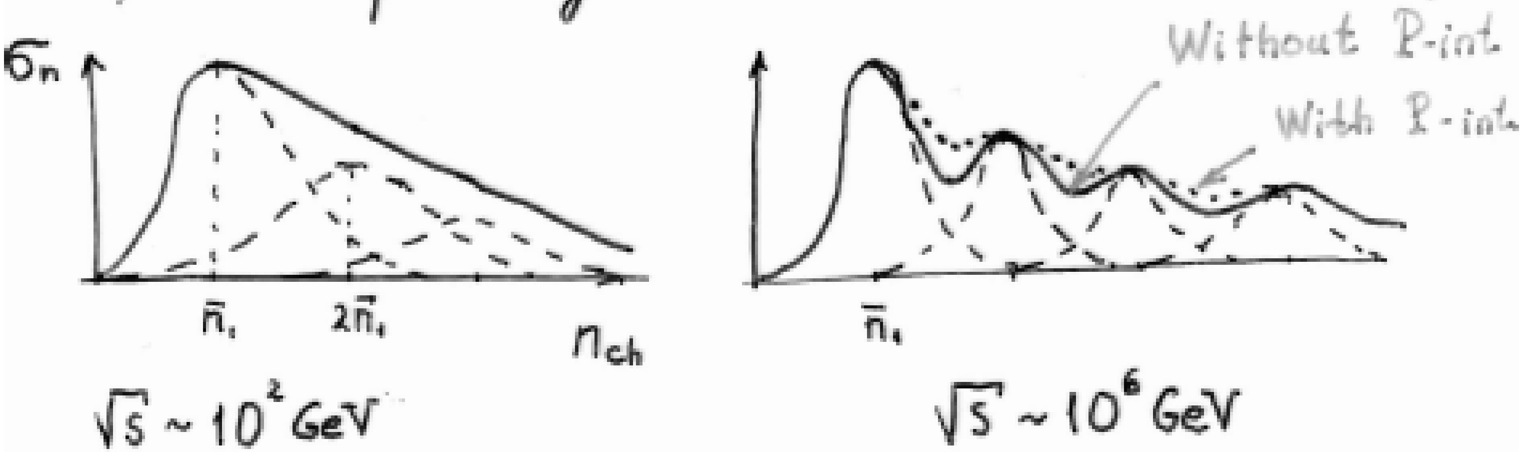

f) Important long range correlations.

Predictions for LHC.

1.	$\sigma^{(tot)}$	$103\ mb$	$\left(\sigma^{(tot)}(s) \sim \ln^2 \frac{s}{s_0}\right)$
2.	$\sigma^{(el)}$	$26\ mb$	$\left(\sigma^{(el)}(s) \sim \ln^2 \frac{s}{s_0}\right)$
3.	$B(0)$	$21.5\ GeV^{-2}$	$\left(B(0) \sim \ln^2 \frac{s}{s_0}\right)$
4.	$\rho = \frac{Re\,T(0)}{Im\,T(0)}$	0.11	
5.	σ_{SD}	$12 \div 13\ mb$	$\left(\sigma_{SD} \sim \sigma_{DD} \sim \ln \frac{s}{s_0}\right)$
6	σ_{DD}	$11 \div 13\ mb$	

$$\sigma^{(el)} + \sigma_{SD} + \sigma_{DD} = 51\ mb \approx \frac{1}{2}\,\sigma^{(tot)}$$

Predictions for LHC.

7. $\langle n_{ch} \rangle$ $\quad 80 \div 100$

8. $\left.\frac{dn_{ch}}{dy}\right|_{y=0}$ $\quad 5.5 \div 6.0$

9. Structures in σ_n

10. Strong long-range (in y) correlations

11. Large amount of minijets.

Charged particles multiplicity (QGSM calc. by M.Poghosyan)

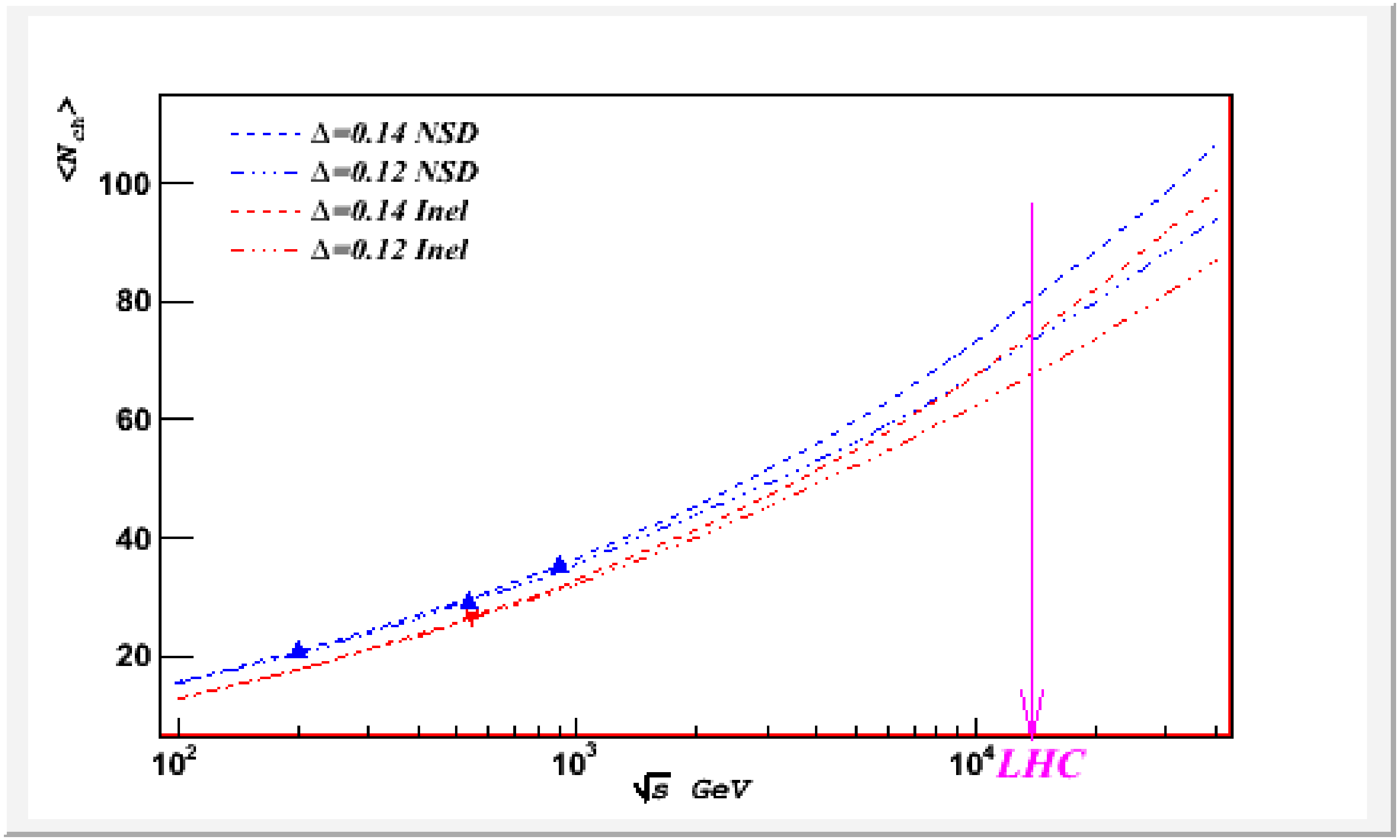

Meson production (QGSM calc. by M.Poghosyan)

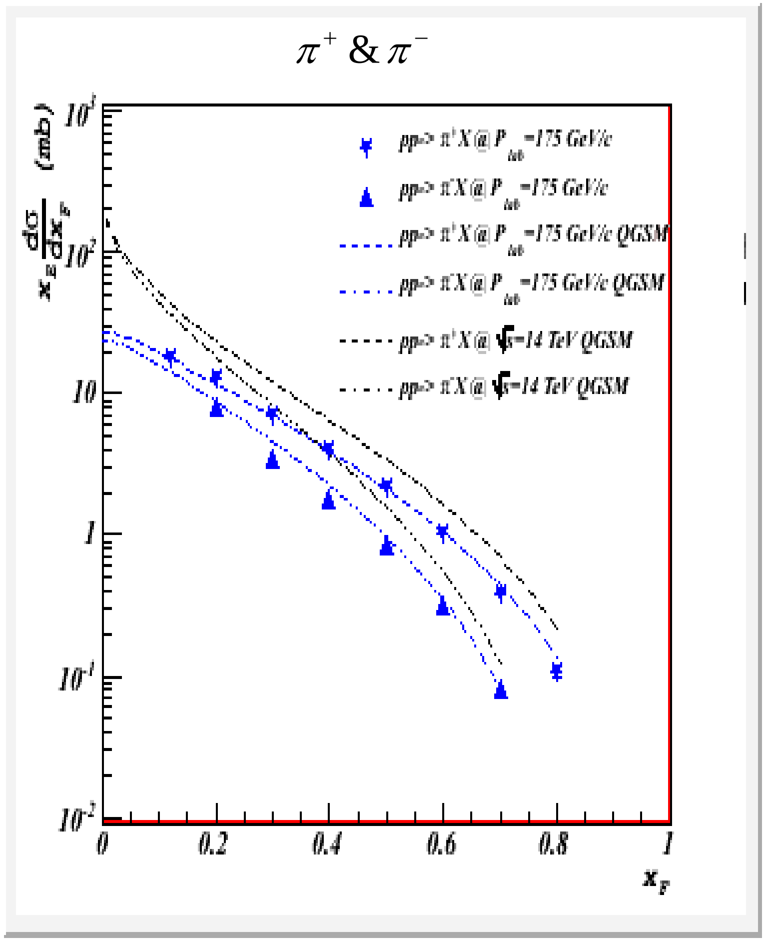

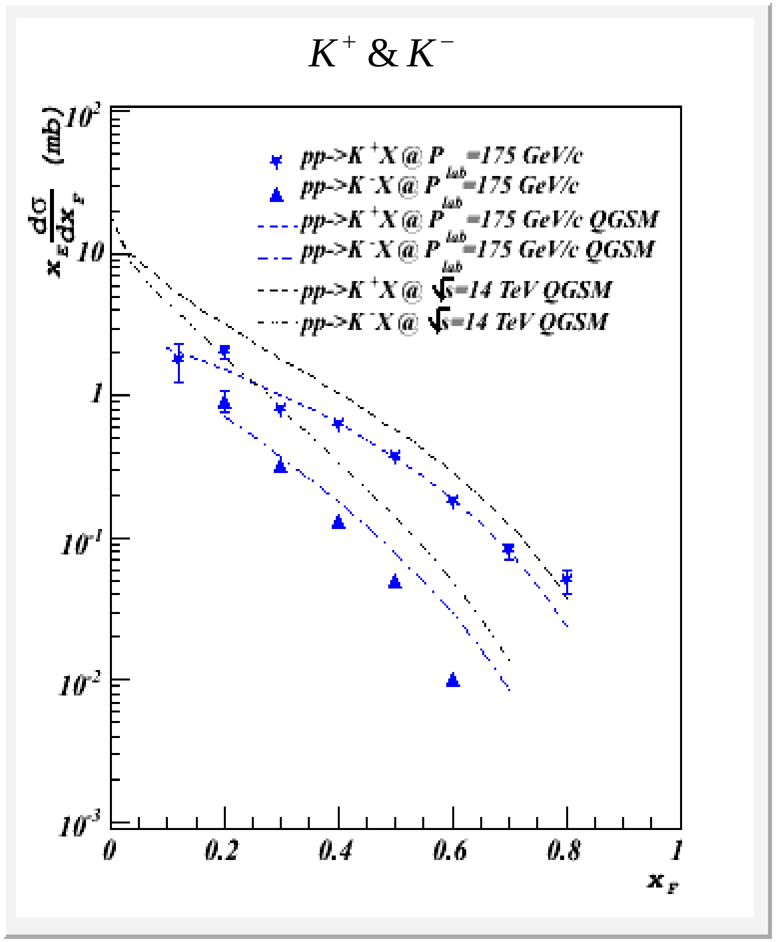

Problems and new developments.

It is necessary to formulate Monte Carlo for multiparticle production, which includes all essential diagrams with interactions of pomerons and gives description of $x \rightarrow 0$ region in DIS.

Existing Monte Carlo:

DPM jet, Phojet	J.Ranft, R.Engel
QGSM (with string fusion)	N.Amelin et al.
Nexsus	K.Werner et al.
QGSjet	S.Ostapchenko

Conclusions

- Notion of Regge pole is “one of the stable truth” in particle physics.
- Striking linearity of Regge-trajectories is related to the confinement in QCD and is a basis of string models of hadrons.
- 1/N-expansion in QCD is a very useful tool.
- Reggeon formalism is a universal approach to investigation of high-energy interactions of hadrons and nuclei.

Conclusions.

- The pomeron is the main building block of the reggeon approach. It has a rich dynamical structure in QCD.
- Many-pomeron exchanges are important for understanding high-energy interactions.
- Models based on reggeon calculus and 1/N –expansion in QCD give a good description of experimental data on interactions of hadrons, nuclei and small-x DIS.

Conclusions.

- Study of diffractive processes gives an important information on dynamics.
- Central exclusive Higgs production at LHC is a useful tool for studying Higgs properties.
- Many predictions for pp-interactions at LHC are formulated and will be soon tested experimentally.